Collision Dynamics Modeling of Crash Energy Management Passenger Rail Equipment

A thesis
submitted by

Karina M. Jacobsen

In partial fulfillment of the requirements
for the degree of

Master of Sciences
in
Mechanical Engineering

TUFTS UNIVERSITY

January 2008

Advisor: Professor A.B. Perlman

ABSTRACT

Crash Energy Management (CEM) is a crashworthiness strategy that incorporates crush zones into the design of passenger railcars. In the event of a collision, crush zones are engineered to collapse in a controlled manner and distribute crush to unoccupied areas throughout a train. This approach manages dissipation of the collision energy more effectively and efficiently than conventional railcar designs.

A train-to-train collision scenario is the basis for evaluation of crashworthiness in passenger railcars. This thesis uses a three-dimensional model of a CEM passenger train to simulate train collisions. The model is evolved in three stages: a single car model, a two-car model, and a train-to-train model. The key features include crush zones at both ends of the passenger railcars with a pushback coupler, suspension characteristics between the trucks and car body, and derailment characteristics to approximate the wheel-to-rail interaction. The results of each model are compared and validated with data from full-scale impact tests conducted for CEM passenger rail equipment.

The three-dimensional collision dynamics model developed for this thesis serves two roles: to explain the events of a CEM train-to-train test and to develop a tool for evaluating other collision conditions and equipment variations. The first role is accomplished and demonstrated through comparison of results with a full-scale test. The second role is accomplished through the documentation and demonstration of the features needed to assess other conditions and demands on CEM. The future uses of the model include investigation of new designs of CEM equipment and

evaluation of crashworthiness performance in more complex collision conditions such as oblique impacts and grade crossing collisions.

ACKNOWLEDGEMENTS

Endless thanks to my advisor, Professor Benjamin Perlman, for his continuous guidance and constant encouragement. Every discussion in the course of this work motivated me to move forward. I have truly enjoyed this experience.

Thank you all my colleagues at the Volpe Center. You inspire me daily with your humility, ability to solve tough problems, and willingness to help others. I am lucky to be an engineer working among such company.

Thank you to my editor, Karin, for polishing my thesis and providing a refreshing perspective. And thank you to my father, for reviewing the entire document. I appreciated every comment you provided. You've taught me a lot over the years and I'm thrilled I could teach you a few new words.

Gratitude to all my favorite suppliers of caffeine for keeping me up and to my favorite shala in the Back Bay for keeping me grounded; without a fine balance of both I never would have finished this thesis.

I want to extend my final appreciation to my mother, father and sister, for their love, encouragement, and support in this and all my endeavors. Thanks for always pointing me in the right direction.

LIST OF SYMBOLS, ABBREVIATIONS AND NOMENCLATURE

AC	anti-climber
APTA	American Public Transportation Association
CEM	crash energy management
CG	center of gravity
DOF	degrees of freedom
DMU	diesel multiple unit
FEA	finite element analysis
FRA	Federal Railroad Administration
MBTA	Massachusetts Bay Transportation Authority
MU	multiple-unit
1D	one-dimensional
PBC	pushback coupler
PEAM	primary energy absorbing mechanism
PTC	positive train control
SCRRA	Southern California Regional Rail Authority
SIV	secondary impact velocity
SNCF	French National Railway Company (*Société Nationale des Chemins de fer Français*)
TOR	top of rail
TSI	Technical Specification for Interoperability
UIC	International Union of Railways (*L'Union Internationale des chemins de fer*)
3D	three-dimensional

TABLE OF CONTENTS

LIST OF FIGURES AND TABLES

1 INTRODUCTION

Crash Energy Management (CEM) is a modern design strategy for railcars that includes crush zones at unoccupied locations of passenger trains. These zones are designed to crush at lower force levels than the surrounding passenger compartments. By engineering the crush zones to act as a system, collision energy can be dissipated into unoccupied spaces through the train, thereby preserving the integrity and safety of the occupied areas. By contrast, accident history shows that in conventional railcars, extensive damage is typically focused on the passenger car closest to the impact point, which can result in fatalities and serious injuries. The CEM approach to railcar design manages the collision energy more effectively and efficiently in a train than conventional railcar designs.

While CEM is not a new concept, implementation of CEM has occurred only in the last two decades. The French and British separately demonstrated the safety benefits through designing, building, and testing of CEM trains in the 1990s [1, 2, 3]. This research led to the inclusion of CEM trains in both countries, and the technology became widely accepted across Europe. However, in the United States, due to a unique operating environment, CEM trains must meet different loading requirements. In particular, much of U.S. passenger rail service is operated on track shared with freight trains. The potential of an impact with a much heavier and stronger freight consist requires passenger cars to absorb more collision energy than in impacts with a like train, the basis of most foreign crashworthiness standards. Additionally, push-pull operation in commuter rail service subjects the cab car to a potential impact with a locomotive-led train. In the U.S., CEM features have been

required for high-speed equipment (speed greater than 125 mph) since 1999 [4]. Over the last few years, the Volpe National Transportation Systems Center, under sponsorship of the Federal Railroad Administration (FRA), has developed and demonstrated the benefits of a prototype CEM design within the context of a collision on the general U.S. railroad system.

A prototype design of CEM passenger railcars has been designed, built and tested in a series of full-scale tests to study crashworthiness performance in an in-line train-to-train scenario. The results demonstrate that significant improvements in occupant protection can be achieved over conventional passenger rail equipment. This thesis evaluates the state-of-the-art crashworthiness technique of CEM within the context of collision dynamics modeling.

1.1 MOTIVATION

The development of a three-dimensional collision dynamics model of CEM passenger rail equipment is presented in this thesis. Test data from full-scale tests is used to validate the model through its stages of evolution. The full-train model is used to evaluate the component level performance of the CEM design in the in-line train-to-train test.

In general, collision dynamics models are used to estimate the gross motions of colliding bodies, impact forces imparted on each body and the gross structural crush of each body. Lumped-mass models have been used as a tool to estimate the crashworthiness and kinematics of trains for a number of collision scenarios [1, 2, 3, 5, 6, 7, 8]. A range of initial conditions can be evaluated in an efficient manner since the computational time is much less than detailed finite element models. Output

from lumped-mass models typically produces two measures of crashworthiness: 1) intrusion into the occupant compartment and 2) severity of the interior collision environment. The metrics can be used to interpret the likelihood of fatality or serious injury.

The most simplified lumped-parameter model of a railcar is a single mass representing the rigid car body and non-linear springs at each car end to characterize the structural force-crush response as the car is loaded in an impact [9]. Train sets can be constructed by linking cars together in series. In the most restricted form of such models, vertical and lateral linear and angular motions are neglected, and the train is constrained to move in one direction, longitudinally, along the track. By constraining the train to longitudinal motion and applying an initial velocity, such models are useful in evaluating general crashworthiness performance in highly idealized collision scenarios. More complex and realistic scenarios, in which significant lateral or longitudinal loads are introduced, require a three-dimensional model to investigate the situation. Simplified representations of structures with connections that allow for some three-dimensional motion can be used to investigate the initiation of complicated collision modes such as override between cars or lateral buckling.

Railcars with crush zones have structural elements that are designed to crush in a controlled manner at prescribed load levels. A one-dimensional single lumped-mass per car model cannot provide information on individual crushable components. Highly simplified models may be appropriate for evaluating car body behavior. However, for a CEM railcar with multiple crushable structures, a multi-

mass representation of each car provides estimates of the train kinematics, the car-to-car interactions and individual crush zone component performance.

A variety of collision dynamics models were developed to support the FRA's full-scale testing program to study train-to-train collisions. The first stage tested conventional passenger equipment to set a baseline of crashworthiness performance. The second stage tested prototype designs of CEM passenger cars in the same collision scenarios as the conventional equipment. Simplified one-dimensional models were used to evaluate the performance of conventional passenger rail equipment. Multi-mass models began to be developed for the single car and two-car tests of CEM equipment [10, 11]. In these models the vehicle-track interaction was idealized and assumed to be in-line. Agreement between the test data and the models was very good in terms of longitudinal car body gross motions and overall crush. In the train-to-train CEM test, one-dimensional models were used to determine crush distribution and gross motions of the train set. The CEM train set performed as expected; override between the impacting equipment did not occur, crush was distributed to all cars in the train, and the cars remained in-line with the exception of the trailing locomotive. The one-dimensional model was sufficient for instrumenting the test and predicting the outcome of the idealized train-to-train test since the train remained on the tracks. The model showed agreement with the test results in terms of crush distribution and the total time of the collision event.

In order to investigate the detailed performance of the CEM system in the train-to-train test, a more advanced lumped-mass model is needed. Important model features include a multi-mass representation of the crush zone, wheel-to-rail interaction, suspension characteristics between the car body and trucks, and a three-

dimensional coupler representation for each railcar in the train. With these features the CEM system can be assessed at a train level, a car level and a component level. Some details about the vertical and lateral motions experienced by the CEM train in the train-to-train test cannot be provided with the one-dimensional model. A three-dimensional multi-mass model is necessary to evaluate such details and how they influence out-of-line motions observed between cars and throughout the train set. Additionally, ideal performance of every crush zone component is unlikely. The multi-body configuration of each crush zone allows for further evaluation of detailed component performance.

The detailed model developed in this thesis will also be a tool for evaluating future concerns of CEM performance. New model features can be applied to evaluating: 1) CEM performance in oblique collisions and grade crossings, 2) inclusion of CEM features on locomotives, 3) compliance of new CEM designs. Testing to date has been focused on highly idealized collision scenarios. Further work is needed to evaluate CEM performance in oblique collisions and grade crossings. With a few changes to initial conditions and the impact object, the model can provide an initial evaluation. Other applications of CEM are likely in future efforts to further improve safety with CEM. The model has the capability of including CEM features on locomotives. Additionally, with CEM design currently being introduced into rail service in the U.S., qualification of these designs is a quickly approaching need. Rotem, a Korean railcar manufacturer, is currently designing CEM bi-level cars for use by Metrolink, Southern California Regional Rail Authority (SCRRA). Austin, Texas is currently developing new commuter railcars that include some CEM features. The detailed three-dimensional collision dynamics

model provides a readily usable tool for addressing a number of future evaluations as CEM enters into general rail service in the U.S.

1.2 RESEARCH APPROACH

The thesis aims to evaluate CEM passenger rail equipment at three levels: train performance, car interface performance and crush zone component performance. To provide appropriate background, Chapter 2 is an overview of past and current passenger rail crashworthiness research. International and domestic research is cited with emphasis on FRA sponsored research.

Chapter 3 provides a description of CEM philosophy and the potential benefits over conventional railcar designs. While CEM philosophy is not new, the evolution of crashworthiness design has been slow and ultimately stimulated by severe accidents in both Europe and the U.S. Research efforts, regulatory development and implementation have followed suit. A variety of CEM implementation strategies have resulted from the distinct operating needs of each country and/or railroad. These include high-speed versus low-speed operation, service on dedicated versus shared track, heavy versus light rail, fixed versus varying train configurations, pull versus push-pull operation. The evaluation techniques investigated in this thesis are illustrated by considering the prototype design developed for commuter rail push-pull operation on shared track. The collision scenario that defines this evaluation is a cab car-led train impacting a locomotive-led train.

A cab end CEM design and a coach end CEM design were developed for the full-scale tests. Chapter 4 describes the design requirements for each of the prototype CEM designs. The required form, features and function of each

component in the prototype CEM designs are summarized. These details define the features needed in the more detailed model.

A three-stage strategy for modeling is described in Chapter 5. This strategy allows the features needed for the train-to-train model to be developed and validated incrementally. The features and desired outcomes are listed in Table 1. First, a single CEM railcar is developed to represent the component crush and the three-dimensional car body motions in an impact with a fixed barrier. Next, two coupled CEM railcars are modeled to evaluate three-dimensional car-to-car interactions and crush distribution. A coupler model is created that includes both conventional coupler motions during typical operation and a pushback feature activated at prescribed collision loads. Finally, a train-to-train model evaluates the behavior of a train of CEM railcars, the car-to-car interactions and the crush zone component performance.

Table 1. Model development

Model	**Features**	**Outcomes/Products**
Single car	- Multi-body crush zone - Suspension characteristics - Derailment characteristic	- Component level crush sequence of events - 3D car body motion - 3D truck motions - Wheel-to-rail forces and indication of derailment event
Two-car	- Coupler-to-bellmouth interaction - Car-to-car interaction	- Coupler swing - Relative motions between cars - Crush distribution
Train-to-train	- Moving train of CEM cars - Standing train of freight equipment - Cab car-to-locomotive interaction	- Crush distribution - 3D train level kinematics - 3D relative car body motions - Component level crush sequence of events

The model development reflects the conceptual design of the full-scale tests. Chapter 5 describes the results of the complete series of full-scale tests. Comparisons are shown between the test data and the simplified models used to prepare for the tests.

Chapter 6 uses the results of the train-to-train test in order to validate the three-dimensional multi-body models. Gross motions and crush are compared to the test results and comparisons are also made against the simplified model results presented in Chapter 5. The more advanced features of the thesis models are demonstrated and shown to correlate well with the behavior observed in each full-scale test. The model is used to explore unexpected component level events in the train-to-train test.

The final chapter summarizes the comparisons made to validate the three-dimensional model. Recommendations are suggested for the prototype design and the final discussion includes anticipated future concerns of CEM in the U.S., recommendations for further research into CEM designs, and applications of the developed model in further work.

2 OVERVIEW OF PASSENGER RAIL CRASHWORTHINESS RESEARCH

2.1 BACKGROUND

While rail travel is the second safest mode of transportation in the United States [12], the few serious rail accidents that do occur highlight areas where improvements can be made to better protect occupants. The FRA regulates rail operation in the U.S. and also evaluates the potential for improvements in rail crashworthiness. The FRA leads working groups made up of railroad stakeholders (i.e. railroad authorities, equipment manufacturers, technology providers and engineering consultants) to discuss revised or new regulations. Through this process, the FRA integrates current federal rail research with practical experience to implement incremental safety improvements through new or revised regulations.

Assessing the need for improvements in passenger rail equipment begins with identifying the most common risks that passengers are subject to in the event of a train collision or derailment. The primary risks are associated with the loss of safe space within the occupant compartment and the subsequent impacts between the occupants and the interior surfaces. The goals of crashworthiness research are twofold: preserve a safe space for occupants to ride out the collision, and minimize the forces imparted to the occupants as they interact with the surrounding interior surfaces.

The Volpe National Transportation Systems Center, a federal research center under the U.S. Department of Transportation, provides technical support to the FRA's rulemaking process through the Passenger Equipment Safety Research

Program. Information from accident investigations, full-scale testing and modeling are used to dissect train-to-train collisions and evaluate the effectiveness of occupant protection strategies. The process shown in Figure 1 guides the research efforts. Statistically analyzing accident databases and conducting accident investigations identify primary collision scenarios of concern [13]. Such scenarios are idealized to conduct repeatable tests. The evaluation strategy establishes the crashworthiness performance metrics and the test requirements needed to provide the appropriate measurements. Existing equipment is evaluated for the chosen collision scenario to establish a baseline level of crashworthiness. Alternative designs are evaluated in the same idealized collision scenario and using the chosen measures of crashworthiness (i.e. energy absorbed, total crush, modes of deformation, etc.) comparisons are made to the baseline level of crashworthiness. The development and validation of analysis techniques play a key role in evaluating alternative designs. Validated models are used to extrapolate to other collision conditions and evaluate the performance of other designs. The research results are used by the FRA to support rule-making that improves occupant protection in rail.

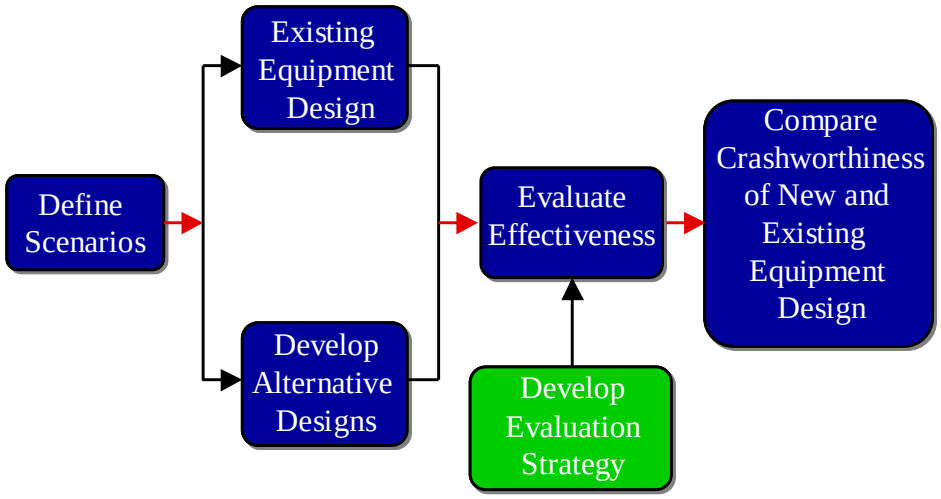

Figure 1. Flow diagram illustrating research methodology for evaluation of alternative occupant protection strategies

Incidents are classified in three groups: collisions with objects (i.e. grade-crossing incidents), single train events (i.e. derailments), and train-to-train collisions. These collision scenarios are studied further with on-going field investigations, full-scale tests and analyses. Accident databases and accident investigations provide the information needed to identify collision scenarios of primary concern for passenger rail equipment. Accident investigations provide physical evidence of the impact conditions that lead to fatalities or severe injuries. Field side evidence helps reconstruct the train kinematics during the collision. By determining the casual mechanisms for fatalities and serious injuries, alternative strategies are developed to improve occupant protection.

Full-scale tests are conducted to study the performance of the rail equipment for an idealized scenario and collect data of key metrics in order to compare baseline equipment performance to alternative designs. The study of overall crashworthiness is broken into two aspects, the structural crashworthiness and the interior occupant environment. As shown in Figure 2, each of these research activities is inter-related

and the information gleaned from each lends to better understanding the likely outcomes of the scenario of concern and what can be accomplished through designing improvements.

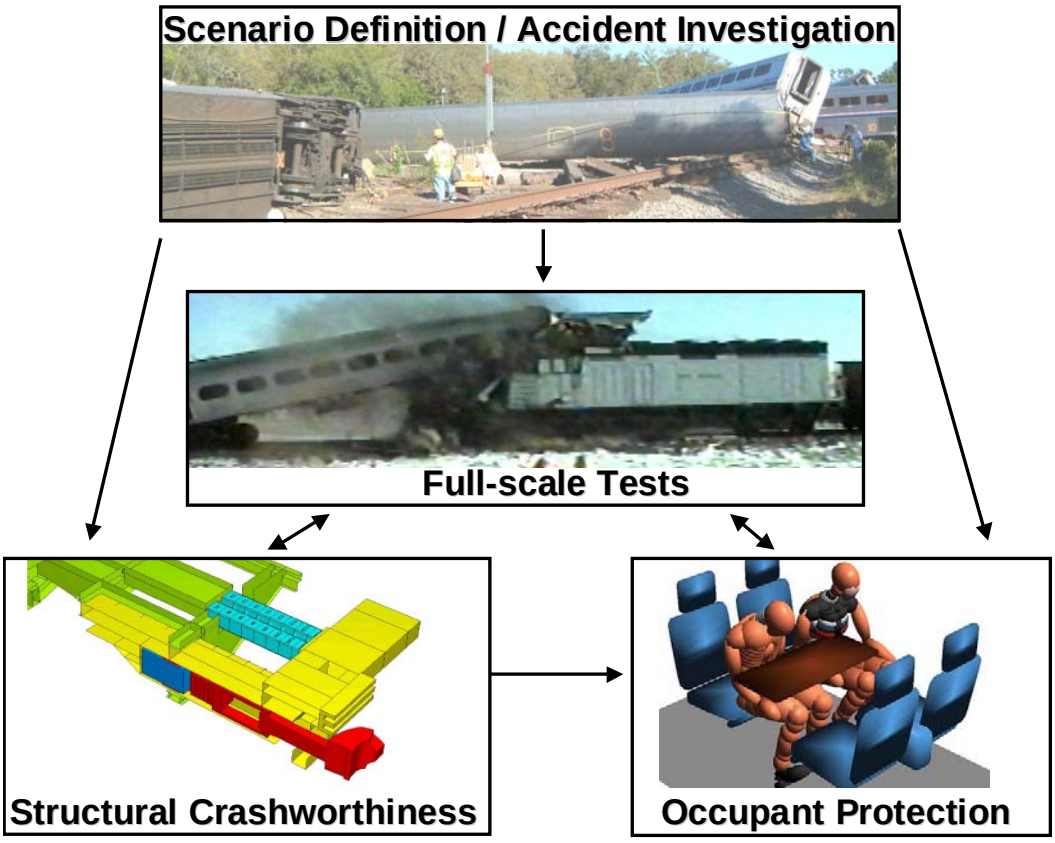

Figure 2. Passenger train research flow diagram

Accident investigations involve reconstructing the sequence of events leading to severe injuries and fatalities and determining the causal injury mechanisms. From this work, three collision modes were identified for conventional North American passenger rail equipment that pose particularly hazardous conditions:

1) Structural damage focused on the impacting equipment
2) Override of impacting equipment
3) Lateral buckling of coupled cars during collisions

Figure 3 - Figure 6 show photographs from four example accidents that demonstrate the undesirable outcome of each collision mode. In January 2005 in Glendale, California, a cab car-led commuter train impacted a sport utility vehicle obstructing the tracks, causing the front of the train to transfer onto a siding and impact a standing locomotive-led freight train [14]. Figure 3 shows the colliding equipment post-impact. The cab car was shortened in length by approximately 26 feet, causing six fatalities due to the bulk crushing. In 1981, a cab car-led passenger train impacted a locomotive-led freight train in Beverly, Massachusetts resulting in override of the locomotive by the cab car as shown in Figure 4 [15]. Haphazard structural crush can deform the underframe structure into a ramp, which promotes override. As one car overrides another, substantial loss of occupied volume typically occurs. In this collision, 29 fatalities occurred. Figure 5 and Figure 6 show photographs from incidents with varying levels of lateral buckling. During collisions, coupled cars tend to buckle out laterally relative to each other. In the New York incident of 1984, a small amplitude sawtooth pattern is observed down the length of the train [16]. In the incident shown from Bourbonnais, Illinois, lateral buckling in the front of the train has progressed into a large amplitude zigzagging pattern of buckling [17]. In this collision, a locomotive-led train impacted a highway vehicle at a grade crossing, which in turn caused the train to derail and led to an impact with a standing freight train on an adjacent track. As demonstrated in this accident, lateral buckling can lead to side-to-side impacts between cars. Such impacts are largely undesirable because passenger railcars are designed with relatively weak side structure and as cars derail and rollover, the likelihood of fire due to fuel tank ruptures

increases. Eleven fatalities occurred in the Bourbonnais accident due to loss of occupied space and a resultant fire.

Figure 3. Train-to-train collision with structural damage focused on the lead cab car; Glendale, California – January 26, 2005

Figure 4. Train-to-train accident with override; Beverly, Massachusetts - August 11, 1981

Figure 5. Incident with sawtooth lateral buckling; New York, New York – July 23, 1984

Figure 6. Incident with large-scale lateral buckling; Bourbonnais, Illinois - March 15, 1999

2.2 CRASHWORTHINESS TECHNIQUES

Crashworthiness is defined as resistance to the effects of a collision. Crashworthiness research focuses on determining a structure's ability to protect its contents, which may range from combustible liquid in fuel tanks, lethal gases in tank cars or passengers in automobiles and railcars. In all instances, the goal is the same – to safely contain the contents by engineering a structure that deforms in a controlled manner. In the area of passenger crashworthiness the objectives are defined as: 1) preservation of the occupied space so that the passengers can ride out the collision and 2) limitation of the secondary impacts experienced by the passengers to within survivable levels. Achieving these goals requires understanding of the collision events that challenge a vehicle. Implementation is constrained by a tradeoff between strengthening the structure and increasing the severity of the secondary impact environment. Weight and design costs influence these decisions.

2.2.1 Crash Energy Management

Crash energy management (CEM) is a strategy for managing the collision energy of a train impact incident by engineering the collapse of dedicated areas of a railcar and distributing the crush throughout the length of a train. Inclusion of crush zones on passenger railcars can significantly increase the crashworthiness of passenger rail equipment over conventional railcar design. Sacrificial crush zones can be designed into unoccupied areas of railcars – typically, the front and back ends – such as electrical and brake service closets, and bicycle or baggage storage areas. A crush zone is made up of structural elements that have predictable crush modes and are engineered to meet energy absorption requirements. Crush zone designs must dissipate collision energy as they deform and act as a system in a train to distribute

the collision energy. As the acceleration pulse moves through the train, crush zones are designed to collapse under lower loads than the occupied volume, such that the crush is distributed among the sacrificial ends of each car.

There are two important performance differences between conventional and CEM railcar designs. CEM cars more efficiently absorb collision energy and transfer crush to the following cars in a train rather than allowing crush to be concentrated exclusively on the lead car. Prototype CEM coach and cab car designs developed for full-scale tests can absorb at least 2.5 million ft-lb in the first three feet of the end structure [18, 19]. This dissipation is accomplished by the controlled crush of three primary components: the pushback coupler/draft gear assembly, primary energy absorbers, and the roof absorbers.

The distinctions between the conventional and CEM equipment can be illustrated in idealized force-crush characteristics, which are shown in Figure 7. A conventional railcar structure is defined primarily by a uniformly strong underframe structure. As shown in the plot, this structure requires a high peak force to instigate damage. Once the peak load is exceeded, there is little resistance to further deformation. Accident investigations and full-scale tests confirm that collision performance of conventional equipment typically concentrates crush at the front end of the lead passenger car of the colliding vehicles. CEM equipment is engineered to have structures outboard of the occupied volume that crush at lower levels than the underframe. The tiered force-crush behavior shown in Figure 7 characterizes a CEM design. The two peaks indicate the initiation of failure for each component in the crush zone. Each component crushes with an average crush load during the progressive collapse of each element. The occupant compartment begins to be

challenged when the third peak of the CEM load characteristic is exceeded. Beyond this point, the passenger car crushes with a load characteristic similar to a conventional car. The increasing double-tiered force-crush behavior of CEM causes the load to be passed to successive crush zones before the leading one is exhausted.

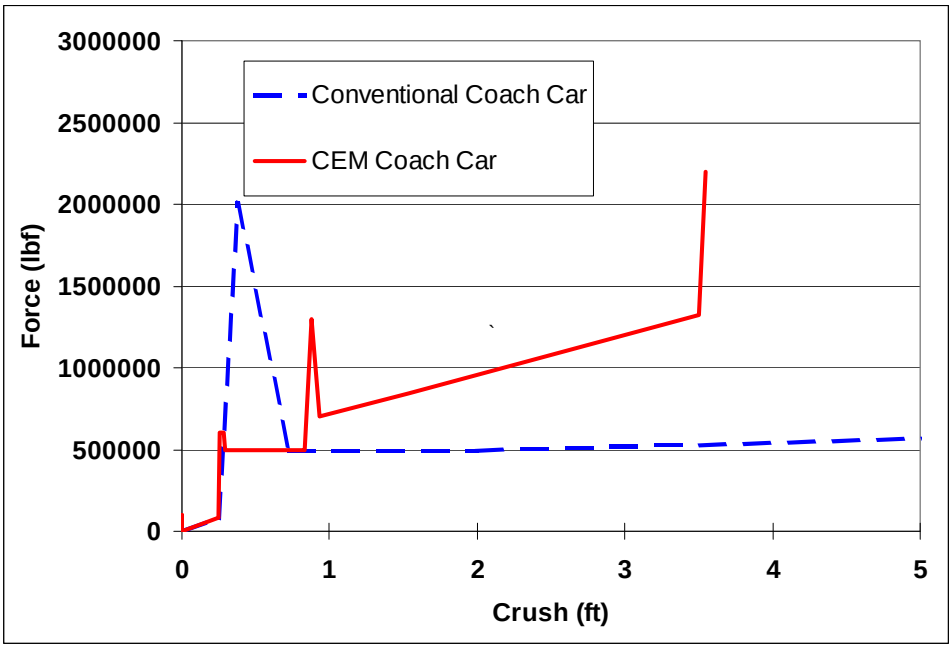

Figure 7. Idealized force-crush curve for conventional and CEM passenger car designs

The CEM strategy orchestrates the crush of multiple cars such that the energy dissipated in controlled crush is distributed. The energy absorbed by each crush zone is the integral of the force-crush characteristics. A comparison of the areas under the curves in Figure 7 shows that the CEM design can absorb almost twice as much energy in three feet of crush as conventional equipment. Three feet is the maximum amount of crush that can occur without intruding into the occupant compartment.

2.2.2 Increased Safety for Passenger Trains

Developments in improving safety measures for passenger rail travel are distinct in design and function, but complementary in purpose and outcome. Improved safety measures range from collision prevention strategies to infrastructure improvements and maintenance, to advanced crashworthiness designs. While this thesis focuses on evaluation of improvements made in the area of train crashworthiness, it should be mentioned that accident avoidance and mitigation strategies are valuable to maximize collision prevention. The advancement of positive train control (PTC) is recognized as a valuable safeguard against precursor collision events such as operator error, obstructions on the track, and signaling errors. The development of PTC systems continues to advance and be implemented in rail operation in the U.S. In the event that a collision occurs, however, train collision performance is the primary concern. The foremost goal of improving rail passenger equipment crashworthiness is to preserve the occupant volume during a collision. The secondary goal is to enable the passengers to ride out the collision by minimizing secondary impact velocities and providing a "friendly" interior environment. Crash energy management, along with strategic modification of rail passenger interior components, has the potential to significantly increase occupant protection during an accident.

The use of crushable structures manages the dissipation of collision energy with a higher average force over a shorter distance than conventional railcar designs so that the total structural crush in the train is reduced. A CEM train is engineered to reduce the likelihood of the three collision modes described earlier in this chapter. Crush zones should be designed to promote engagement between impacting

equipment. Engagement and controlled in-line crush inhibits override. Pushback design features on couplers can help prevent lateral motions between cars and reduce the risk of large amplitude lateral buckling. Ultimately, the prototype CEM design provides a more controlled collision response than conventional equipment.

The effects of a collision between a cab car-led passenger train and a locomotive-led train can be significantly improved over conventional equipment. A passenger train equipped with CEM end structures can more than double the train's crashworthy speed (the speed at which all occupied space is preserved). In addition to full-scale testing, studies have been conducted to evaluate CEM equipment for varying collision scenarios [20], to assess the capability and performance of incremental introduction into service with existing conventional equipment [21, 22], and determine the influence of operational factors on the overall performance [23]. These studies show that CEM cars can be introduced into service with minimal risks and with great potential benefit. The crashworthiness performance of a consist which combines conventional and CEM equipment is never worse than the performance of all conventional equipment in a train-to-train collision and is always better when a CEM car is the impacted cab car. The impacting end of a CEM car can absorb more energy before intrusion into the occupant volume than the impacting end of a conventional car. Consequently, the crashworthy speed of a consist with a CEM car leading is higher than the crashworthy speed of a consist with a conventional car leading. The crashworthy speed for the consist with a CEM car leading depends on the number of CEM cars immediately following the lead car. The results of these studies also show that crush zones are beneficial for multiple

units (MU) and push-pull service, and that CEM makes train crashworthiness nearly independent of the range of train lengths typically used in passenger service.

The results of this research indicate that the benefits of CEM can be practically achieved through incremental incorporation of CEM into service. In the rail industry, a typical passenger railcar lifespan can range from 20-40 years. With the cost of a new passenger railcar currently about $2-$3 million, railroads generally replace only a few railcars at a time, rather than an entire fleet, and opt to retrofit existing equipment, when possible, to make improvements. Metrolink, SCRRA, is an example of a railroad that is actively improving safety by strategically transitioning to CEM equipment [24] for use on the general railroad system. In February 2006, Metrolink awarded a contract for a new generation of multi-level CEM passenger railcars that will be incorporated into service with their existing fleet [25]. Metrolink plans to replace all their existing cab cars with CEM cab cars and incrementally phase in CEM coach cars, as funding allows. Southern Florida Regional Transportation Authority (operators of Tri-Rail commuter train service) will receive a smaller order of CEM cab cars and CEM trailer cars. Metrolink is additionally investigating the retrofit of its existing fleet to include pushback couplers. Furthermore, federal regulatory and industry standard development are under consideration for the retrofit of existing passenger cars with pushback couplers.

2.3 ANALYSES

In an industry in which building and testing a railcar is a mutli-million dollar effort, analysis plays an important role in the design and qualification of new railcars. In the rail industry, preparation includes hundreds of detailed design drawings,

thousands of pounds of material and months of skilled laborers' time to build a single vehicle. As a result, analysis of railcar crashworthiness has been developed over the last couple decades alongside the evolution of CEM railcar designs.

Analyses are broken into a few levels of modeling: structural crush, collision dynamics and occupant modeling. Figure 8 shows a diagram that maps out some of the inter-related analyses and the output each produces. Each model provides important measures used to assess the overall crashworthiness performance of the rail equipment. The finite element model evaluates the various modes of deformation that occur and the load path through the structure. This is especially important in the design phase in order to design crashworthiness features that collapse for prescribed loads and the surround structure to support the collision loads and protect the occupant compartment. The force-crush behavior of the system is used as a model input to define characteristics in the lumped-parameter collision dynamics model. The most simplified collision dynamics model produces the gross motions of the car bodies and crush experienced by the railcar for a defined collision speed. The crash acceleration pulse can be used as input for models of the occupant environment (the secondary impact environment). These models generate the secondary motions experienced by the occupants in various seating arrangements. These three models can guide the design, testing and evaluation process.

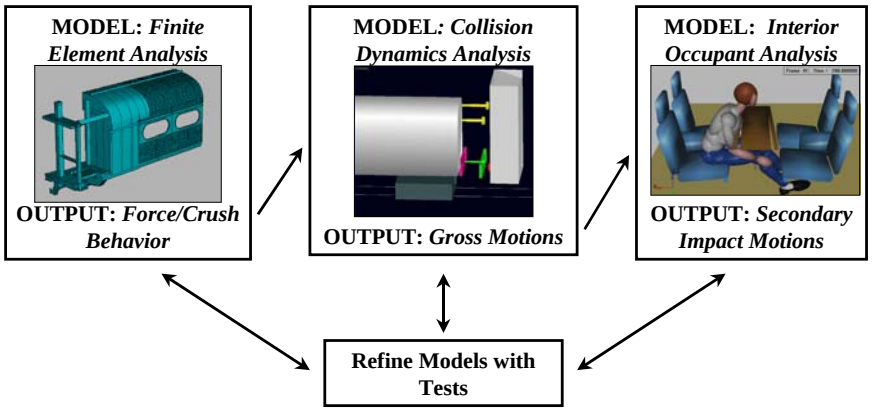

Figure 8. Rail crashworthiness analyses flowchart

Over the last two decades, these three types of models have become standard tools for evaluating crashworthiness in the rail industry. A review of other work shows that both simple and detailed analyses are used to produce results ranging from energy dissipation and gross longitudinal motions to structural behavior and three-dimensional motions. This thesis work draws upon the validated techniques of collision dynamics modeling and further develops features specifically for evaluating CEM equipment in a train-to-train impact.

In the 1970s, Tong [9] demonstrated the use of two types of models to describe train level mechanics. A simple one degree-of-freedom lumped-parameter model is compared with full-scale test data of a train-to-train collision. In his model, a railcar is represented as a single mass and a linear elastic spring represents the car's structure. The impact scenario is simplified to investigate the impact forces that are transferred between cars when a single car impacts a like car coupled to a freight locomotive. The cars are constrained to travel in the longitudinal direction. The spring-mass systems were represented by equations of motion and the results numerically calculated. Tong shows that the simple model produces reasonable comparisons with full-scale test data. Tong also describes the use of a finite element

model in which the underframe of the car is represented as a beam element and includes inertial properties. This model produces good agreement of the longitudinal forces at the ends of each car with full-scale test data. In his conclusions, Tong cites the need for a detailed model to simulate the three-dimensional motions of the car.

Models that follow simple representations of each railcar, similar to Tong's, produce gross estimates of motion in idealized collision scenarios. For situations where the damage is assumed to be primarily longitudinal these models can provide good estimates of the deceleration and collision time of an event. This information can be used to design an impact test. The gross motions also provide an estimate of the severity of the interior environment.

In the 1990s, both the British and the French undertook full-scale testing programs to demonstrate and measure crashworthiness features of new railcar designs. Chatterjee and Carney [26] numerically simulated several hundred train collisions as part of a study for British Rail Research. In this study, finite element and lumped-mass models were compared. A one-dimensional model represented the railcar as three masses, two crush zones at the ends and the remaining car body and truck weight lumped into a single mass at the center of gravity (CG). Chatterjee and Carney concluded that the lumped-mass model and finite element model produced near identical results for accelerations and velocity; the total plastic deformation results were identical. In light of these comparisons, Chatterjee and Carney cite user-friendliness as the explanation for carrying out the remainder of the study, which includes hundreds of simulations, with the lumped-mass model. Shorter computational time and fewer input parameters likely influenced this decision. Chatterjee and Carney also compare two lumped-mass models, one which

lumps the entire railcar into a single mass and the second in which the railcar mass is distributed among three masses. The results show very similar force-time histories. The multi-mass representation of the railcar force-time histories have high frequency content.

Cadete, Dias and Pereira [26] have conducted studies of lumped-mass modeling to optimize railcar crashworthiness design. These experiments highlight the usefulness of simplified models in the design phase of new railcars with crush zones. Cadete, Dias and Pereria use one-dimensional models of a three-car consist and seek to optimize the crush zones for a head-on train-to-train scenario, a grade-crossing scenario and an impact with a line end. In further work, Dias and Pereira [5] discuss the application of these models to support the SAFETRAIN project [3], research initiated in 1997, and sponsored by the UIC to improve safety in rail travel throughout Europe. The practices described by the UIC are widely used in crashworthiness design and evaluation throughout Europe.

In the United States, the FRA has sponsored the largest body of research in improving crashworthiness for passenger trains. The effort has included the development of finite element models to assess the structural behavior of CEM prototype designs under dynamic loading conditions. In crush zone component testing, detailed component models verified that the components crushed as expected. A full-car finite element model was built in accordance with the assembly drawings used for the integration of the CEM design onto Budd Pioneer and Budd M1 passenger cars. The finite element model produced the initial representation of the composite force-crush characteristic of the coach car CEM system, as shown in

Figure 9. An idealization of this behavior is a key input for collision dynamics models.

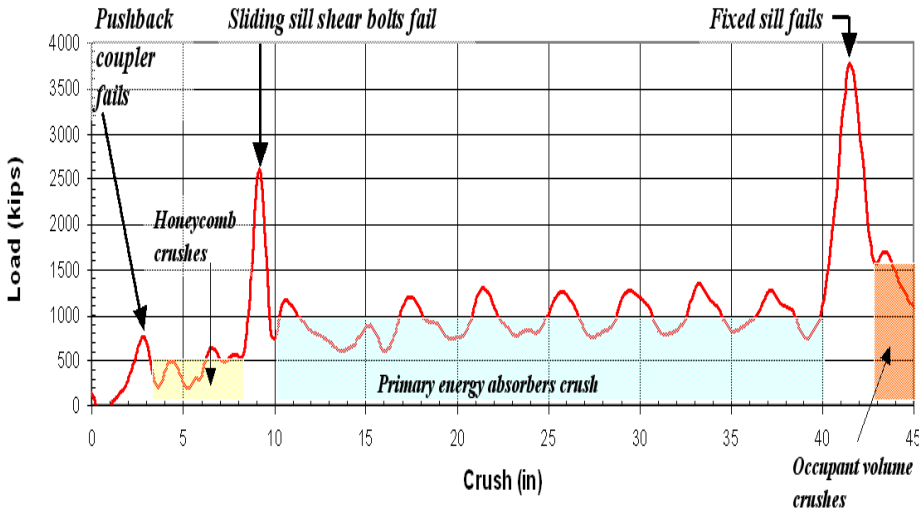

Figure 9. CEM force-crush curve of the coach car prototype design, estimated by a finite element model

Collision dynamics models have been used throughout the research conducted for the FRA. In 1995, Tyrell, Severson and Marquis [28] used one-dimensional lumped-mass models to evaluate crashworthiness features of high-speed railcars. In 2000, Severson [29] used lumped mass models to predict the outcome of the single car and two-car full-scale tests of conventional North American passenger railcars. The railcar models are multi-mass railcars, including trucks connected to the car body and to the rails. The wheel-to-rail interaction is based on in a lateral buckling study of railcars [6]. The results shown in Severson's study include a parametric study of impact parameters to simulation the car-to-wall interaction and the car-to-car interaction, a non-linear force-crush characteristic implemented with a FORTRAN subroutine that accounts for an unloading characteristic, and three-dimensional rigid body motions of the car. Perturbations were used to instigate the lateral motion and bound the range of expected responses. The full-scale test

observations of longitudinal motion agreed well; but vertical and lateral motion did not match the predictions. Severson recommended that the suspension characteristics and the wheel-to-rail connection could be modified to improve estimates.

2.4 TESTS

Manufacturers of railcars that include crushable structures typically conduct various levels of dynamic, static and component tests to confirm performance of their designs and to complement their analyses. Much of this information is proprietary and not available in open literature. Some full-scale tests have been conducted by federal research centers and collaborative research groups which do openly provide the results.

The British have conducted full-scale tests to validate concepts for energy absorption in crush zone designs. Lewis [1] describes a series of tests conducted by British Rail Research in 1994 to demonstrate and measure the performance of crush zones on railcars. Tests included a train-to-train impact which demonstrated energy absorption capabilities and crush distribution through the train. A car-to-car impact showed that the crush zone, which included pushback couplers and anti-climbers prevented override. Photographs of the test show that although the end frames engaged, the end structures crushed asymmetrically so that the end frames were positioned diagonal to the ground.

Similarly, in 1994-1996, the French National Railway Company (SNCF) sponsored a number of full-scale tests of TGV equipment. Cleon, Legait and Villemin [2] describe the full-scale tests used to qualify the crashworthiness features

in the bi-level TGV and the XTER DMU. Both bi-level passenger railcars and DMU equipment appear to be in growing demand in the U.S.

Beginning in 1997, the UIC sponsored a research effort called SAFETRAIN [3], with the aim of designing improved railcar structures to reduce the number of fatalities and serious injuries associated with railway in Europe. The research results provided by its members with technical information to make recommendations and guide standards for all rail used throughout Europe. A series of tests were planned to be conducted to test the program's prototype design in 2000.

In 2006, Indian Railway conducted full-scale tests of redesigned GS and SLR passenger railcars which included crush zones [30]. During the test of these redesigned passenger cars, the crush zones were activated, but damage also occurred at the transition of the crush zone and the occupant compartment, which suggests that particular attention must be paid to the collision loads that the crush zone support structure must sustain. Although vertical and lateral motions were minimized at the colliding interface, the damage that occurred inboard of the crush zone warns of the potential for mid-car override under more severe collision loads without modifications to the support structure.

As part of the FRA's Equipment Safety Research Program a series of full-scale impact tests have been conducted in the United States. The purpose of this program is to propose strategies for improving occupant protection under common impact conditions for passenger rail equipment. A unique feature of passenger rail operation in the U.S. is the use of passenger rail equipment on shared track with freight equipment and the frequency of push-pull service on these routes. The set of full-scale tests is consequently, a collision scenario in which a cab car-led train

collides with a locomotive-led train. Example collisions include the Beverly, Massachusetts collision between a commuter train and a freight train [15], the Silver Spring, Maryland collision between a commuter train and an intercity passenger train [31], and the Glendale, California collision between a commuter train and a freight train [24].

Six tests have been conducted to measure the crashworthiness performance of existing equipment and to measure the performance of equipment incorporating CEM features. The collision scenario addressed by these tests is a cab car-led passenger train colliding with a conventional locomotive-led passenger train. The tests conducted for each equipment type include:

1. Single-car impact into a fixed barrier
2. Two coupled car impact into a fixed barrier
3. Cab car-led train collision with standing conventional locomotive-led train

This arrangement of the tests allows comparison of the existing equipment's performance with the performance of improved-crashworthiness equipment. The sequence of impact tests allows an in-line train-to-train collision to be studied in incremental levels of complexity. These tests are intended to measure the crashworthiness of a single passenger car, then the interactions of two such cars when coupled, and finally the behavior of complete trains, including the interactions of the colliding cars.

The results from these tests show that the CEM design has superior crashworthiness performance over existing equipment. In the single-car test of existing equipment at a closing speed of 35 mph, the car was reduced in length by approximately 6 feet, with intrusion into the occupied area [32]. The draft sill was

crippled during the impact, with plastic deformation extending past the buff stops. As a result of the crippling of the car body structure, the car lifted by about 9 inches, raising the wheels of the lead truck off the rails. Under the single-car test conditions at a closing speed of 34 mph, the CEM car crushed about 3 feet, preserving the occupied area. As a result of the controlled crush of the car body structure, its wheels remained on the rails [10].

In the two-car test of existing equipment at a closing speed of 26 mph, the impact car again crushed by approximately 6 feet [33]. No crush of the trailing car occurred. The crippling of the car body structure again caused the car to lift about 9 inches. The conventional couplers caused the cars to buckle laterally. As a result of this misalignment of the coupled cars, the trucks immediately adjacent to the coupled connection derailed. In the two-car test of CEM equipment, at a closing speed of 29 mph, the cars preserved the occupant areas [11]. The lead car crushed at the front and rear, and the trailing car crushed at the front. The pushback couplers allowed the cars to remain in-line with all of the wheels on the rails.

In the train-to-train test of existing equipment at a closing speed of 30 mph, the colliding cab car crushed by approximately 22 feet [34]. Due to the crippling of the cab car structure, the cab car overrode the conventional locomotive. The space for the operator's seat and for approximately 47 passenger seats was lost. During the train-to-train test of CEM equipment, at a closing speed of 31 mph, the front of the cab car crushed by approximately 3 feet [35]. The controlled deformation of the cab car prevented override. All of the crew and passenger space was preserved.

This thesis work focuses on the second half of full-scale tests conducted for the FRA. Many modeling techniques are drawn from previous research. The Adams

software package is used to develop multi-body railcars and non-linear force-crush characteristics are calculated through a FORTRAN subroutine developed at the Volpe Center [29]. The multi-body railcar representation developed for this thesis is unique to CEM railcars. It draws upon techniques used to predict the results of the single and two-car CEM full-scale tests. Jacobsen, Tyrell and Perlman [10, 11] describe the multi-body model and present the comparisons with test data in two journal papers. The models compare favorable with longitudinal gross motions and total crush. This thesis develops a coupler representation that captures the swing and pitch motions of conventional coupler operation and longitudinal motions of the pushback feature when activated. Modeling this feature allows the timing of events and transfer of car-to-car loads to be investigated. Suspension characteristics are defined between each truck based upon measured characteristics. Forces are defined between the trucks and include a prediction of derailment. Model development is described further in Chapter 4.

2.5 EVALUATING TESTS AND ANALYSES

Collision dynamics models are valuable tools for planning tests and evaluating test results. Once a model is validated, it can be used to extrapolate to other collision speeds or loading conditions. In this thesis, full-scale tests of CEM equipment are used to validate the model based on gross motions, crush and sequence of events. The model can then be used to investigate variations of input parameters that differ from the values in the test. The critical measurements in the CEM full-scale tests are summarized below. Results are presented in Chapter 5.

In the single-car test, the critical measurements are made to obtain a force-crush characteristic and to measure the gross motions of the test equipment. The two-car test adds consideration of the interactions of the coupled connection. Vertical and lateral motions of the cars respective to each other are measured to assess the potential for sawtooth lateral buckling. The train-to-train test focuses on the interactions of the colliding equipment: how the equipment engages, the potential for override of the colliding vehicles, and the effects of the collision throughout the train.

The tests of conventional equipment established a baseline for crashworthiness performance of current passenger rail equipment. The following events occurred in the conventional train-to-train test: override of the colliding equipment, lateral buckling between coupled cars and loss of 47 seats in the lead passenger car. In the corresponding CEM tests, the following events demonstrated an improved level of crashworthiness over conventional equipment: the colliding equipment engaged (did not override), the railcars remained in-line and on the rails (did not laterally buckle), and all occupied space was preserved.

Lumped-mass collision dynamics models were used to design the full-scale tests (test speed, vehicle weights, instrumentation specifications, etc.) and predict the collision outcome. For the conventional tests and initial comparisons between alternate designs, one-dimensional collision dynamics models were developed to predict the gross motions of the test vehicles and crush estimates (structural damage) for each railcar. The models were modified based on the test results. For the single and two-car tests of the CEM equipment, multi-body representations of the crush

zones were developed for the collision dynamics models to investigate the triggering of individual crush zone components at each car end.

The need for further development of a three-dimensional multi-body railcar model in the train-to-train scenario was identified post-test. A one-dimensional model was used for instrumenting the CEM train-to-train test and provided sufficient estimates of deceleration ranges and the overall gross motions of the car bodies. A three-dimensional model can provide further information of the vertical and lateral motions experienced at each car and the effect of the resultant vertical and lateral forces on the functioning of the crush zones. Additionally a three-dimensional model can be used to look at the performance of a CEM train in non-ideal collision conditions such as oblique impacts and curved track.

3 CRASH ENERGY MANAGEMENT TECHNOLOGY

The concept of crash energy management as a strategy for improving occupant protection in collisions was acknowledged as early as 1850 [36, 37]. The general philosophy entails designing a vehicle's structure to collapse at specified unoccupied locations, in an effort to preserve the occupied compartment. This is accomplished by designing crushable structures that deform in a controlled manner at lower loads than the occupied compartment. The goal is to dissipate the collision energy through the deformation of these crushable structures before it reaches the passengers. By preserving the occupied space, the passengers then have a chance to ride out the collision. The key to designing a crush zone that protects the occupants is defining the amount of collision energy that must be absorbed by the crush zone. With kinetic energy estimated in a collision as the product of one half the mass times velocity squared, the problem is dependent on both speed and mass of the colliding equipment. Consequently, crashworthiness of a system must be described in relation to a scenario. As a result, the specific requirement for a crush zone is typically defined in terms of an amount of energy that must be absorbed by the crush zone for the prescribed condition while all damage is confined to the designated location.

In the 1970s, the U.S. government took measures to reduce the number of deaths in motor vehicle accidents by pushing the automotive industry to incorporate crashworthiness testing in the design process of automobiles. Automotive crashworthiness requirements worked their way into regulations by the early 1980s in the form of requirements for ensuring occupant survivability in barrier impact tests and rollover tests [38]. Significant research was accomplished to design collapsible

structures into existing automotive designs in order to preserve the occupied space and reduce the severity of the collision environment. The basic principles of crush zones were implemented in these designs. If the collapsible structures are designed to crush at a lower load than the structure protecting the occupied space, then the damage during a specific type of collision (head-on, side impacts and every orientation in-between) could be contained to the unoccupied areas of the car (i.e. the bumper, hood, trunk, door, etc) up to a given speed. Additionally, because automotive collisions occur at high speeds, which cause severe crash pulses additional measures are necessary to restrain the passengers and protect against severe impacts with the interior. Providing restraints limits the distance a passenger can travel during a collision which reduces the severity of the impact. Seat belts, air bags and inflatable structures have become standardized crashworthiness features in automobiles over the years.

Train crashworthiness can apply similar philosophies in the design of individual passenger cars, but the coordination of the forms and features vary due to unique differences in the operating constraints of railcars. Railcars operate as a series of vehicles linked together by couplers and are travel along the curve defined by the rail. An automobile collision can occur for a large number of collision scenarios, but because trains are confined to move along a set of rails, the operating environment greatly reduces the number of likely collision scenarios for trains. This makes defining the kinematics of the collision extremely different because the interaction of the railcars as a system is just as important to understand as how a single railcar acts. The collision must be evaluated at a train level, a car level and a crush zone component level.

At a train level perspective, the design of crush zones in railcars can include a variety of strategies to control energy absorption. One strategy for controlling collision energy is the use of a sacrificial (unoccupied) car that is strategically placed in a train and is designed to collapse at a lower load than the other cars so that collision energy is dissipated primarily through its collapse. Some railroads position baggage cars as sacrificial cars at the front or back of the train with this intention. This practice does not address the subsequent kinematics of the rest of the cars in the collision which can lead to highly undesirable collision modes. The French have employed a more tactical approach for the TGV train sets, by designing long areas of crushable structure into portions of the power cars. The TGV train sets are operated in a set configuration with power cars at the front and the rear of the train. The issues of design and loss of revenue have not made this a popular strategy in the U.S.

In a CEM train, crush is distributed to unoccupied areas throughout the train. The collision force moves through a train in a slinky-like manner producing a delay in the deceleration of each successive car. The U.K. has explored the collision delay in inter-railcar behavior and investigated designing a CEM train set that controls the deceleration and crush of each car in order to reduce the severity of the secondary impacts occupants experience. Crush zones are designed into a train with an optimized "intercarriage gap" between each car in order to isolate each car's deceleration as a separately occurring event in the collision, down the length of the train [26]. Such specifically designed systems within a CEM train set may increase occupant protection for trains that operate permanently in a set configuration, as do many trains in Europe [3]. However, in typical passenger rail operation in the U.S., passenger train lengths vary dramatically depending on service demands which may

vary throughout the day and cars are moved around between consists regularly due to maintenance. Such irregular configurations and varying consists create an operating environment such that a CEM system cannot be designed for a standard operating configuration. The focus leans toward ensuring a more robust CEM design that can accommodate a variety of collision conditions.

3.1 PHILOSOPHY OF CEM

The underlying principles of CEM are similar throughout all applications of crashworthiness design: absorb collision energy through the controlled collapse of unoccupied areas of vehicles in order to preserve the occupant volume. The strategies will differ depending on the likely types of collisions and the operating environments. An automobile as discussed, must be designed against a large number of collision scenarios (i.e. side impacts, front impacts, rear-end impacts, and rollover). For each scenario, certain areas of the automobile are designed to collapse in a manner that allows the space containing the passenger to be maintained. Passive and active interior protection are used to protect the passengers against secondary impacts.

Similar strategies can be used for improving train crashworthiness, but the details of the train kinematics and interactions of impacting equipment present some unique challenges that must be addressed by more of a systems design approach. A 30 mph impact of a single car into a wall requires a crush zone to absorb approximately 4 million ft-lb. At the same speed a typical commuter train requires dissipation of about 30 million ft-lb. At the train level, distribution of crush and energy absorption are the primary design considerations. At the car level, the

sequence of events in car-to-car interactions (i.e. locomotive-to-cab car impact, coupled car interaction, etc.) must be addressed through specific design features. At the component level, specific functions must be achieved. By addressing each of these levels with CEM design, a train can be designed to have a more predictable and less hazardous response during a collision.

A likely and challenging collision scenario for passenger trains is a head-on train-to-train impact scenario. In train-to-train collisions of conventional passenger equipment, the lead passenger railcar typically sustains extensive damage while the trailing cars remain relatively intact. Railcars are traditionally designed with a uniformly strong continuous center sill and relatively weak superstructure. When a railcar experiences a high collision force and the underframe begins to buckle, the resultant load required to crush the structure is relatively low. A passenger train made up of CEM railcars can be designed to perform as a system of crashworthy cars by sharing the dissipation of collision energy by all the cars. Because the cars in a train are coupled together, the impact forces as transferred through the train. With crush zones on the ends of each railcar, crush can be distributed through the length of the train. If the crush zones are designed to collapse at a lower load than the supporting car body protecting the occupied space, the crush zones at the ends of each railcar can share the damage while preserving all the occupied space in the train.

3.2 DEVELOPMENT OF RAIL CRASHWORTHINESS STANDARDS

Internationally, several accidents occurred that motivated the development of CEM specifications. In the U.K., a head-on accident at Clapham Junction resulted in many fatalities and injuries. It prompted discussion on how to better design a

platform-like railcar structure to collapse in a controlled manner in a collision scenario [39]. An accident that inspired change in France was a grade crossing collision in Voiron, where a passenger train rounding a curve at 68 mph impacted a road transport weighing about 80 tons. The lead power unit derailed and the first trailer was ripped open by debris resulting in over 60 injuries and two fatalities. As a result of this accident, all future generations of TGV designs incorporated crash testing of safety features and included crush zones at the front and rear of the power unit and first trailer. The High and Low Speed Technical Specification for Interoperability (TSI) [40] guides all members of the International Union of Railroads (UIC). The TSI includes crashworthiness requirements for all trains operated on the European rail network. The crashworthiness requirements define three collision scenarios (including a cab-car led train impacting a locomotive) and include requirements for minimum energy absorption and allowable lengths for crush zones.

Additional regulations, specifications and industry standards have been adopted in the U.S. since the early 1990s. In an accident in Chase, Maryland in 1987, a locomotive-leading Amtrak Colonial Express passenger train impacted a freight consist at 130 mph, resulting in 16 fatalities [41]. This high speed accident prompted the development of increased crashworthiness standards and regulations for Tier II equipment (trains operating at speeds between 125 mph to 150 mph). In 1994 FRA worked with Amtrak to incorporate crush zone requirements into the specification for the high-speed Acela train sets, which were being introduced at that time to the Northeast corridor [42]. In 1999 FRA published passenger equipment safety standards in the Federal Register to mandate that all Tier II equipment include crush

zones that meet energy absorption requirements for a prescribed train-to-train scenario [4]. The standard defines an in-line train-to-train collision scenario of identical trains at a given speed. Minimum energy absorption requirements are defined for both passenger cars and locomotives and crush is restricted to the ends of the car, but no limits are placed on the allowable crush stroke. Also, in 1999 the American Public Transportation Association (APTA) issued a Standard of Recommended Practices that includes energy absorption requirements for new passenger rail equipment including locomotive hauled, MU and cab cars for three collision scenarios, including an in-line train-to-train collision [43].

3.3 PASSENGER RAIL CRASHWORTHINESS NEEDS IN THE U.S.

Three factors influence the development of CEM in the United States. The U.S. has a unique operating environment, particularly in comparison to Europe. Lessons can be learned from European CEM strategies, but ultimately, requirements for CEM designs in the U.S. must coincide with existing requirements. Finally, CEM designs must specifically address prevention of the typical collision modes observed in North American incidents.

3.3.1 Operational Environment and Service Needs

The U.S. has specific needs for operating passenger rail equipment which differ from those of many other countries. The UIC reports [44] that in 2005, passenger operation accounts for less than 0.6% of total traveled railroad miles in America. America accounts for only 1% of all passenger-miles traveled in the world, whereas, America accounts for nearly 38% of all tonne-miles traveled in the world. Since passenger rail travel in the U.S. accounts for such a small fraction of track use, the

establishment of dedicated passenger track is not economical and the use of shared track (mixed freight and passenger traffic) is inevitable. As a result, in terms evaluating passenger train crashworthiness, the worst threat is the scenario of a locomotive-led freight impacting a passenger car.

A second uniqueness of U.S. passenger rail service is the regular use of push-pull operation. Push-pull operation refers to the practice of running a train made up of a locomotive followed by passenger cars in two directions of travel without altering the orientation of the consist. The locomotive "pulls" the consist in one direction of travel and the locomotive "pushes" the consist in the other direction of travel. In pull-mode, a cab car serves as the passenger car, with a control stand at the end, in which the operator resides. In the U.S., 16 railroads operate in push-pull mode, which makes up nearly 65% of U.S. commuter rail service [14]. The second most common operating configuration for commuter passenger train service in the U.S. is MU service. An MU is a self-propelled railcar with passenger seats. An MU can be operated without a locomotive as a single unit or as a consist of MUs (typically as a pair or a triplet).

Approximately 8.3 billion commuter rail passenger miles are traveled annually in the U.S. and the number is increasing [14]. With freeways overcrowded, the price of fuel dramatically increasing and a growing sense of environmental awareness, many people are looking for alternatives to driving. As a result, most metropolitan areas, which are growing in both area and population, are looking to build or expand commuter rail service to their surrounding suburbs and neighboring cities. Examples include: development of a new commuter rail in Austin, Texas; an extension to existing Caltrans commuter rail in the Bay Area [45]; reopening

commuter rail lines in the Massachusetts Bay Transportation Authority (MBTA) [46]; construction of the first commuter rail line in Oregon (serving suburbs of Portland) known as the Washington County Commuter Rail Project [47]; and development of Northstar Commuter Rail Service between downtown Minneapolis to suburbs 40 miles away [48].

Cab car and MU locomotive-led trains present a challenging situation in collisions. The presence of passengers in the front or rear vehicle of a consist presents a mismatched contest in the event of a collision with a conventional locomotive. Conventional locomotives significantly outweigh passenger cars and locomotive end structures are built to meet higher strength requirements than passenger car end frames. In order to address this exposure, FRA has conducted research on strategies intended to improve the crashworthiness of cab cars and MU locomotives [7, 19, 49, 50, 51].

3.3.2 Existing Strength Requirements

According to federal regulations [4], cab cars, MU locomotives and conventional coach cars are required to support an 800,000-pound longitudinal static load applied at the buff stops without permanent deformation. This requirement assures a minimum strength of the vehicle's occupied volume. Buff stops are typically located about 6 feet from the end of the vehicle and support the compressive longitudinal loads applied through the coupler. Meeting this requirement using conventional design practices has resulted in structures that are nearly uniform in their axial strength. These structures are as strong at the ends as at the mid-length.

When a cab car, MU locomotive or a conventional coach car is loaded longitudinally, the structure of the vehicle's body is initially very stiff. When a critical

load is reached, local buckling occurs which indicates the body beginning to cripple. Once crippled, the vehicle's ability to further support a longitudinal load is compromised. As a result, a much lower load is required to continue longitudinal deformation of the vehicle body. When a longitudinal collision load is introduced to a train set, the car closest to the impact is typically the first to cripple. In a collision, a railcar that begins to crush in this manner will singularly absorb much of the collision energy as its occupied volume crushes. If the collision is extreme, this situation can result in the colliding vehicle being destroyed.

The development of CEM in the U.S. adds further safety benefits onto traditional railcar design practice. The 800,000-pound buff strength requirement, which dates back to the early 1900s, prescribes the strength of the main car body structure, which in turn, defines the strength of the occupant compartment. Crush zones are placed outboard of the buff stops and are intended to collapse at a lower load than the occupant strength. As a result, for North American railcars, the buff strength requirement dictates the maximum crush loads for a crush zone, which influences the amount of energy that is absorbed. Greater buff strength allows greater crushing forces to be supported, and likewise, greater energy can be absorbed for a given crush distance.

By controlling the structural crushing in the CEM zones of the trailing cars, occupant volumes can be preserved. Severity of the secondary impacts can be limited by managing the deceleration of the occupied volume with strategic modifications of the interior. For example, the use of rear-facing seats in CEM cab cars can limit the severity of the secondary impacts.

In CEM cab cars and MU locomotives, measures are required to provide protection for the train operator, who is located closest to the impact in a train-to-train collision. One alternative is to move the operator back from the end of the cab car/MU locomotive, inboard of the crush zone. Similar interior measures as used for the passengers can be used to protect the operator. Another alternative is to keep the operator at the end of the cab car/MU locomotive, ahead of the crush zone. In this alternative, the operator's cab is surrounded by a structure that can slide back as the energy dissipation elements are crushed. The area behind the operator is unoccupied but could be used as a utility closet for brake or electrical equipment. This arrangement allows for preservation of the operator's volume in the event of a collision but exposes the operator to higher deceleration than the passengers. To protect the operator in this arrangement, additional measures, such as seatbelts, airbags, or other inflatable structures, may be necessary.

3.3.3 Observed Collision Modes

Typically, for conventional North American passenger rail equipment, an impact may result in 1) uncontrolled haphazard crush, 2) override and/or 3) buckling between cars. These three modes are illustrated schematically in Figure 10. Each is undesirable events in the progression of a collision and decrease the likelihood of passengers to survive the collision.

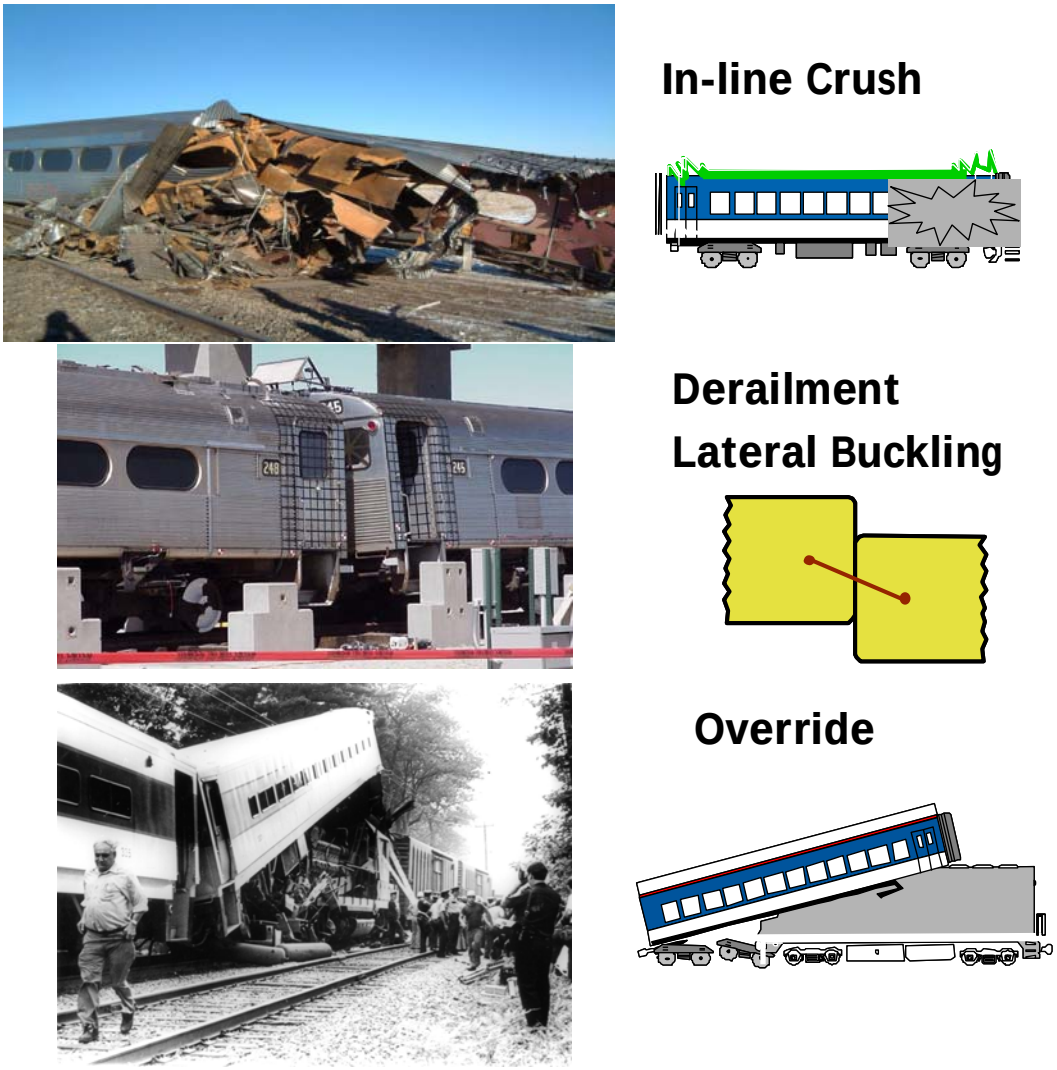

Figure 10. Observed collision modes

For conventional equipment structural damage tends to focus on the lead passenger railcar. North American passenger cars have historically been built with a strength-based design. Accident data, tests and analysis show that once a center sill has been compromised, crush is focused on that railcar in the train. In train-to-train collisions the lead car typically experiences the brunt of the impact and intrusion into the occupant compartment is highest at the cars nearest the impact. Crush zones can distribute the crush throughout the train, rather than focusing the damage on a single car.

Override is often associated with substantial loss of occupant volume and consequent fatalities. During a collision, as the underframe of a railcar is loaded, analysis from full-scale testing and observations from accident investigations show that the haphazard deformation of a conventional railcar underframe can create a mechanism for override. Figure 11 shows the progressive collapse of an example underframe from a single level conventional passenger railcar [52]. As a single conventional car deforms, the shape and position (below the center of gravity of the car) of the deformed underframe can serve as a catapult in a collision for an adjacent railcar, causing an override situation. CEM designs that collapse in a controlled manner will prevent the haphazard and unpredictable crush shown below. Additionally, CEM features can be designed to engage the impacting equipment to further prevent vertical motions.

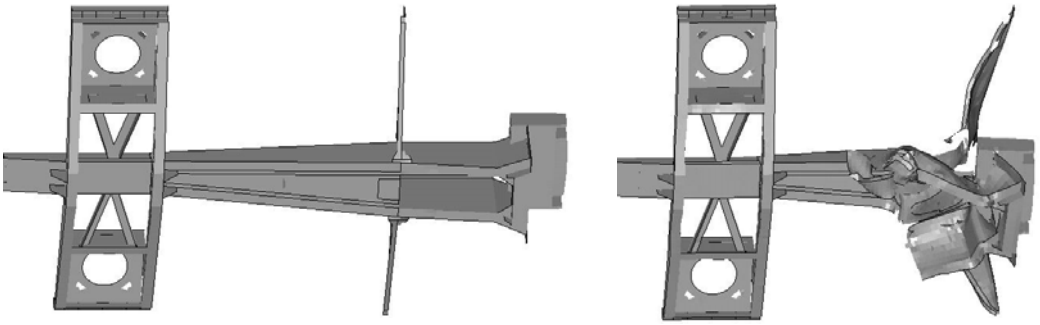

Figure 11. Schematic of conventional draft sill pre- and post-impact

The third undesirable collision mode is buckling between cars. A traditional coupler acts as an essentially rigid link between the cars. In a collision where there are high longitudinal forces present as the cars rapidly decelerate, a small lateral perturbation can cause the cars to become misaligned. When misaligned, the large longitudinal force transferred through the coupler places a lateral force on the adjacent car. Such behavior not only leads to derailment, but can propagate

throughout the length of a train and large scale buckling may occur in the formation of an accordion-like zigzagging pattern between cars. As the cars pile up, side impacts are more likely. Figure 6 shows an example incident in which the progression of severe lateral displacements can be observed. Lateral buckling and derailment in the first few cars progresses into saw-tooth buckling toward the back of the consist. Since passenger cars are, apart from the door structure, typically weak along the sides, the passenger compartment is particularly vulnerable in side-impacts. Crashworthiness features that reduce the potential for vertical and lateral motions are critical in preventing buckling modes during a collision.

3.4 PROTOTYPE CEM DESIGNS

There are two important performance differences between conventional and CEM designs. CEM cars can more efficiently absorb collision energy and crush is transferred to the following cars in a train rather than being concentrated exclusively on the lead car. A variety of CEM designs exist around the world to address unique operating environments. The prototype design described in this section was designed to address the operating environment in North American passenger rail travel which includes frequent mixed traffic of freight and passenger operation, many operating configurations, and push-pull operation. Full-scale test results of this equipment are described in Chapter 5.

The CEM design developed for these tests is intended to absorb at least 2.5 million ft-lb in the first three feet of the end structure [18]. This dissipation is accomplished by the controlled crush of three primary components: the pushback coupler/draft gear assembly, primary energy absorbers and the roof absorbers.

The CEM design developed for these tests is characterized by a collection of trigger mechanisms supported by crushable elements. Figure 12 is a cross section taken from a finite element model developed for analysis of the CEM system during design. This schematic identifies the primary components and the layout of the system. The first set of bolts shear at a prescribed load, allowing the coupler/draft gear assembly to slide back and crush an aluminum honeycomb module. When the coupler has receded longitudinally inside the bellmouth and reached its full stroke, the load is then transferred to the anti-telescoping plate and the end beam via the anti-climber. A second series of shear bolts act as a fuse for the sill, which slides back into the underframe causing the end frame to crush the primary energy absorbers. Simultaneously, rivets fail in shear, triggering the collapse of the roof absorbers which crushes additional aluminum honeycomb modules.

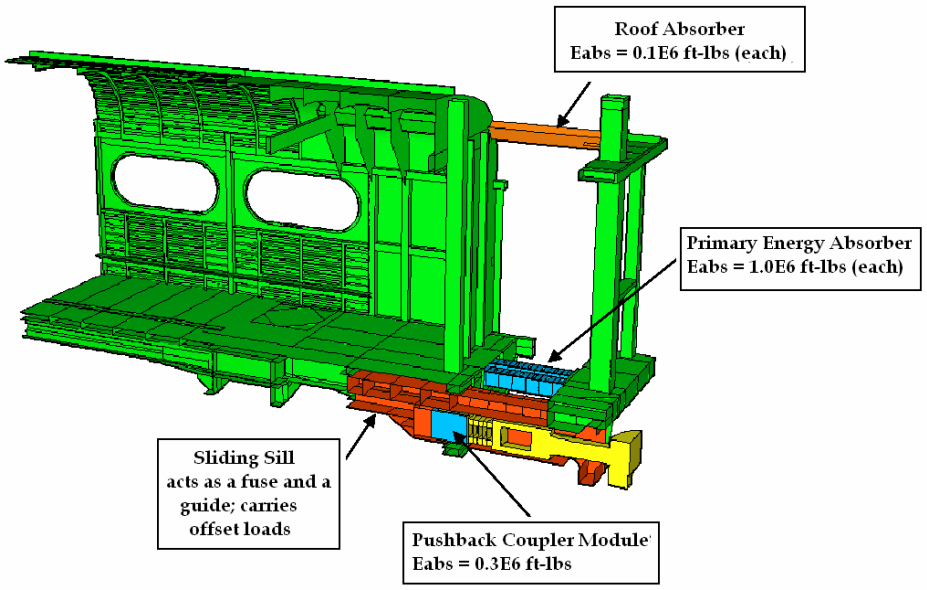

Figure 12. Cross section of the prototype CEM coach car design

The end structure has a multi-tiered load path, allowing for service loads and collision loads to be accommodated separately. Low-level service loads are absorbed by the elastic deformation of the conventional draft gear and the pushback feature of the coupler can absorb higher service loads. The primary energy absorbers are activated only when this system is exhausted, as in a collision condition. This feature ensures the integrity of the crush zone by preventing the primary energy absorbers from being inadvertently triggered during daily operation.

The prototype design crush zones were designed in two phases: a coach end crush zone and a cab end crush zone. Idealized force-crush characteristics are shown in Figure 13 for the two designs. Both designs include the same main components, pushback couplers and primary energy absorbers. The cab car additionally includes a pushback coupler with a longer stroke to accommodate an impact with a conventional coupler, a deformable anti-climber integrated into the end frame design to engage an impacting locomotive and an operator's cage to preserve the space for the operator.

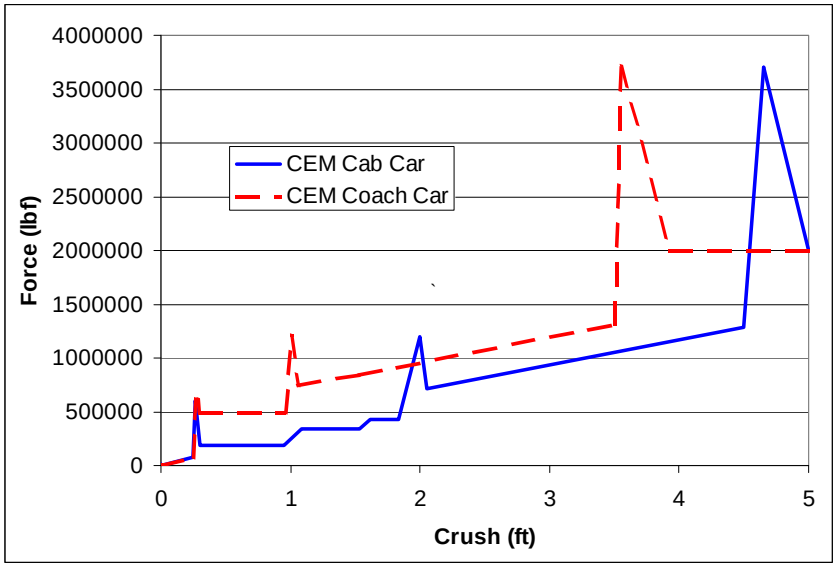

Figure 13. Idealized CEM force-crush characteristics

Figure 14 shows an image of the prototype cab car crush zone design. The activation of the pushback coupler initiates the crush zone. When the coupler triggers and pushes back, an energy absorbing element crushes. The travel of the shear-back mechanism accommodates the coupler of the impacting equipment to the extent necessary for the anti-climber and integrated end frame to engage the impacting equipment appropriately.

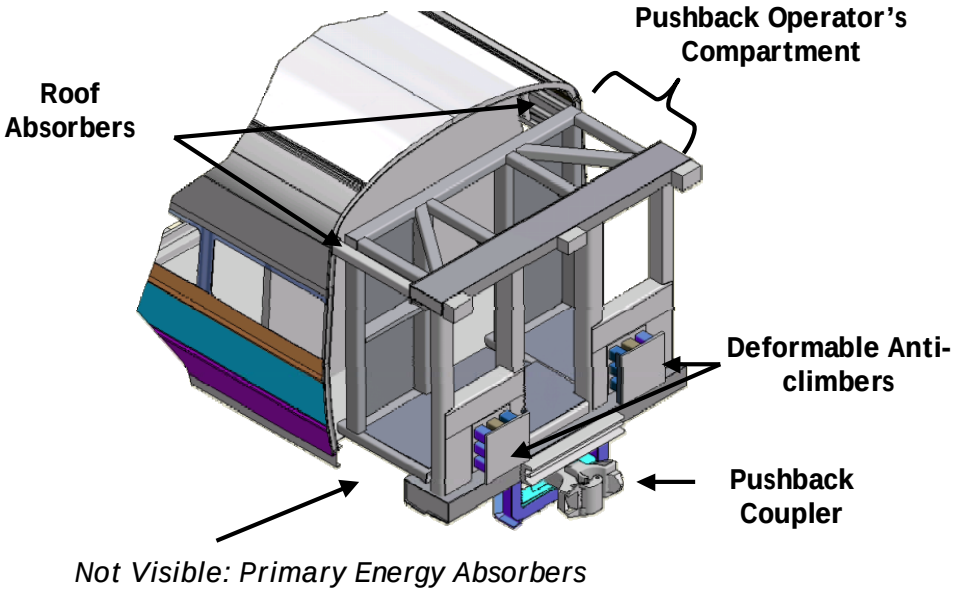

Figure 14. Prototype CEM coach car design

As the anti-climber begins to deform it incorporates the geometry of the locomotive and distributes the load over as large an area on the integrated end frame as can be reasonably achieved. The collision posts carry about 60% of the crushable anti-climber loads and the corner posts about 40%. The anti-climber is designed to crush in a controlled manner to avoid forming a ramp or a catapult by limiting the potential for material failure. The anti-climber can sustain off-center impact loads and transmit longitudinal loads into the end frame.

The integrated end frame is designed to remain sufficiently stiff in transmitting the impact load to the energy absorbers to assure the proper functioning of these elements. The integrated end frame can appropriately trigger and allow crushing of the energy absorbers when the coupler and the anti-climber share the impact load, or when the load path is through only the coupler or the crushable anti-climber. The structure attached for assuring survival volume of the operator can be pushed straight back into space normally taken by electrical and/or brake service closets. The expected structural deformation does not interfere with ready egress from the operator's compartment before and after the design crush zone stroke has been exhausted. The structure allows for the operator's seat to be attached with sufficient security to remain attached during the test. (Means of protecting the operator from the expected decelerations are currently being explored, including the use of inflatable structures and placement of the operator's compartment behind the crush zone.)

When the integrated end-frame is subject to a high-energy impact load, the cab car crush zone deforms in a controlled manner, activating both the roof and primary energy absorbers. The energy absorbers are able to properly function while accommodating the deflections of the integrated end frame. These devices can absorb more than two million foot-pounds of energy.

A conventional car body structure, between the two body bolsters (i.e., the sub-floor structures at each end of the car that provide support for the suspension), is sufficient to support the loads from the cab car crush zone as it crushes over its design stroke. The cab car crush zone design was developed for retrofit onto an existing M1 car.

Figure 15A shows the target force/crush characteristic used in the design of the cab car crush zone and the five states that define the prescribed sequence of events. Figure 15B illustrates the corresponding kinematics of the cab car crush zone design during an impact with a conventional locomotive. Initially the couplers meet in state 1. The stroke of the draft gear is eventually exhausted and the load increases on the structural fuse which then releases in state 2. In state 3, the anti-climber is also engaged, and the load is shared between the anti-climber and the coupler. When the combined load on the coupler and anti-climber is sufficient, the energy absorber structural fuse releases in state 4. The primary and roof absorbers crush and reach state 5 when their stroke is exhausted.

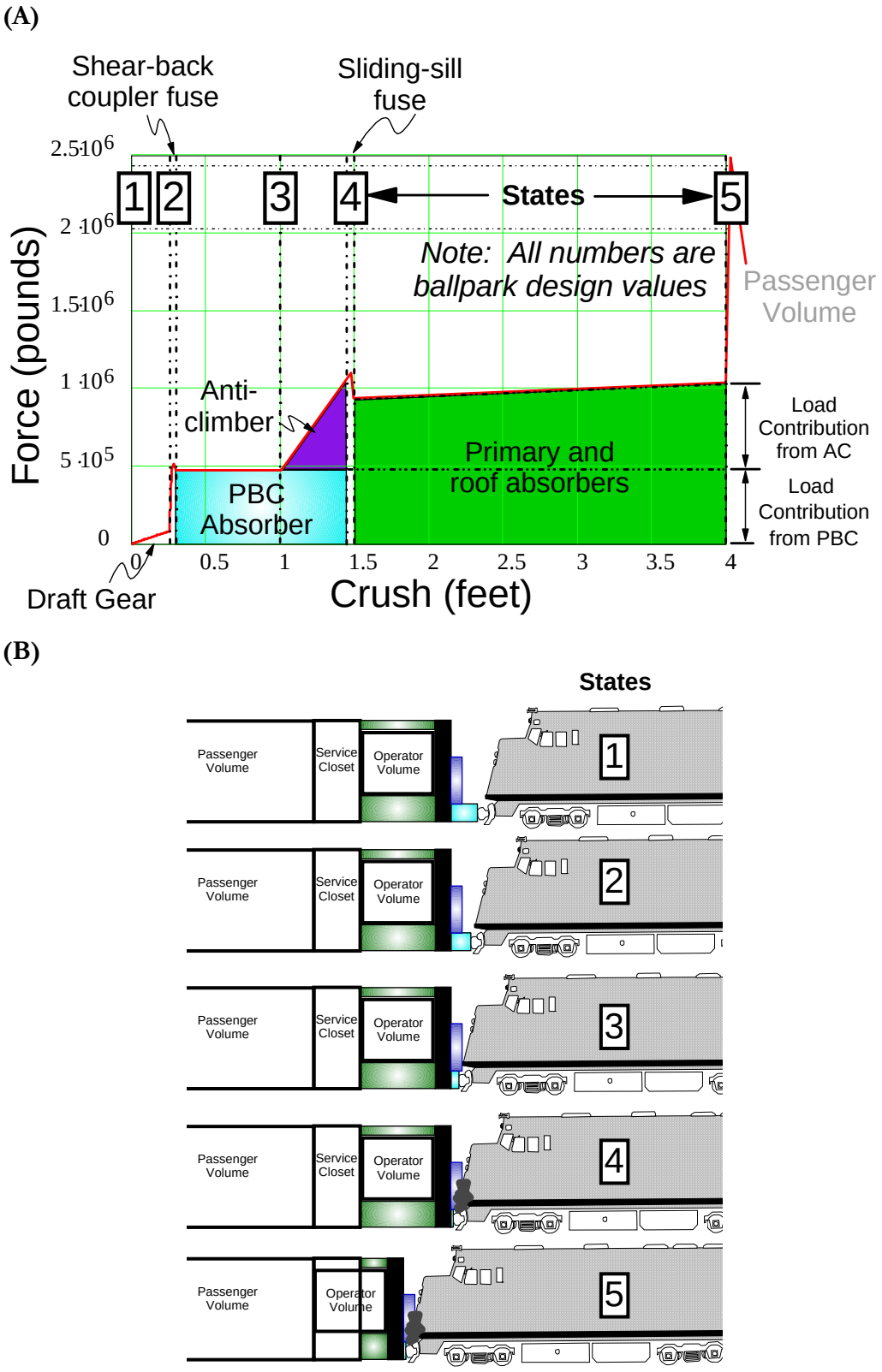

Figure 15. Cab car CEM design requirements: (A) idealized force-crush characteristic and (B) the desired collision kinematics

The cab car crush zone is designed to function for a range of initial conditions, including lateral and vertical misalignments of the colliding bodies of up to 3 inches, pitch and yaw of the cab car body of up to 0.4 degrees and pitch and yaw of the colliding locomotive of up to 0.5 degrees. These limits correspond to an end-to-end difference in elevation of approximately 6 inches for both the cab car and the locomotive.

3.5 MODELING NEEDS

Collision dynamics models were used to prepare for the full-scale tests of the prototype equipment. One-dimensional models were used to determine the instrumentation and the target impact speed. The models were used to predict the gross motions and the estimates of longitudinal crush of each car end. Additionally, for the single car and two-car tests, a model was developed which included a multi-body lumped parameter representation of each crush zone. These models were used to evaluate the sequence of events within each crush zone, but provided limited information about the three-dimensional motions of the cars.

The overall objective of this work is to simulate the three-dimensional motions of CEM equipment in a train-to-train impact. This objective will be accomplished with a three-dimensional collision dynamics model using a commercial software package for simulating dynamic mechanical systems. The model is developed in three incremental stages: a single car model, a two-car model and a train-to-train model. The results of each model will be compared with complementary results from the full-scale tests of CEM passenger rail equipment.

A single car model will establish the multi-body configuration to be used for each passenger car. The railcar mass is divided into sub-systems: two trucks, a crush zone on each end and the car body between crush zones. Each body is defined with inertial properties and connected by springs that represent each component's structural stiffness or suspension characteristics. Various connecting joints approximate the appropriate multi-dimensional movement between each rigid body and constraints are applied to account for additional limitations of degrees-of-freedom. The truck sub-system and connections to car body allow the car body to pitch, bounce and yaw relative to the trucks. Force-displacement characteristics define the primary and secondary suspension between the car body and the trucks. Derailment characteristics are applied between the truck/wheel set and the track. The three-dimensional capabilities of the model are tested by applying initial lateral perturbations and comparing the motions to those measured in the single-car test data.

The two-car model builds upon the single-car model by developing coupled connections between two railcars. The coupler connection allows for vertical, lateral and rotational motion between the two cars. The bellmouth structure is approximated so that the appropriate constraints are applied to the coupler swing for a conventional coupler. Joints are constructed so that lateral buckling of the railcars can be simulated when an initial lateral perturbation is applied.

The train-to-train model is constructed from the two-car model. The moving consist is a set of the multi-mass coupled cars. The stationary consist is constructed of simplified lumped-mass cars. The train-to-train model is compared to the full-scale test data for agreement. The full-train model will be used as an investigative

tool of specific events of the train-to-train test. Future uses of this model include investigation of oblique impact conditions on a CEM train and evaluation of future CEM designs.

4 COLLISION DYNAMICS MODELING

Collision dynamics models have been used to estimate the train-level and car-level performance of CEM equipment in the series of in-line full-scale tests conducted by the FRA [10, 11, 35]. The full-scale tests were conducted for idealized in-line conditions. For in-line conditions, the predominant force is longitudinal. Simplified lumped mass, one-dimensional collision dynamics models are valuable tools for estimating the longitudinal crush and gross motions. For the series of CEM tests conducted by the FRA, the longitudinal gross motions of the train and crush of each car were predicted with close agreement to the CEM test results. While CEM is designed to help keep the train on the tracks in a collision and promote controlled collapse of unoccupied areas of the train, some details of the full-scale tests have prompted the need for further investigation into the train and car body motions in three-dimensions. The goal of the three-dimensional model is to evaluate the limits for which the train does not remain in-line and on the tracks. A three-dimensional model provides a tool for investigating train collision behavior on curved track and for oblique collisions.

4.1 MODELING STRATEGY

The strategy for building the three-dimensional model follows the full-scale testing approach of incrementally evaluating a train-to-train collision through a series full-scale tests. The model was developed using the same software, solver, subroutine implementation and principles as the one-dimensional models developed for the FRA full-scale tests [6, 7, 2, 1]. The model was developed in three stages: a single-car model to validate the features of the car and trucks; a two-car model to

develop the coupled connection and validate the car-to-car interactions; and a train-to-train model to validate the full-train behavior. Comparisons with the full-scale tests were used to verify key features of the model (results are presented in Chapter 6).

The targets of the model developed for this thesis include capturing the three-dimensional motions of the train, each car and its set of trucks. An analytical model was developed in which each car is represented with multiple masses, each with six degrees of freedom. Joints are used to constrain kinematics between various parts as necessary to represent structural and mechanical connections. Non-linear springs connect the masses and individual spring characteristics define the relative structural displacements and deformations between each mass. The features of the model include a representation of a wheel-to-rail interaction including a derailment characteristic, three-dimensional truck suspension, three-dimensional coupler swing, and crush of each component in the crush zones.

While the impact forces in an in-line train-collision are initially predominantly longitudinal, the introduction of vertical or lateral forces can cause significant out-of-line motions. A railcar's geometry can be described in the most simplified representation, as shown in Figure 16, as a long slender object. If the large longitudinal forces present in a collision are slightly offset vertically or laterally, significant vertical or lateral motions may develop, such as override or lateral buckling between cars. For example, as two coupled cars begin to experience a lateral displacement of a few inches, a lateral force develops. A large load applied to a small displacement for a long slender geometry causes a significant moment. A displacement of a few inches between cars can lead to a large moment applied to an

85-foot passenger car, and can result in lateral buckling between cars. Furthermore, as the car-to-car lateral buckling progresses down the length of a train, sawtooth lateral buckling may occur. In sawtooth buckling the railcars pile up in an accordion-like pattern, during which car-to-car side impacts are likely. To prevent such collision events, it is important to investigate the initiation of lateral buckling between cars.

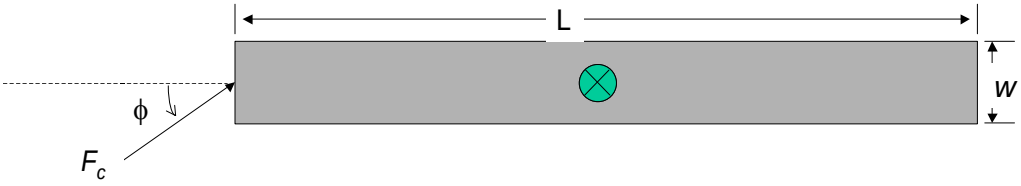

Figure 16. Free body diagram of simplified railcar geometry with diagonal force applied

An important modeling feature for investigating lateral buckling is the detail of the coupler connection. A typical coupler connection between cars has three degrees of freedom: pitch, yaw and longitudinal translation. These motions are limited by the coupler housing and mechanical connections.

To investigate out-of-line motions some representation of wheel-to-rail motions must be captured. Because of the wheel and rail geometries, as the lateral forces build up between the wheel and the rail, the potential of the car to lift off of the rail increases [53]. Derailment is represented in the model terms of lateral truck forces.

Additional features in the model include a multi-mass representation of each railcar. During collision conditions, vertical motions cause the car body and trucks to lift off the rail. Mechanical stops keep the trucks attached to the car body, but as the trucks lift off the rail, they experience three-dimensional motions (in particular, pitching) separate from the car body.

4.1.1 Single Car Model Description

A multi-body representation of a single car with crush zones and trucks is shown in Figure 17. The single-car model developed in this first stage is subsequently used to represent each car in the passenger train consist. The nonlinear spring characteristics are easily varied by editing an input file.

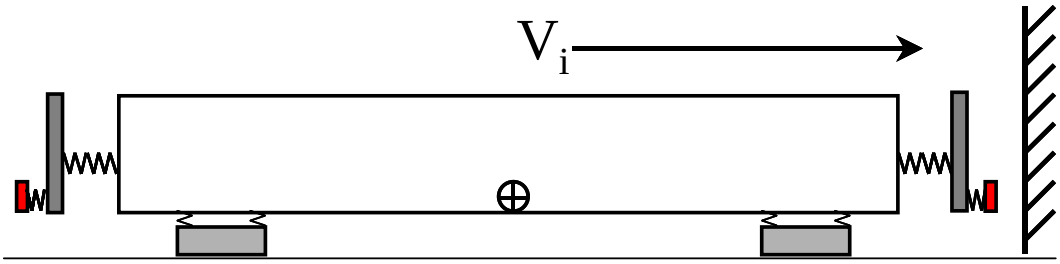

Figure 17. Schematic of a simplified spring-mass representation of a CEM railcar impacting a fixed barrier

The railcar is broken into smaller lumped-mass sub-systems (i.e. main car body, individual components of the crush zone, trucks) connected by springs to represent their structural stiffness or suspension characteristics. Various connecting joints allow for the appropriate multi-dimensional movement between each rigid body. Constraints are applied to simulate structural limitations. Point-to-point impact forces are tuned to classify the interaction of colliding surfaces. From this three-dimensional model, the gross motions of each rigid body can be produced for any set of initial conditions. Additionally, the crush distribution and sequence of events, both within each crush zone and at each crush zone can be simulated.

The pushback coupler is shown by the small red mass at the outermost end of railcar and is the first component to contact the wall during an impact. The dark grey mass represents the end frame and sliding structure of the crush zone. The long slender white box represents the main car body mass. The car body center of gravity (CG) is located at the longitudinal and lateral center of the car about 5.2 feet above

top of rail (TOR). The longitudinal mass-spring series is 85 feet long from car end-to-car end. The coupler extends past the end frame and has a force-deformation characteristic appropriate for the known pushback coupler. Each component of the crush zone is assumed to stay in-line and crush longitudinally. Translational joints are used to constrain the motions as such.

The collision dynamics model was developed using Adams™, a commercial software package used for building mechanical systems and solving them under dynamic conditions [54]. For this case, a collision scenario is developed along with approximate geometry of rigid bodies, connections, contact forces and initial conditions using Adams™/View. A user-defined FORTRAN subroutine is called by the Adams™/Solver to calculate forces at each time increment. The subroutine accesses a data file containing known spring characteristics for the non-linear springs used to represent the structures of the railcar intended to crush for prescribed loads in a collision. The subroutine then calculates the loading and unloading of each spring over the duration of the simulation, which in turn is fed back into the model. Contact forces define interactions between colliding bodies. Joints appropriately constrain DOF between rigid bodies. Each model takes less than five minutes to run a one-second interval of the impact scenario with a time step of 0.0005 seconds. The crush events occur in the first 0.25 seconds for the single car and two-car impacts and in less than one second for the train-to-train collision.

The test car used in the single car test, which had previously been stripped of all electrical equipment, seats and interior panels weighed approximately 75,000 pounds (including the trucks). As shown in Figure 17, the single-car model is a system of masses and springs that represent the motions and interactions of selected

components of a railcar in relation to the wall and ground. The inertial properties of each lumped-mass are listed in Table 2 for the baseline model of the single car test. The car body and truck properties were measured prior to the full-scale test. The crush zone and pushback coupler properties were estimated from the fabrication drawings and material properties.

Table 2. Baseline multi-body CEM railcar inertial properties

Property	***Car body***	***Crush Zone***	***Pushback Coupler***	***Truck***
Mass (lb)	35,590	6,000	638	13,000
Centroidal Roll (lb-ft^2)	9.67E5	6.8E5	2.03E2	7.23E3
Centroidal Pitch (lb-ft^2)	2.22E7	4.6E5	1.72E2	7.23E4
Centroidal Yaw (lb-ft^2)	2.245E7	2.55E5	50	7.23E4

The force-crush curves for each spring are shown in Figure 18. The combination of spring characteristics represents the forces required to deform the structure of the CEM coach car crush zone during an impact. The composite force-crush characteristics are described in the preceding chapters and are shown in Figure 13. The component characteristics permits the contribution of each component to be simulated in the overall performance of the cab car crush zone. This layout provides for varying load applications (at the coupler only, at the end frame only, etc.) to be evaluated.

(A)

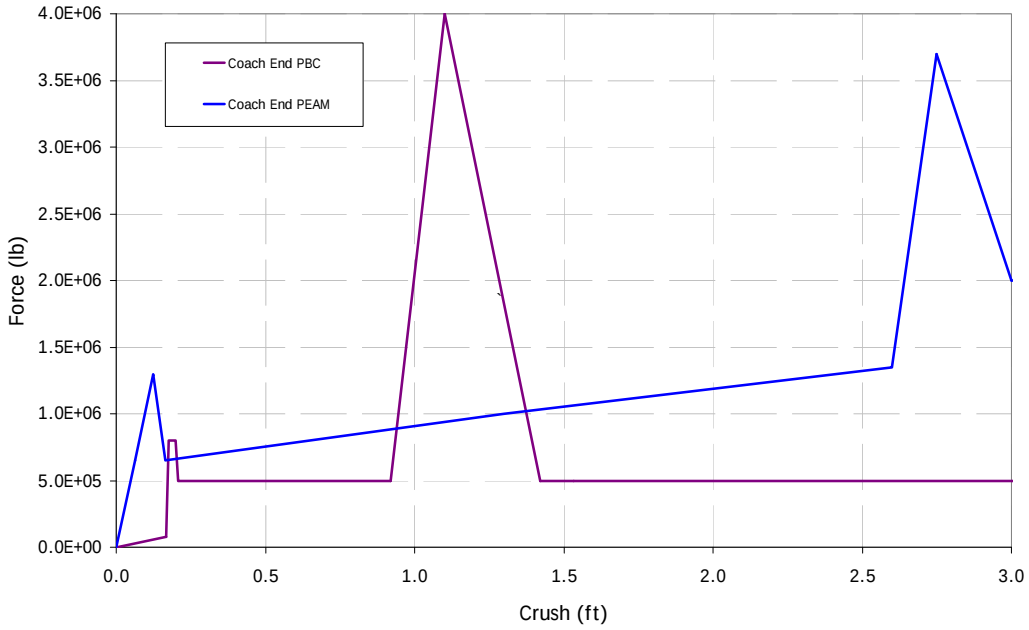

(B)

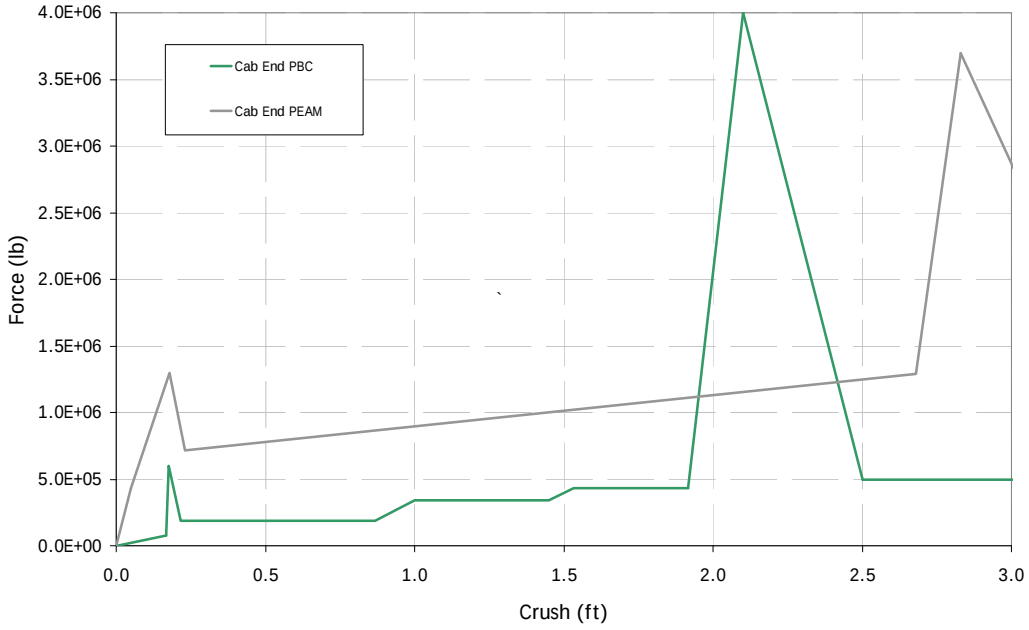

Figure 18. Force-crush characteristics for each crush zone component in the (A) coach car and (B) cab car

4.1.1.1 Truck and Track Connections

The two trucks are each modeled as independent masses from the car body. The dynamic interaction between the car body and trucks are defined through non-

linear spring characteristics. The arrangements of joints simulate appropriate constraints of the mechanical connections. Trucks are able to pitch, yaw and translate vertically through connections with the car body. Representing the truck-to-car body and truck-to-track interaction is critical for investigating the likelihood of derailment.

Figure 19 shows a schematic representation of the connections used to constrain the motions appropriately between the car body, truck and rails. The bottom edge of the car body is seen at the top of the schematic. Below the car body there are three parts used to represent the truck: the primary truck, which includes inertia properties of a truck, and two dummy masses for which mass is neglected. A dummy pivot part connects to the car body by a cylindrical joint and connects to the truck part by a revolute joint. This allows the truck to pitch and yaw relative to the car body.

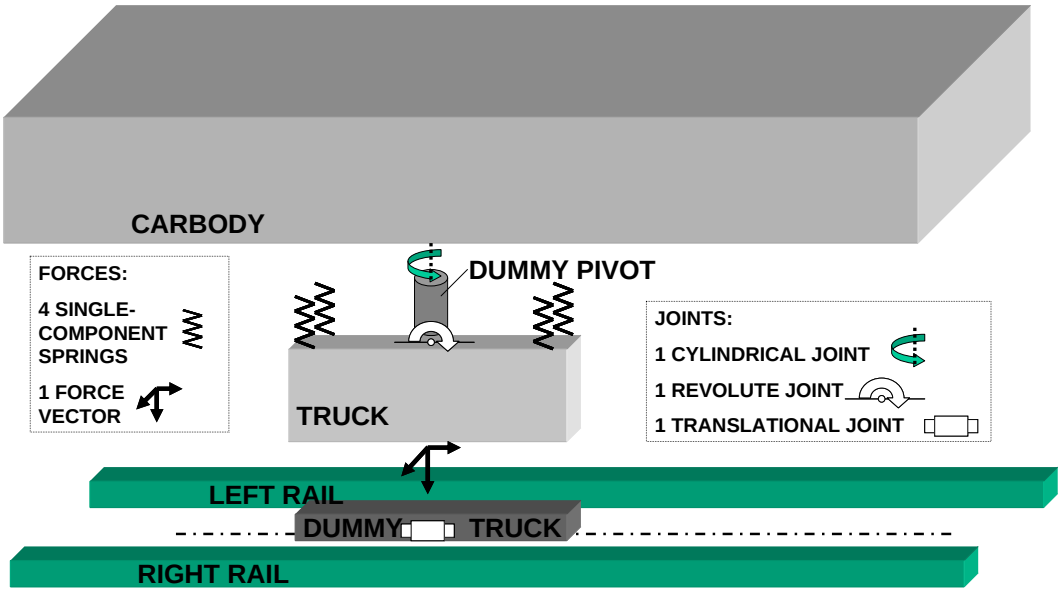

Figure 19. Schematic of joints between the car body, truck and rail

The suspension to the car body is represented by four forces connected with a vertical orientation at the corners of the trucks. A function was defined to apply the

tension and compression forces associated with the secondary suspension and simulate the mechanical stops present when the suspension reaches full extension or bottoms out. Appendix A shows details of the derailment characteristic.

The trucks are constrained to follow the rails using a dummy mass and a point-to-curve constraint. The dummy mass is forced to follow the indicated centerline of the two rails. This arrangement of parts and connections allows the truck to move along the track and transmit longitudinal, lateral and vertical forces. In typical operation, a wheel set moves laterally between the rails approximately +/- 2 inches. For these small displacements, lateral forces are transmitted between the truck mass and dummy mass as the dummy truck part moves along the tracks. Under high lateral forces, the truck can derail. A ratio of L/V is used as an approximation for estimating derailment, in which L is the lateral force and V is the vertical force (i.e. the weight of the railcar and trucks) between the wheel and the rail. The general industry estimate says that when L/V = 1, derailment begins to occur [53]. In the model, for greater than two inches of lateral displacement, the lateral load becomes constant and artificially high, indicating the wheel set dragging on the ties or ground with a high coefficient of friction. Appendix A shows further details of the developed function and test cases showing a simulated derailment condition. This model is not designed to determine an exact derailment or the collision events once derailment occurs. The truck-to-rail connections are intended to measure the loads transferred between the wheel set and the rail and provide an indication of large lateral loads, which may indicate a derailment event.

4.1.1.2 Contact Forces

A plane-to-plane contact force is activated when the coupler mass first contacts another rigid body. Parametric studies conducted by Severson [9] show that this value is rate-dependent and bounds the range of the impact parameters for similar impact conditions. The impact stiffness and damping coefficients are 7.0E+07 lb/ft and 2.0E+04 lb-s/ft, respectively. A second contact force is defined for the impact between the end frame and the wall. The impact stiffness and damping coefficients are 7.0E+07 lb/ft and 2.0E+04 lb-s/ft, respectively.

Additionally, a high coefficient of friction was added to the contact force to limit the vertical and lateral motion between the car and the wall. During the tests with the fixed barrier it was observed that although there was car body pitch, the end frame essentially "sticks" to the wall during the crushing of the end structure. In the CEM prototype design, the sliding sill in fixed sill mechanism used to allow pushback of the crush zone essentially prevents vertical and lateral motion of the car end.

4.1.2 Two-car Model Description

The two-car collision scenario is illustrated in Figure 20. The single-car from the single-car model was duplicated and translated 85 feet back so that the coupler masses are adjacent. In the single-car model the coupler was constrained to translate only in the longitudinal direction as pushback was the first event to occur and the swing and pitch of the coupler did not need to be represented. For the two-car scenario, the motions of the coupler are critical to evaluate the vertical and lateral motions of the car body, as well as the likelihood of lateral buckling. As described

earlier, the relative motions between cars can additionally increase the likelihood of derailment of one or both cars.

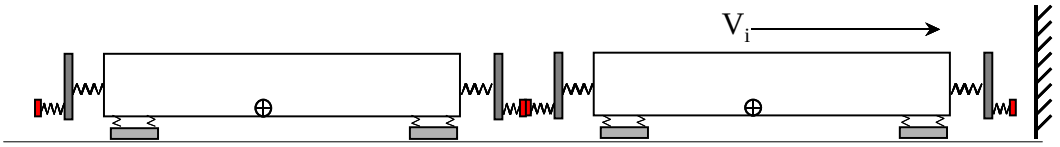

Figure 20. Schematic of spring-mass representation of a two coupled CEM railcars impacting a fixed barrier

4.1.2.1 Coupler Motions

The motions of the coupler and its connection to the railcar were modeled with a collection of masses and joints in order to allow for coupler pitch and swing, as well as translation in draft and when the coupler fuse has been triggered. The mass of the coupler is lumped into a single rigid body and connections to a dummy part of negligible mass allow the appropriate motions, while not over-constraining the model. Additionally, contact forces were used to represent the interaction with the coupler and the bellmouth, which limits the coupler pitch and swing. Figure 21 shows the connections between the railcar end structure, the dummy mass, the coupler and the coupled connection to the adjacent car's coupler. The coupler dummy mass is attached to the first car by a spherical joint, which constrains all translational motions and allows for all rotational motions. A nonlinear spring characteristic is connected between the main coupler mass and dummy mass and represents the load-deformation behavior of the fuse/pushback mechanism in the coupler. A translational joint connects these two masses and assures that pushback occurs in-line, as the pushback coupler is designed to occur. A fixed joint is used to represent the locking mechanism of an H-lock type coupler (allowable motions are negligible at this connection). The adjacent coupler is constructed identically. This

method of construction allows for ease of duplicating the cars and building trains, and minimizes the joints and contacts that must be connected between similar cars.

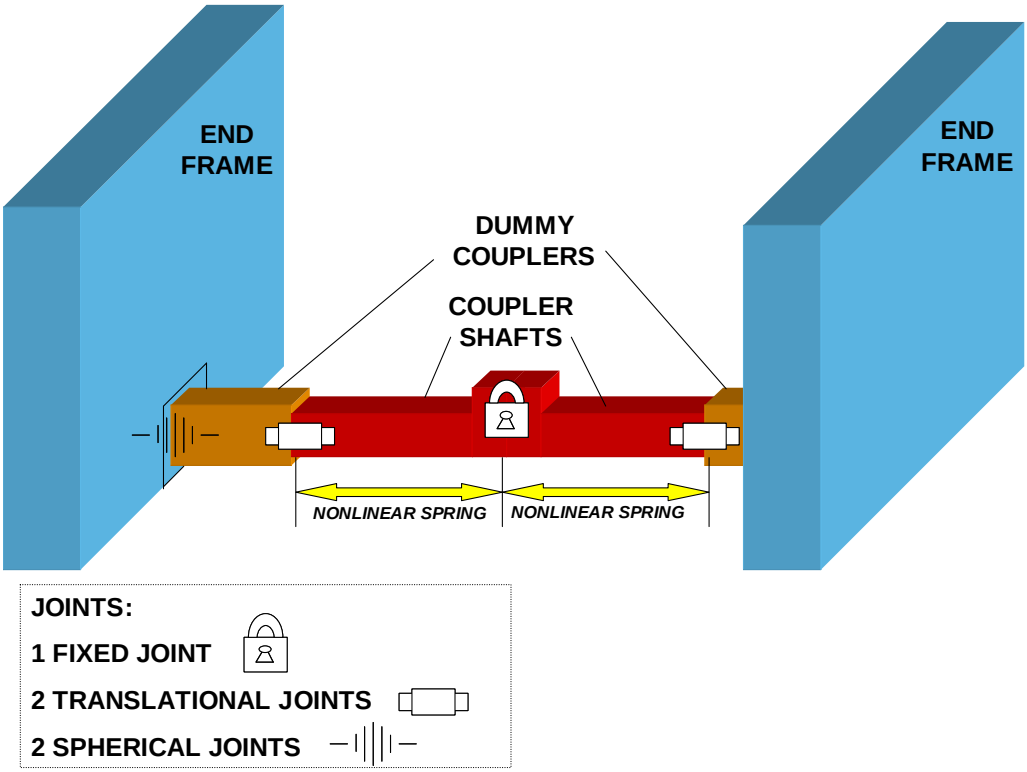

Figure 21. Schematic of the joints at a coupled interface

The coupler swing and pitch motions are limited by interaction with the surrounding structure. The maximum pitch and swing are about +/-7 degrees and +/-15 degrees. These limits were placed on the coupler by building geometry into the end frame/sliding sill part to represent the interior surfaces of the bellmouth. Figure 22 shows an image from the model. The outline of the bellmouth structure is shown in yellow and the end frame outline is in blue. The coupler (solid red and pink geometries) impacts the bellmouth at maximum swing and pitch limits. The dummy bellmouth structure is locked to the mass representing the end frame. Four sphere-to-sphere contact forces are defined to place upper and lower vertical and

lateral limits on the swing and pitch of the coupler. The details of these contacts are described in Appendix A.

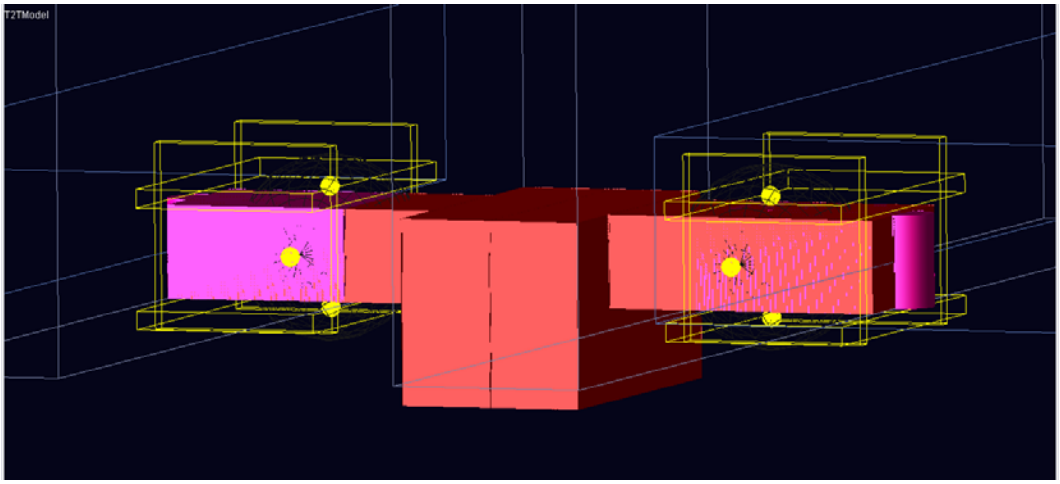

Figure 22. Image of the multi-mass coupler arrangement showing the coupler shaft (red and pink geometries) positioned in the bellmouth structure (outlined yellow geometry)

The fixed connection between mated couplers allows forces to be transmitted between cars during a simulation. In the case that a collision conditions cause the pushback coupler to be triggered and exhausted, the end frame of the coupled cars come into contact. Initially, a fairly rigid contact force was defined between end frames. Simulations showed that the end frames came into contact and rebounded off each other. The contact force was softened in order to prevent rebound and a large friction coefficient was added to simulate the fingered anti-climber protruding from each end frame which limits the vertical motion of the cars when the end frames come together.

4.1.3 Train-to-train Model Description

The train-to-train model was constructed from the cars developed in the two-car model. Features of the train-to-train model include coupled connections (with pushback and pitch and yaw), derailment representation, full suspension between

trucks and car body, potential of override between the impacting equipment. The details of the two-car model allow for the coupled cars to be duplicated and linked together with minimal connections to form a train. A single fixed joint locks the coupler masses together and a contact force is defined between the adjacent end frames of the coupled cars. Initially, baseline mass properties were used for the full-train to confirm the general functioning of the model. To validate the model with the results of the train-to-train test, individual mass properties were specified for the test equipment as well as force-crush characteristics for the known variations in each of the ten crush zones. These details are provided in Appendix A.

4.1.3.1 Standing Train

The train-to-train impact scenario is shown in Figure 23, below. The fixed barrier in the one- and two-car models was removed and a simplified representation of the standing train consist was developed. The mass of the standing consist is lumped into two locomotives. The two masses are linked by linear springs and their motions are constrained to translate in-line with the rails since no vertical or lateral motions are expected of this train for the given impact conditions. Typically, a wheel-to-rail coefficient of friction is around 0.2 for a train with emergency brakes applied. In the test, the handbrakes were applied to the standing train. During the test, the initially standing train traveled approximately 1,200 feet from the impact point. A coefficient of friction was defined at 0.05 to approximate the brakes on the standing train and the appropriate travel distance. The lead locomotive has the simplified geometry of a conventional coupler. Expected to be essentially rigid in comparison to the impacting passenger equipment, the force-crush behavior of the

locomotive is modeled as a relatively stiff linear spring, i.e. for these impact conditions there is less than two inches of crush experienced by the locomotive.

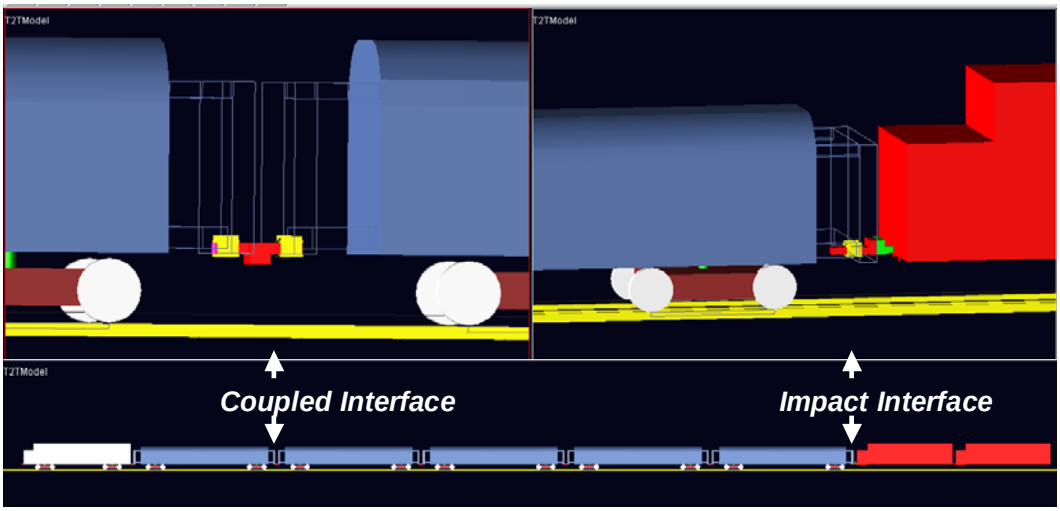

Figure 23. Schematic of three-dimensional train-to-train collision dynamics model

4.1.3.2 Impact Interface

Contact forces were defined at the locations of expected impacts between key structural elements of the locomotive and cab car. The initial impact occurs between the locomotive coupler and the cab car coupler. The secondary impact between structures occurs between the locomotive platform and the load distributor on the end frame structure. The impact stiffness and damping coefficients for these contact forces are 7.0E+07 lb/ft and 2.0E+04 lb-s/ft, respectively. Adams™ estimates surface-to-surface contact parameters based upon the shape and material properties of the impacting bodies. These values were adjusted to match the timing and peak acceleration values of full-scale test data. A high coefficient of friction is defined to simulate the engagement between the locomotive and load distributor, which is designed to prevent vertical motions that lead to override of the locomotive.

5 FULL-SCALE TESTS AND ANALYSES

As part of the FRA's Equipment Safety Research Program, a series of full-scale impact tests were conducted. The purpose of this program is to propose strategies for improving occupant protection under common impact conditions. The sequence of tests shown in Figure 24 allows the study of in-line collisions in increasing levels of complexity and produces a direct comparison between the crashworthiness performance of conventional passenger equipment to a modified design under similar collision conditions. The prototype CEM equipment demonstrated an achievable level of crashworthiness improvement over the current equipment.

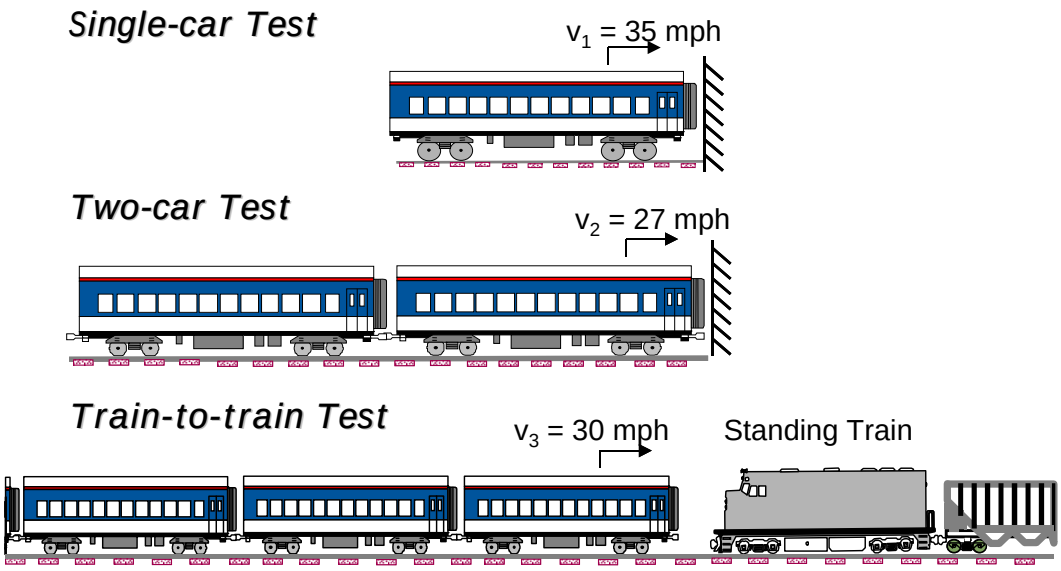

Figure 24. Schematics of the in-line full-scale impact tests

In the single-car test, the critical measurements are made to obtain a force-crush characteristic and to measure the gross motions of the test equipment. The two-car test adds consideration of the interactions of the coupled connection, i.e. measuring the vertical and lateral motions of the car respective to each other and observing the potential for sawtooth lateral buckling to occur. The train-to-train test focuses on

the interactions of the colliding equipment, i.e. how the equipment engages and the potential for override of the colliding vehicles. Additionally, the effects of the collision throughout the train are measured.

The completed conventional tests established the baseline performance of an existing fleet of single-level passenger rail equipment. The tests of the modified design (conventional cars retrofitted with CEM end structures) showed that all occupied space could be preserved under the same conditions as the conventional equipment.

Table 3 lists the key measurements made during each test. The italicized text in the two right columns summarizes the test results Table 3. The modified design enhances the crashworthiness performance of the passenger car by limiting the vertical and lateral motions of the vehicle and allocating crush to the designated crush zones at each end of the passenger cars.

Table 3. Test descriptions, critical measurements and outcome

Test Description	Critical Measurement	Results	
		Conventional Equipment	CEM Equipment
Single-car Test	Occupant volume	*Loss*	*Preserved*
	Force-crush characteristic	*Decreasing*	*Increasing*
	Mode of deformation	*Ramp*	*Controlled*
Two-car Test	Occupant volume	*Loss*	*Preserved*
	Interaction of coupled cars	*Sawtooth buckled*	*Remained in-line*
	Distribution of crush	*Focused on impact car*	*Distributed*
Train-to-train Test	Occupant volume	*Loss*	*Preserved*
	Colliding equipment interaction	*Override*	*Engagement*
	Distribution of crush	*Focused on impact car*	*Distributed*

For the CEM tests, a single coach car retrofitted with CEM end structures impacted a fixed barrier at 34.1 mph and two coupled coach cars retrofitted with CEM end structures impacted a fixed barrier at 29.3 mph. In the train-to-train test a CEM cab car, followed by four CEM coaches and a locomotive impacted a standing locomotive-leading train of equal mass. The following sections present the key results of each test and comparisons with the simplified collision dynamics models used to prepare for the tests.

5.1 SINGLE CAR TEST

The test of a single CEM coach car was conducted on December 3, 2003. During this test, a coach car retrofitted with a CEM end structure impacted a fixed barrier at 34.1 mph. The kinetic energy in the test was approximately 2.8 million ft-lb. The specific objectives for this impact test are as follows:

1) Measure the force-crush behavior of the end structure
2) Observe the primary modes of deformation
3) Measure the gross motions of the passenger car
4) Verify that the triggers and crushable elements perform/deform as designed

5.1.1 Crush

In the CEM single car test, the coach car crush zone was activated in the impact with the wall and crushed in a progressive and controlled manner, as designed. Crush was constrained to the first three feet of unoccupied space at the end of the test vehicle. For comparison, in the corresponding impact test of conventional equipment, the railcar crushed by approximately five feet. This demonstrates that

the CEM car is an incremental improvement over conventional equipment and that collision energy can be managed in a more efficient manner through the controlled collapse of structures to provide improved occupant protection.

The photographs in Figure 25 show three stills taken from high-speed cameras of the CEM and conventional tests. These shots depict the time at which 1) the end frame contacts the wall, 2) midway through the collision and 3) full penetration of the test vehicles.

As seen in the bottom half of Figure 25, the conventional car climbed the wall, causing the front truck to lift off the tracks. These significant lateral and vertical motions are a result of the multiple modes of deformation seen by the draft sill. By employing longitudinally crushable elements in the CEM design, the crush is engineered to remain in-line, which in turn reduces the vertical motion.

Figure 25. Sequential still photographs of CEM (top) and conventional (bottom) in the single car impact tests

The load path moved through the crush zone as predicted and triggered the crush of each of the energy absorbing mechanisms. Upon impact the load path

initially triggered the shear bolts of the pushback coupler, causing the coupler to slide into the underframe of the car end. The impact load then transferred to the buffer beam and anti-telescoping plate of the end frame, which initiated the primary energy absorbers and the roof absorbers.

Figure 26 shows the controlled collapse of the CEM design with the key components identified. The pushback coupler and sliding sill become neatly encased under the passenger compartment, allowing the primary energy absorbers to crush. For comparison, Figure 11 shows the conventional underframe counterpart. Its draft sill has multiple modes of deformation and crushes into a contorted shape. The post-test results indicate that the CEM design did perform as intended to allocate crush to specific zones.

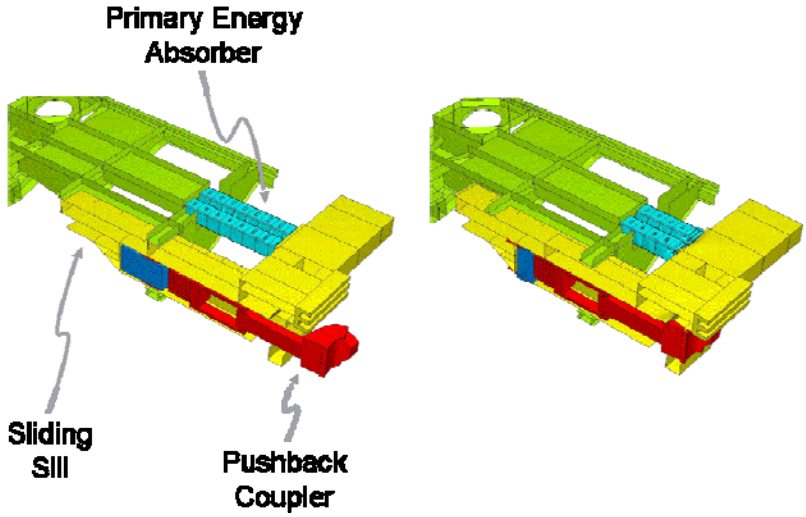

Figure 26. Image of the sub-floor CEM system pre- and post-impact

5.1.2 Gross Motions

Figure 27 compares the velocity-time histories of the collision dynamics model (dark blue dashed trace) and the test results (solid light blue trace). The plot shows good agreement between the model and test in terms of capturing the average

deceleration. The steep slope of the velocity plot shows the intensity and the timing of the collision. The CEM design completes crushing 3 feet in less than 120 milliseconds. This plot is an indication of the higher levels of acceleration in the CEM design in this test compared with the longer deceleration time in the conventional test [32].

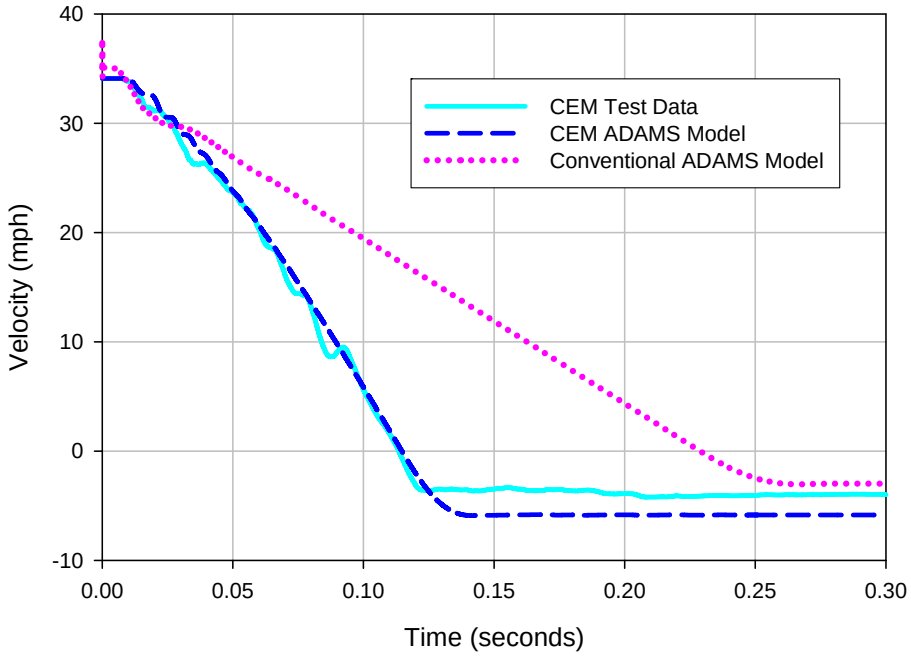

Figure 27. Single car impact velocity-time histories

5.2 TWO-CAR TEST

During the CEM two-car test the lead car crush zone was nearly exhausted, crushing 3 feet in less than 120 milliseconds. At the coupled interface, both pushback couplers failed, allowing the anti-climbers to engage and both crush zones to activate; the coupled interface crushed a total of 2 feet. Intrusion into the occupant volume was prevented and the vertical and lateral motions were limited. The three crush zones absorbed approximately 3.5 million ft-lb.

5.2.1 Crush

The photographs in Figure 28 compare the damage of the lead car in both the conventional and CEM tests. Using the trucks as a reference point in each photograph, the difference in the amount of structure crushed is easily compared. The conventional car impacted with the wall and climbed the wall as the car body crushed a total of 6 feet. The sill is the most significant structural member of the underframe and tends to deform gracelessly into a contorted mass of metal, causing uncontrolled crushing of the end. The conventional tests established that the draft sill can have varying modes of deformation under similar impact conditions [32]. Further, the uncontrolled crush of the draft sill at the base of the structure causes the car to climb the wall as it crushes.

Figure 28. Post-test photographs from the two-car impact test of the lead conventional (left) and CEM (right) vehicles

As shown in the photograph on the right of the CEM coach car, the lead car crushed a total of 3 feet, with controlled collapse of the crush zone. This measurement includes the crush of the coupler in the total crush measurement.

Each element of the crush zone is designed to crush in a controlled manner, which effectively limits the vertical and lateral motions of the car body during the impact. The CEM end structure collapsed in the prescribed series of events shown in Figure 9. The coupler initially impacted the wall, causing the bolts to shear at a load of approximately 600 kips and the honeycomb module to crush as the coupler slid back. The end frame was then loaded to approximately 1,300 kips, activating the trigger mechanisms in the sill and the roof absorbers. The primary energy absorbers and the roof absorbers subsequently crushed as the gap between the end frame and the vestibule wall/bolster diminished.

Crush was successfully passed to the coupled interface as the first crush zone collapsed. At approximately 60 milliseconds, both couplers triggered and began to recede into the underframe. The anti-climbers engaged as the end frames came together and load then passed into the crush zones of both ends. The load pulse through the two cars triggered the rear crush zone of the lead car slightly before the second car crush zone. The bolts of the sliding sills failed causing the primary energy absorbers to begin to crush as predicted. The primary energy absorbers of the trailing end of the lead car crushed a total of 10 inches. The second car's energy absorbers just began to crush, deforming approximately 1 inch.

5.2.2 Gross Motions

Figure 29 shows the final positions of the two cars during the conventional and CEM tests. During the conventional two-car test, sawtooth lateral buckling occurred at the coupled connection and the left track buckled under the lateral load. During the CEM two-car test the cars remained in-line relative to their mechanically allowable vertical and lateral variations of 3-5 inches. The lead vehicle in the

conventional test lifted approximately 6 inches off the track. The lead CEM vehicle lifted by about 2 inches.

Figure 29. Post-test photographs from the two-car test of the conventional (top) and CEM (bottom) coupled connections

Figure 30 shows an overhead view of the stills from the high-speed camera for the conventional and CEM tests. The first photograph shows the cars at the time of impact (indicated by the flash of light). Relative lateral offset of the cars is marked with white lines in the photographs. In both tests, at the time of impact the cars were offset laterally by approximately 1.5 inches. The second still shows the offset at the time of maximum crush for each test. Sawtooth lateral buckling occurred in the conventional test causing the rail to roll. As observed in the top photograph of

Figure 29, the cars rested approximately 13 inches out-of-line at the end of the collision. In contrast, the CEM test cars remained in-line as the coupler pushed back and the anti-climbers engaged (indicated by the dotted oval). The test shows that the controlled collapse of the crush zones effectively helps keep the cars inline.

Figure 30. Still photographs of the coupled interface in the conventional (top) and CEM (bottom) tests at time of impact (left) and maximum crush (right)

The one-dimensional collision dynamics model developed prior to these tests showed good agreement predicting the general crush distribution between the front end of the impacting car and the total crush at coupled interface. In the post-test analysis of the force-crush measurements it was observed that the average crush force of the primary energy absorbers had a slight upward slope. With this adjustment applied to the force-crush behavior of the primary energy absorbing spring element in the model, the gross motions were improved. After refining the

input force-crush behavior in the collision dynamics model, the velocity-time histories matched the deceleration rates more closely throughout the collision.

The two-car test verified the force-crush behavior observed in the single-car test, particularly that the primary energy absorbers require an increasing force to sustain crush. Understanding this behavior improved the overall agreement of the gross motions. With these changes all the important dynamic car body features were captured in both the single-car and two car tests. The detailed performance of the CEM components were observed and documented but not further evaluated with the simplified collision dynamics model.

Figure 31 shows the agreement of the model and test data in relation to the sequence of events. The lead car initially decelerates as the pushback coupler crushes. The change in slope indicates the initiation of crush in the primary energy absorbers of the lead crush zone. Crush at the coupled connection begins at approximately 60 milliseconds. The lead car then rebounds off the wall at around 150 milliseconds, but the trailing car continues moving forward and pins the lead car to the wall until it comes to a stop. The trailing car rebounds off the wall traveling at a higher speed than the lead car. This behavior differs from the corresponding velocity history of the conventional two-car test. In that case, the lead car begins to crush and the two cars decelerate together as a single mass [33].

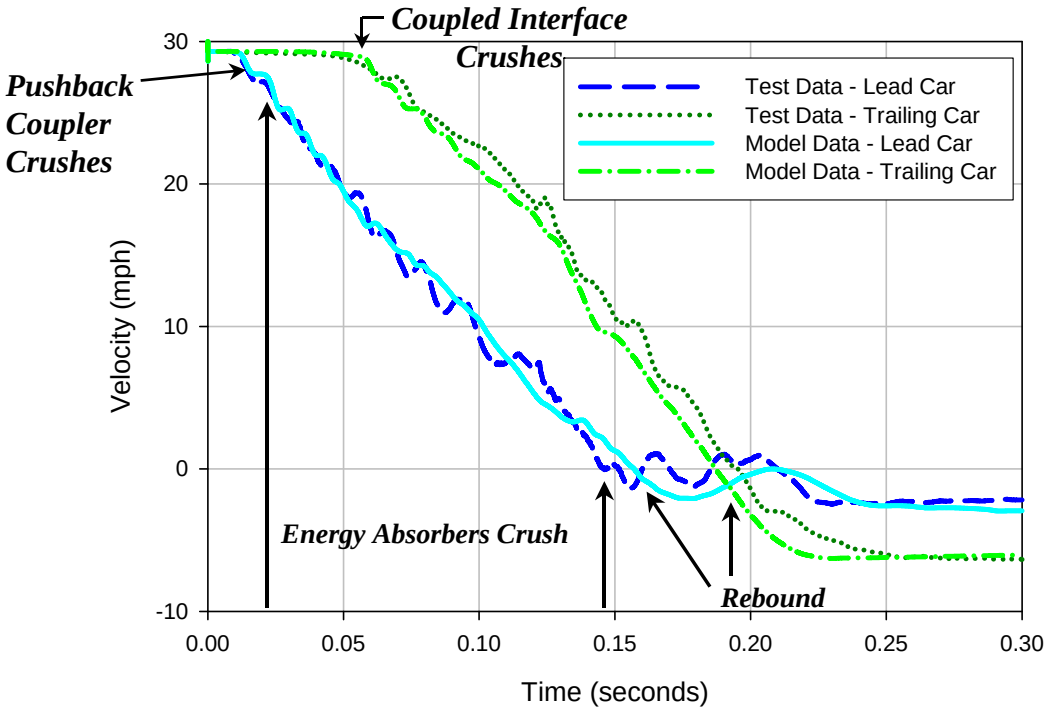

Figure 31. Two-car velocity plots

The velocity plot shows that the simplified multi-mass model captures proper timing of the initial crush of the pushback coupler, indicated by the matching initial slopes of the lead car. This model served the purpose of predicting overall crush distribution and the longitudinal car body gross motions. This test demonstrated that the CEM system could perform as intended and minimize the non-longitudinal motions observed in the conventional test.

5.3 TRAIN-TO-TRAIN TEST

The train-to-train test setup for CEM passenger equipment is shown in Figure 32. Each train weighed approximately 648,000 lb. The individual car weights are listed in Appendix A – Modeling Parameters.

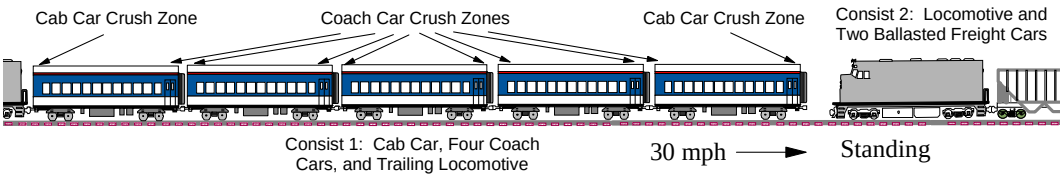

Figure 32. Schematic of CEM train-to-train test

5.3.1 Test Results

The train-to-train test provides crashworthiness performance results at three levels: train level, car level and component level. The train level performance is dependent upon the proper functioning of the system crush zones in order to achieve the required energy absorption and crush distribution through the train. The car-level collision behavior is dependent upon the performance of each component in the crush zone in order to achieve the desired kinematic sequence at each impact or coupled interface. The component level performance reflects upon design and manufacturing details. The test results of the train-to-train test are described in three levels in the following sections.

5.3.1.1 Train-level Results

In summary, overall comparison of the conventional train-to-train test to the CEM train-to-train test showed a marked improvement in occupant protection. In the conventional test there were 20 feet of crush of the lead cab car and override occurred between the passenger train and standing train.

Figure 33 shows results from the train-to-train tests of conventional and CEM equipment. In the conventional equipment test, structural crush was focused on the colliding cab car; there was negligible crush imparted to the trailing equipment. The space for the operator's seat and for approximately 47 passenger seats was lost. In the test of CEM equipment under the same collision conditions, there was no

intrusion into the operator or occupant compartments, crush was shared by unoccupied areas of each passenger car, no override of the impacting vehicles occurred and no derailment of the cars occurred. Comparison of train-level performance shows a more efficient management of the collision energy through controlled collapse of the unoccupied areas distributed throughout the length of the train.

Figure 33. Photographs of crush distribution in train-to-train tests of CEM (top) and conventional (bottom) equipment

5.3.1.2 Car-level Results

The principal functions of the cab and non-cab crush zones are to deform in a controlled manner while providing the appropriate force-crush characteristics to distribute crush. For the cab car crush zone, deforming in a controlled manner includes managing the impact interface to prevent override. There were three types of car-to-car interfaces in the test: the colliding interface between the impacting cab car and locomotive, the coupled interfaces between passenger cars and the coupled interface between the last passenger car and the trailing locomotive. Figure 34 is comprised of frames taken from a high speed movie of the interaction of the impacting cab car and locomotive. These frames show the kinematics of the cab car crush zone as it impacts the standing conventional locomotive. Initially the couplers met, in state 1. The stroke of the draft gear was eventually exhausted; the load increased on the structural fuse, which then released in state 2. In state 3, the deformable anti-climber was engaged, and the load was shared between the anti-climber and the coupler. When the combined load on the coupler and anti-climber

was sufficient, the energy absorber structural fuse releases in state 4. The primary and roof absorbers crush and reach state 5 when crush stops progressing and sufficient energy is absorbed at the impact interface. During the impact, there was little deformation of the locomotive; in essence the locomotive acted as if it were rigid.

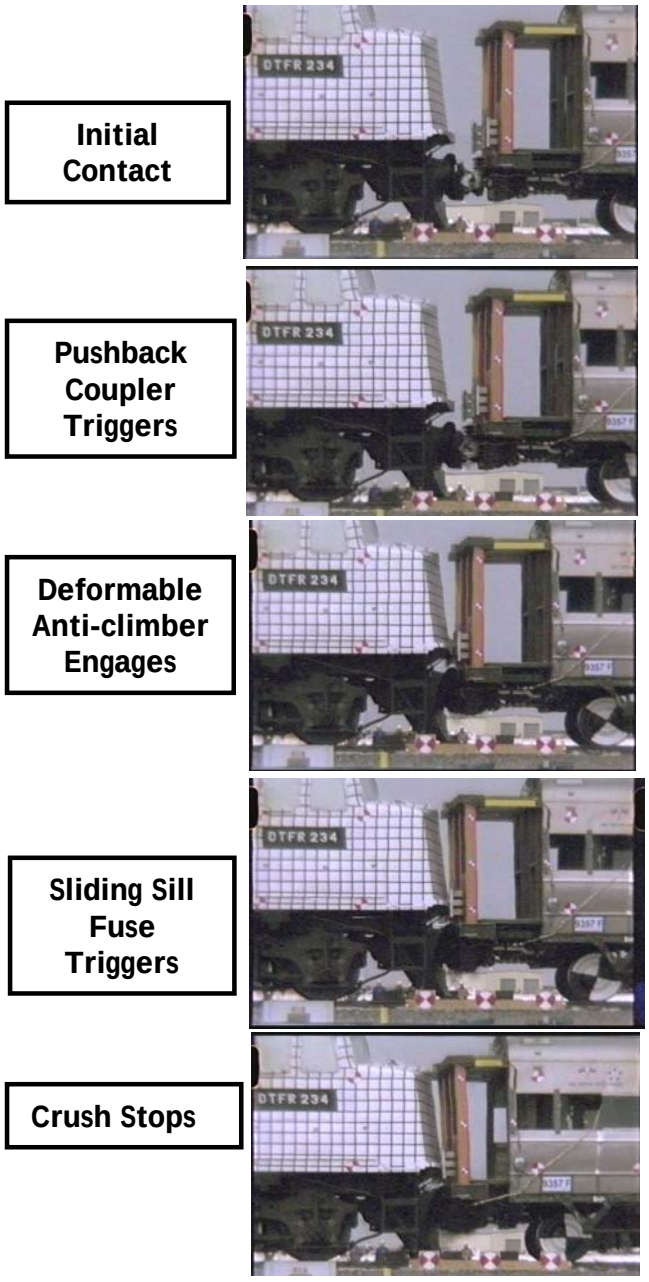

Figure 34. Sequential stills of the colliding interface showing the kinematics of impact crush zone

Figure 35 is comprised of frames taken from a high-speed movie of the interaction of two coupled passenger cars. These frames are representative of the kinematics of all of the coupled passenger car interfaces. Initially the cars were coupled, in state 1. The stroke of the draft gear was eventually exhausted, the load increased on the structural fuse, which then released in state 2. In state 3, the coupled end anti-climbers engaged, and the load was shared between the anti-climbers and the couplers. When the combined load on the coupler and anti-climber was sufficient, the energy absorber structural fuse released in state 4. The primary and roof absorbers crush and reach state 5 when crush stops progressing and sufficient energy is absorbed at the impact interface.

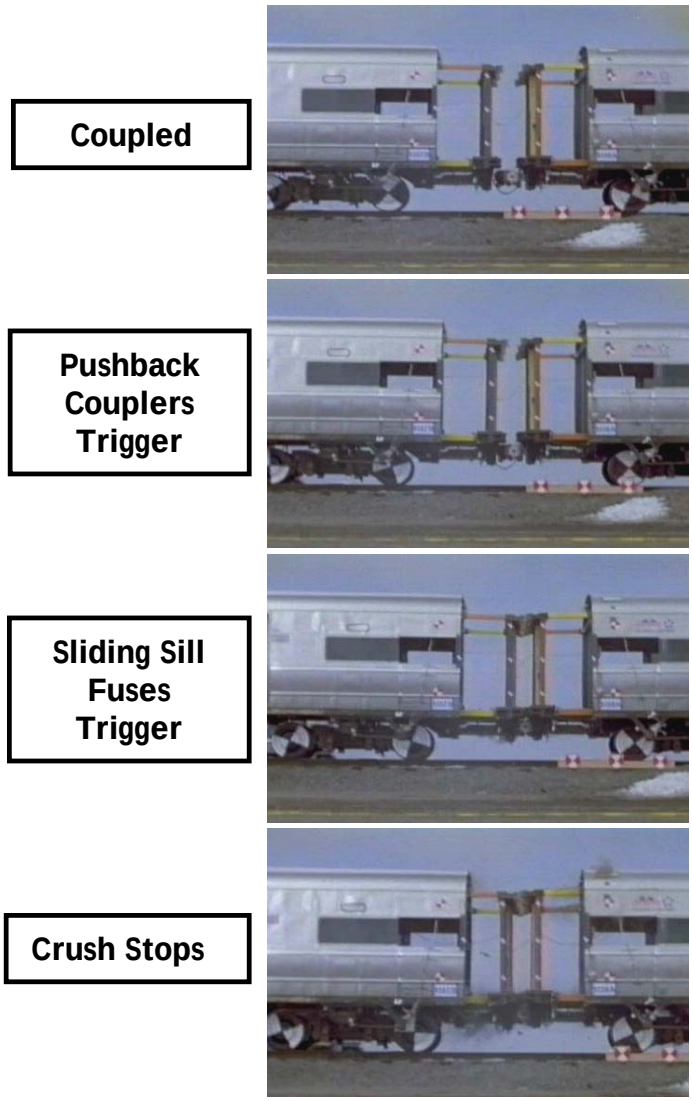

Figure 35. Sequential stills showing kinematics of coupled CEM coach cars

Figure 36 shows the kinematics of the trailing cab car crush zone coupled with the trailing conventional locomotive. The frames are from a high-speed movie taken with a camera mounted on board the trailing cab car. The cab car had a pushback coupler, while the locomotive had a conventional coupler arrangement. Since it was a cab car crush zone, the pushback coupler had sufficient stroke to accommodate a conventional coupler while allowing the ends of the coupled equipment to come together. The first frame shows this coupled interface shortly before the impact.

The middle frame shows the interface shortly after the pushback coupler has triggered. As can be seen in the middle frame, the centerlines of the cab car and locomotive are offset by about four inches. This offset grew from the initial impact until the pushback coupler shear bolts triggered. Once the shear bolts triggered, the offset remained but did not continue to grow. After the cab car and locomotive ends came together, the locomotive end began to crush in an uncontrolled manner. The uncontrolled crush increased the relative lateral displacement of the locomotive and the cab car. In addition, the uncontrolled crush of the locomotive caused the end of the locomotive to rise and the end of the cab car to be pushed down. This motion did not progress to override, but the associated non-longitudinal load into the support structure was sufficient to cause the failure of a few welds around the structures making up the end beam and a crack near the back of the end beam and the front of the sliding sill.

The final frame of Figure 36 shows the final position of the locomotive relative to the cab end crush zone at maximum crush. The rear end of the locomotive's skirt initially contacted the deformable anti-climber and the consequent lateral motion caused the locomotive to contact the collision posts. The integrated end frame accommodated this non-ideal loading condition and shed the load into the sliding sill, successfully triggering the sliding sill fuse.

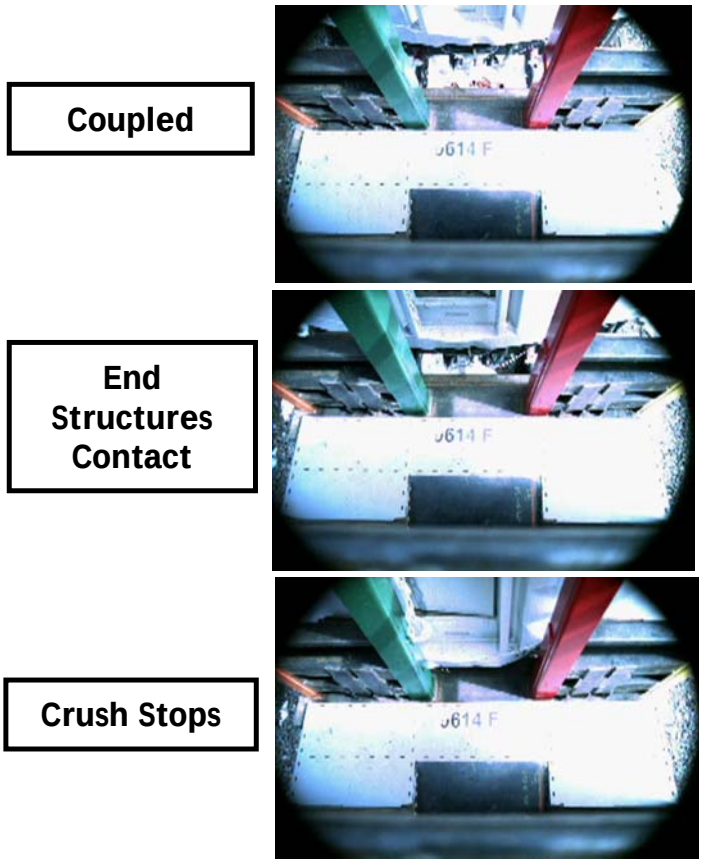

Figure 36. Stills showing kinematics of coupled cab and locomotive

5.3.1.3 Component-level Results

The cab and non-cab crush zone components functioned as designed. For several of the components, the test results suggest that the form of these components could be improved. Alternative designs could be developed which achieve the same function in a more aesthetically pleasing manner.

As shown in Figure 37, the primary energy absorbers exhibited material failure as a result of the test. This material failure did not influence the function of the energy absorbers during the test – they absorbed energy as intended. However, material failure is difficult to simulate with fidelity, and does increase the uncertainty in analytic predictions of the mode of deformation and the force/crush characteristic of the energy absorber design. For the test equipment, this uncertainty was reduced

by prior component, single-car, and two-car tests. A similar level of confidence in the force/crush characteristic of alternative designs may be achieved with fewer tests if material failure is not expected for such designs.

Figure 37. Post-test photograph of a primary energy absorber, showing material failure along the bottom folds of the crushing cells

The design development and performance of the deformable anti-climber suggests that material failure in the primary energy absorbers can be greatly reduced, and potentially eliminated. The deformable anti-climber also performed as designed, and, as shown in Figure 38, deformed as intended without any material failure. The deformable anti-climber was required to be able to support vertical and lateral loads that may arise from the interaction with the colliding locomotive. Consequently, the deformable anti-climber was required to deform without material failure in order to maintain the load path for any vertical and lateral loads. Key differences with the primary energy absorber include thinner, more ductile material, and annealing of the deformable components to relieve residual stresses from forming. Developing primary energy absorbers that incorporate these features would likely result in a design that is not as prone to material failure.

Figure 38. Post-test photograph of the deformable anti-climber, showing no material failure

As seen in accidents investigations, some of the cars uncoupled during the test. This occurred in the test due to the interaction of the coupler carrier and the coupler pin. As the coupler pushed back, the coupler carrier deformed in such a manner as to push the pin up, releasing the coupler. The couplers functioned as designed as long as there was a buff load between cars. Design modifications can prevent an unwanted uncoupling interaction between the coupler pin lifting mechanism and the coupler carrier. Additionally, there are alternative pin arrangements currently in service that are less prone to uncoupling than those used in the test.

The side sill of the M1 cars wrinkled during the test. (There was no visible permanent deformation of the center sills after the test.) While there was no measurable occupant volume lost, the form could be improved by eliminating the permanent deformation of the side sills. The side sills of the M1 cars are open channel sections. In the area where they wrinkled – just inboard of the reinforcements for the quarter point doorframes – the side sill was not attached to the body sheeting for about six inches. Elsewhere on the car, the side sills are spot welded approximately every inch. The wrinkling of the side sill could potentially be

eliminated by the addition of more spot welds, or by closing the cross section. Either approach would reduce the potential for column buckling.

The operator space was preserved, and there are no obvious improvements in form for the operator's compartment. The end frames for both the cab end and non-cab end crush zones performed as intended. These translated the loads applied to the car into the loads required to crush the primary and roof energy absorbers.

5.3.1.4 Other Events

A post-test autopsy was conducted as a more detailed inspection of the crush zone and its components [55]. The results identify a few events that occurred in the test that reflect upon detailed design issues and influenced the component level performance of the CEM design. Chapter 6 investigates the following events/topics:

- Cars uncoupled during pushback
- Uneven crush of PEAM
- Crush distribution pattern
- Asymmetric crush and loading of coupled cab car
- Crush of the coupled locomotive
- Makeup and configuration of the standing consist

5.3.2 Comparison of Analyses and Test Results

The following model results compare the test results to the one-dimensional pre-test model run with the appropriate test speed of 30.8 mph. Comparison of the results from the pre-test collision dynamics model and the test measurements show close agreement for the allocation of crush throughout the passenger train, gross motions of the car bodies and severity of the occupant environment.

5.3.2.1 Crush

The test results demonstrate that a CEM train can manage the collision energy by sharing the required energy absorption due to structural crush in a train-to-train test through multiple dedicated crush zones, and consequently prevent damage to the occupied areas of the cars. The initial kinetic energy of the collision was 20.5 million ft-lb. Each crush zone is designed to absorb at least 2.5 million ft-lb. Approximately 14 feet of crush was distributed among the crush zones. By deducting the stroke of the pushback couplers from the total crush, the total shortening of the cars or loss of space in the train is 5.7 feet.

Figure 39 shows the crush distribution for the cars in the CEM consist. Crush is shown at the lead end of the cab car and summed at each successive coupled interface. The test data represents the measurements of the string potentiometers for total stroke of a crush zone (i.e. the stroke of the pushback coupler and the car body energy absorbers).

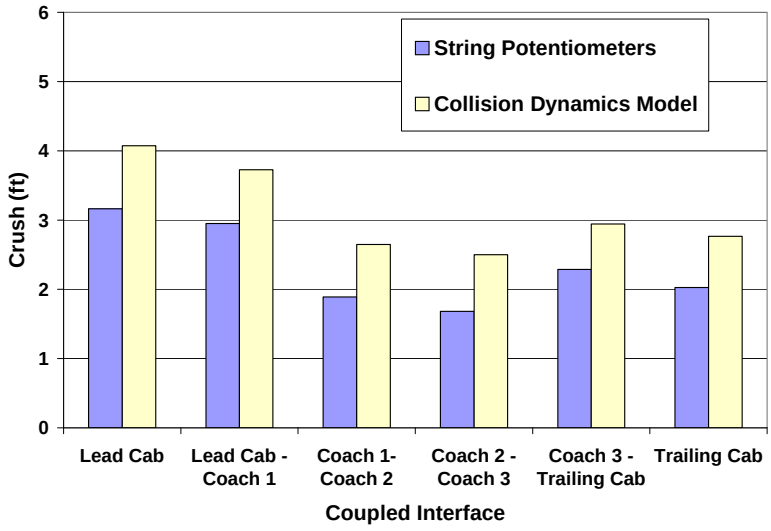

Figure 39. Train-to-train test crush distribution (summed at coupled interfaces)

In the train-to-train test of conventional equipment, the impacted end of the leading cab car crushed by approximately 22 feet and the impact end of the leading locomotive sustained minor structural damage. There was no other structural damage observed in the conventional coach cars of the passenger train. The cab car overrode the locomotive during the test. The force-crush characteristic of conventional passenger cars prevents the distribution of crush to successive cars. After a single high peak load is exceeded, the car continues to crush at a relatively low uniform load. The buckling of the primary longitudinal structural support, the draft sill progressed into ramp formation, which initiated override of the locomotive by the cab car (despite the cab car underframe beginning substantially lower than the locomotive underframe).

The crush distribution plot in Figure 39 shows how the crush was shared between the crush zones of the CEM consist. At the 30.8 mph impact speed, the crush zone of the lead cab car is crushed the most; crush is passed back to the following crush zones. Each car in the CEM system is characterized by an increasing, stepped force-crush behavior. When the force level on the first crush zone reaches the second step, and the primary energy absorbers crush, force levels also begin to be passed to the successive cars causing those crush zones to trigger. Because the pushback couplers trigger at a lower load than the primary energy absorbers, crush is distributed to additional crush zones before the third peak load level is exceeded at the lead crush zone.

The pushback couplers and sliding sills where triggered in every crush zone. The crush zone of the lead cab car came closest to being exhausted, but no crush

zone was completely exhausted. The residual crush in each crush zone allows for the CEM system be effective in a variety of collision scenarios.

The pre-test collision dynamics model captures the trend of crush distribution, but consistently overshoots the total crush at each interface. This is attributed to the material properties of the primary energy absorbers. The crush zones manufactured for the single-car and two-car tests of CEM equipment were a different order of steel than the ten crush zones manufactured for the train-to-train test. When a sample was tested, the material properties were found to be about 10% higher than the material specification. Accordingly, the average crush load of the PEAM would be higher than estimated by the idealized force-crush curves developed from the previous full-scale testing.

5.3.2.2 Gross Motions

Figure 40 shows the overlay of the test and model results for the velocity-time histories of each vehicle in the CEM passenger consist and the lead locomotive of the initially stationary freight consist. The red traces are the test measurements calculated from the accelerometers at the center of gravity of each vehicle. The blue traces are the corresponding model results. As the lead car impacts the freight consist and begins to crush, it slows rapidly. As the impact load travels through the passenger consist, each crush zone progressively triggers and crushes at a similar load, causing each successive car to slow down at a similar rate to the first car. The velocity trace of the initially standing locomotive is representative of the standing consist, as it sustained no damage during the train-to-train test and the three vehicles essentially moved as a single mass.

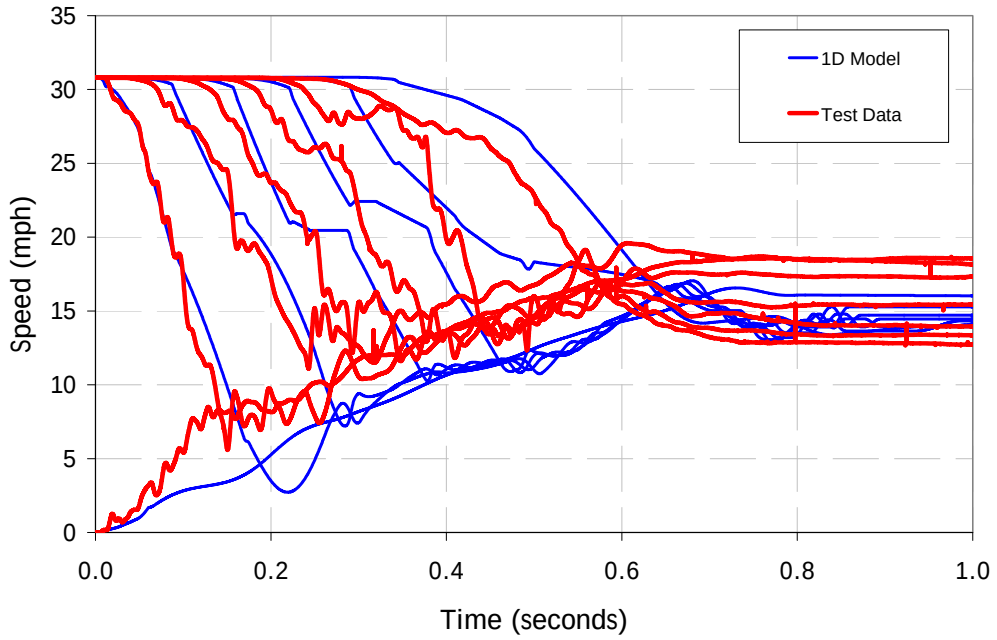

Figure 40. Velocity-time histories of each vehicle in the moving consist and lead locomotive in the initially standing consist

Overall, the model predictions agree with the test results. The crushing and decelerations of the collision are complete at 0.75 seconds and the passenger and freight consists are moving together down the tracks at approximately 15 mph. The decelerations of the first two cars in the CEM train show reasonable agreement with the test data, but the decelerations of the subsequent CEM cars do not agree as well. The model does not have good agreement between the acceleration of the initially standing locomotive. These issues will be addressed in Chapter 6.

6 THREE-DIMENSIONAL MODEL RESULTS

The three-dimensional CEM train-to-train model was developed in three stages. Results are presented in this chapter. Comparisons are made with the test data and simplified models. For the single car test, the three-dimensional model is validated by demonstrating agreement in overall energy absorption, crush and gross motions. The two-car model results are shown to agree with the test data in terms of crush, three-dimensional gross motions and behavior at the coupled connection. The model is used to identify the sequence of crush events for each crush zone and the resultant car body motions are explained in terms of these events. A full train of CEM cars is shown to be a useful tool in evaluating the train kinematics, the car-to-car interactions and individual crush zone component performance. Some modifications are made to improve the agreement with the test data. The more advanced features are demonstrated which were previously neglected in the pre-test train-to-train model. Finally, the model is used to investigate and explain selected details of the crush zone component performance observed in the train-to-train test.

6.1 SINGLE CAR MODEL COMPARISON

The single car model will be validated through comparisons with the test data. Gross motions, crush and event timing are used as metrics to evaluate the quality of the model. Once general agreement is established, modifications will be made to improve the agreement at a component level. Additionally, the three-dimensional features will be demonstrated.

The three-dimensional single-car model of a CEM railcar includes crush zones on both ends with pushback couplers, trucks with suspension and wheel-to-rail

forces to estimate derailment. Selected results are shown in this section for the model run with the single-car impact test conditions. Further details are in Appendix B. The key comparisons include the total crush values for each component in the crush zone, the longitudinal gross motions of the CG of the cars and the sequence of events within crush zone. Additionally, the vertical and lateral motions of the car and trucks are explained in the collision.

In the single-car impact test, a CEM railcar impacted the test wall at 34.1 mph. The crush zone was activated and crushed a total of about 3 feet. The draft gear accounted for about 3 inches of elastic stroke, the pushback coupler about 7-9 inches of stroke and the PEAM approximately 24 inches.

6.1.1 Force-crush Behavior

The force-crush behavior used in the model is an idealization of measured test data. Accelerometer data is used to estimate the force-crush behavior of a single car. Estimates of car body velocity and displacements are estimated by integrating the accelerometer data. This section shows that the acceleration and force comparisons with the model do not show good agreement for the detailed behavior, but the overall collision energy and average forces are within reasonable agreement. The next section demonstrates that the car body velocity-time histories show very good agreement and the model is useful for evaluating more detailed events during the collision.

Accelerometer data is used to measure the force-crush behavior in the full-scale test. The red trace in the top plot of Figure 41 shows the data of an accelerometer located at the longitudinal CG of the car body. This data is filtered according to SAE J211-1 standard for vehicle structural accelerations [56]. The

corresponding car body acceleration from the collision dynamics model is overlaid on the test data. The model average acceleration over the collision time is within 6% of the test data average acceleration, which is about 13 Gs.

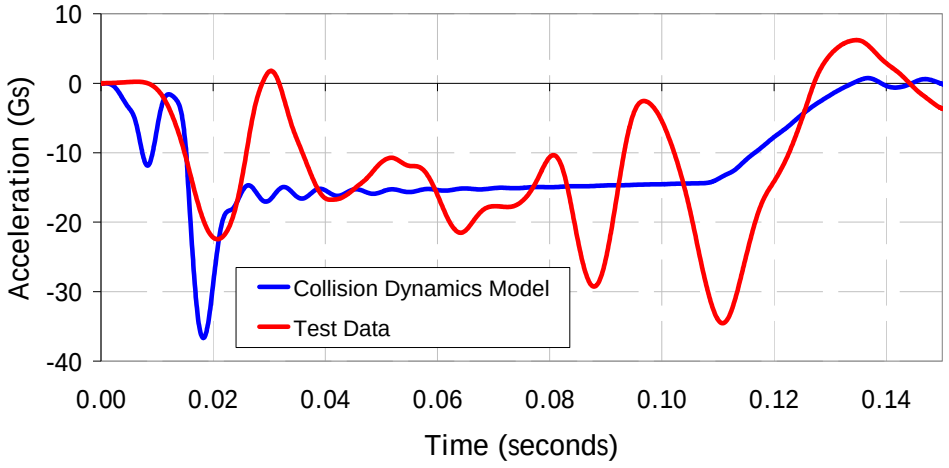

Figure 41. Single car test: car body CG accelerations

Accelerometer data is integrated twice over time to plot the displacement of the car body. The car body decelerations are multiplied by the mass of the vehicle to estimate the force on the wall during the collision [9]. The force and displacement data sets are cross-plotted to show the force-crush data shown in the red trace on the top plot of Figure 42. The idealized force-crush characteristic used as input in the model is plotted in black against this data. The idealized curve was developed from the finite element model used in the design of the CEM prototype crush zone. The bottom plot in Figure 42 shows the idealized curve and the FEA force-crush estimate. The salient features of the behavior can be identified with this comparison. The energy under the idealized curve is within 6% of the kinetic energy in the collision. Since the accelerations measured at the CG of the car body are a gross approximation of the rigid body car motion, the data is in reasonable agreement with

the lumped mass model. Likewise, the average force over the period of crush agrees with the average crush force known for the collapsible elements that make up the crush zone. The test data has an average force of 9.85E5 lb and the average crush load of the PEAM is about 1 million lb. The exact values of the peak forces are affected by the data processing, and the oscillations in the processed force data are an effect of the structure being dynamically loaded.

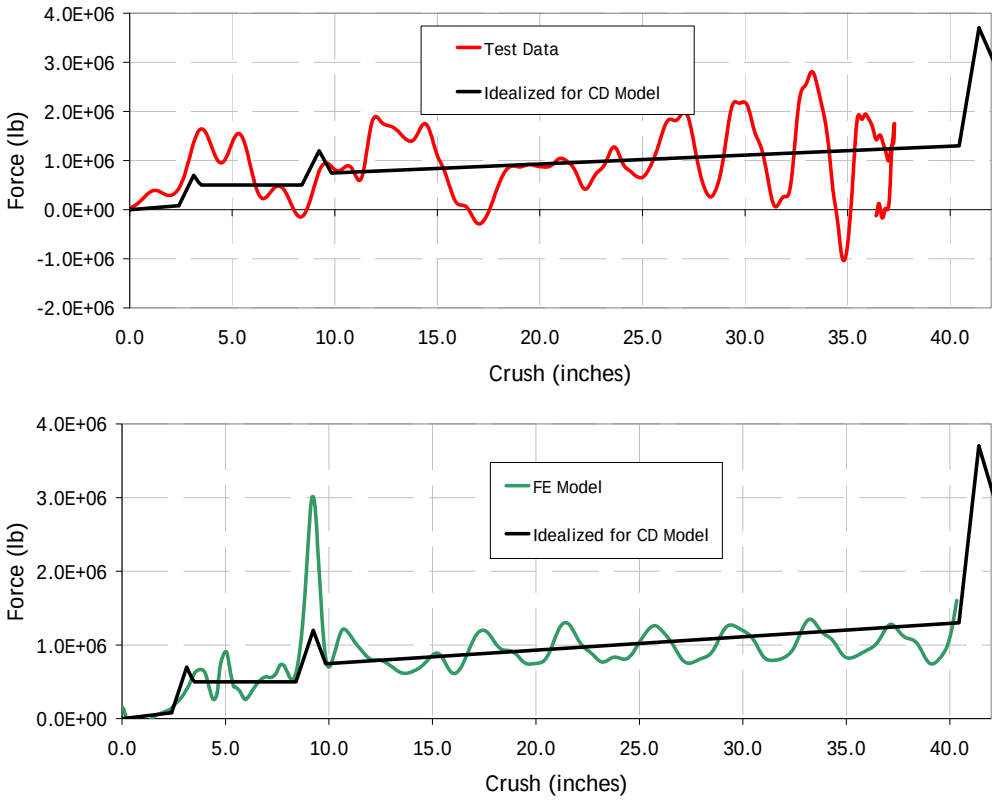

Figure 42. Comparison of the idealized force-crush characteristic to test data (top) and finite element model (bottom)

Figure 43 shows the force-crush of each component in the crush zone for the single car test scenario. In the model, the pushback coupler and the primary energy absorbers are modeled as separate mass-spring systems. The output of each component's force is cross-plotted against each component's spring displacement. The red trace shows the behavior of the draft gear and pushback coupler. In the

first three inches, the draft gear compresses. Next, the pushback coupler triggers, and the coupler absorbs energy as it crushes to its full stroke of about nine inches. The peak at the end of the pushback coupler characteristic indicates that the element has reached its full stroke (a hard physical stop at the base of the pushback coupler box). The blue trace shows the required force to activate and crush the crush zone inboard of the end frame. The initial peak represents the trigger force for activating the sliding sill. The primary energy absorbers and roof absorbers then crush at an average force of one million pounds, with a positively increasing slope on the crush load. A comparison of initial kinetic energy to energy absorbed through crush provides an indication of general agreement in the model and test data. The total energy absorbed by the crush zone represents the energy required to bring the test vehicle to rest from an initial speed of 34.1 mph. The kinetic energy in the test condition is estimated using the equation, $KE = \frac{1}{2}mv^2$, to be about 2.8 million ft-lb. The energy absorbed by the crush zone is estimated by integrating the area under the curves (since $E = \int Fdx$); the energy absorbed by the crush zones is about 2.6 million ft-lb.

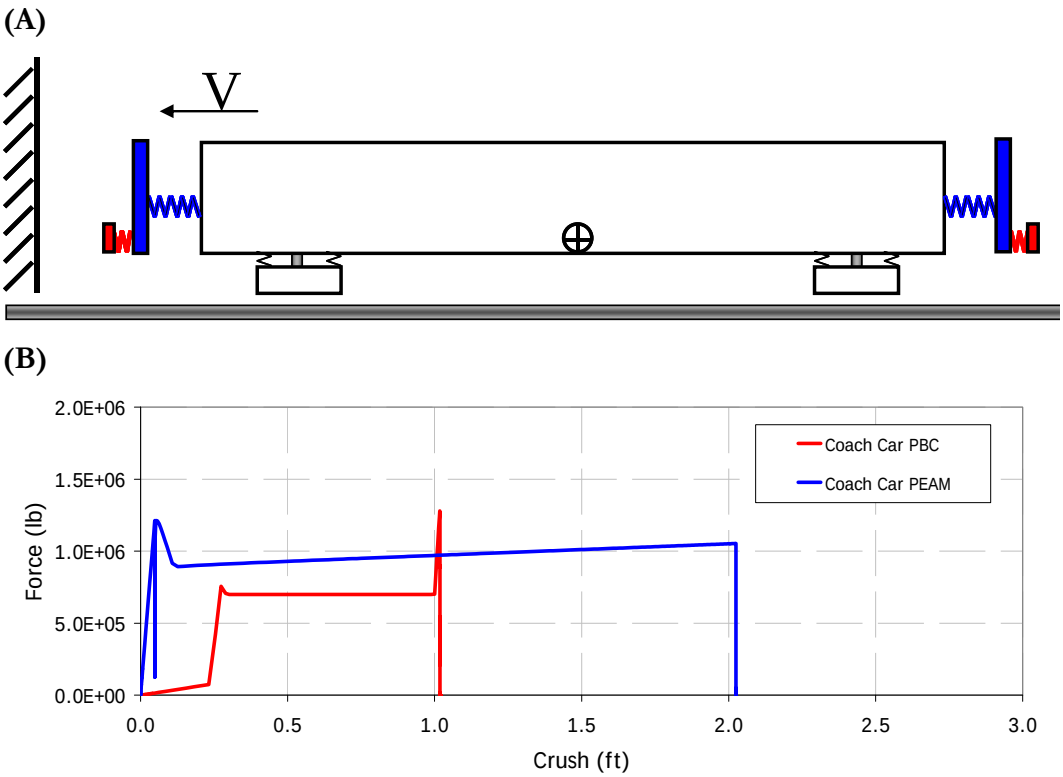

Figure 43. (A) Schematic showing idealized lumped mass model and (B) corresponding model output of crush zone force-crush characteristics for each component

6.1.2 Gross Motions

Although the input force-crush characteristic used in the collision dynamics model is idealized, correlation between the car body gross motions is very good. The plot in Figure 44 shows a comparison of the velocity-time histories of the car body test data and the single car collision dynamics model. The accelerometer data from the car body CG was integrated over time to calculate the velocity-time history. There is very good agreement between the model and test in terms of capturing the timing of the collision and the average deceleration for the car body. Consequently, in evaluating how variations in the force-crush behavior affect the overall motions of a railcar, the model is provides valuable information.

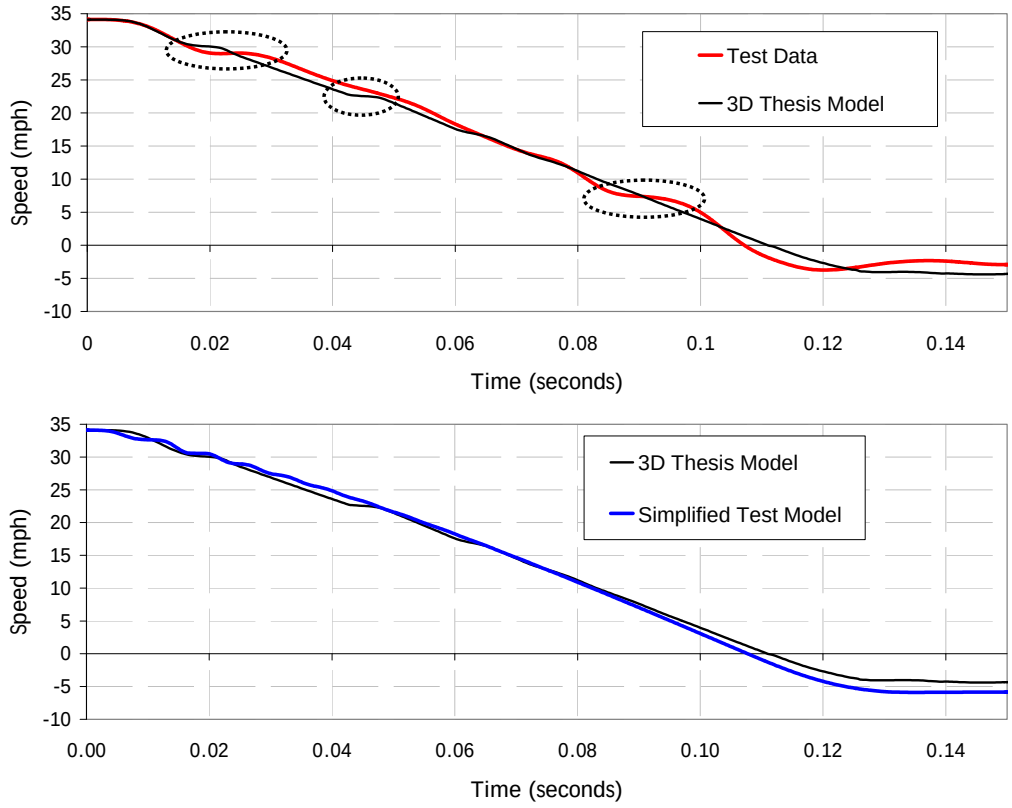

Figure 44. Velocity-time histories of the single car test for the test data and the 3D thesis model (top) and the simplified test model and the 3D thesis model (bottom)

The deceleration of the car is marked by relatively uniform decelerations between the time of impact and 0.11 seconds. Several distinct "plateaus" exist in both the test data and the three-dimensional model, where the negative slope of the velocity approaches zero. By referring back to the accelerometer data in Figure 41, the plateaus in the velocity trace correlate to the most dramatic drop-offs in deceleration. These occur when the deceleration approaches zero, at just after 0.02 seconds and 0.09 seconds. The force measurements from each spring-mass element in the model provide useful information for investigating the reason for such changes in decelerations. The first plateau (indicated by the first dashed oval in Figure 44) at 0.015 seconds is due to a drop-off of force in the sliding sill/PEAM

mass after the pushback coupler triggers, but just before the end frame makes contact with the wall. The second plateau in the model data, at about 0.045 seconds, is due to the drop-off of force post-sliding sill trigger. This sort of scrutiny of the results helps to identify the crush sequence of events and to correlate them to the post-test observations.

For example, during the test it was observed that the primary energy absorbers did not crush exactly as expected. The primary energy absorbers are made up of eight cells that are designed to collapse in a graceful and uniform folding pattern (see Figure 37). During the test, some material failure occurred as the primary energy absorbers crushed. Individual cells toward the rear of the PEAM elements "burst" instead of gracefully folding. If the build up of material caused an interference with the surrounding structure of the PEAM, such an event could explain the plateau in an otherwise constant deceleration of the car body test data seen at about 0.085 seconds.

6.1.3 Sequence of Events

The results for gross motion of the car body match up very closely. The impact occurs at time zero while the car is moving at 34.1 mph. The car body reaches a complete stop at about 0.11 seconds and then rebounds off the wall and comes to a speed of about 5 mph moving away from the wall.

The single car test provided important data for breaking down the sequence of events in the crush zone and the contribution of each component. By developing the three-dimensional model and evaluating the results in stages, details of a single crush zone are understood before investigating the effects of multiple crush zones. Figure 45 shows a key result of the single car model. The forces acting on each

crush zone component are plotted against time. Information in this plot can be used to determine the timing of important events in the velocity-trace. Figure 46 shows the velocity trace from the model with the sequence of events identified. The elastic response of the draft gear occurs in the first 0.005 seconds. The pushback coupler is then triggered as indicated by the peak force in red and crushable structure of the pushback coupler crushes at a constant force. As the pushback coupler reaches the end of its stroke, the end frame contacts the wall (as indicated by loading of the blue dashed line) and begins to load the sliding sill. The shear bolts trigger at 0.02 seconds and the PEAM begin to crush at an average force of about one million pounds.

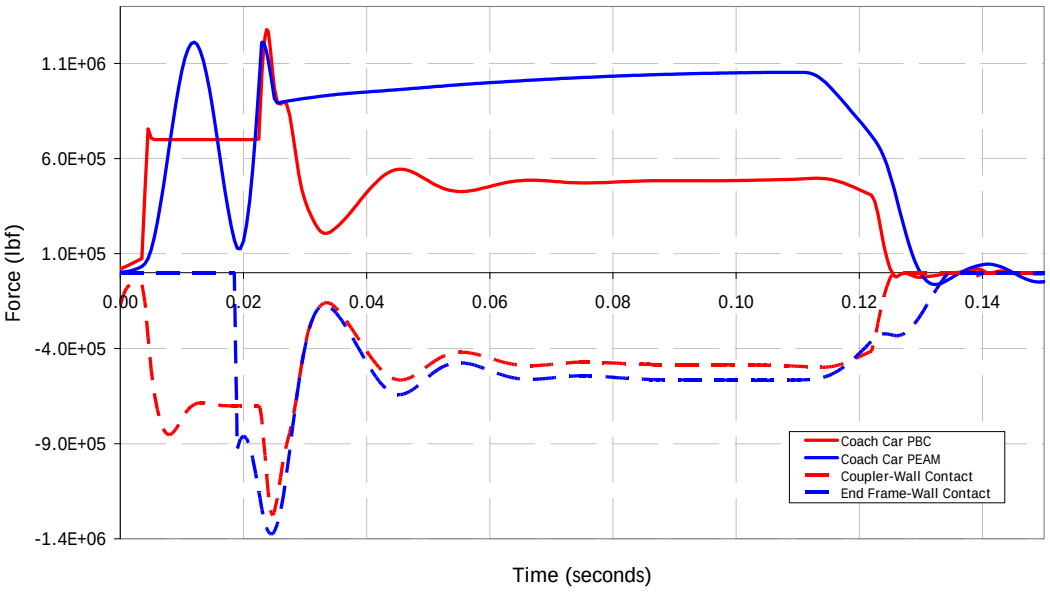

Figure 45. Force-time histories for each crush component and contact force in the single car impact scenario

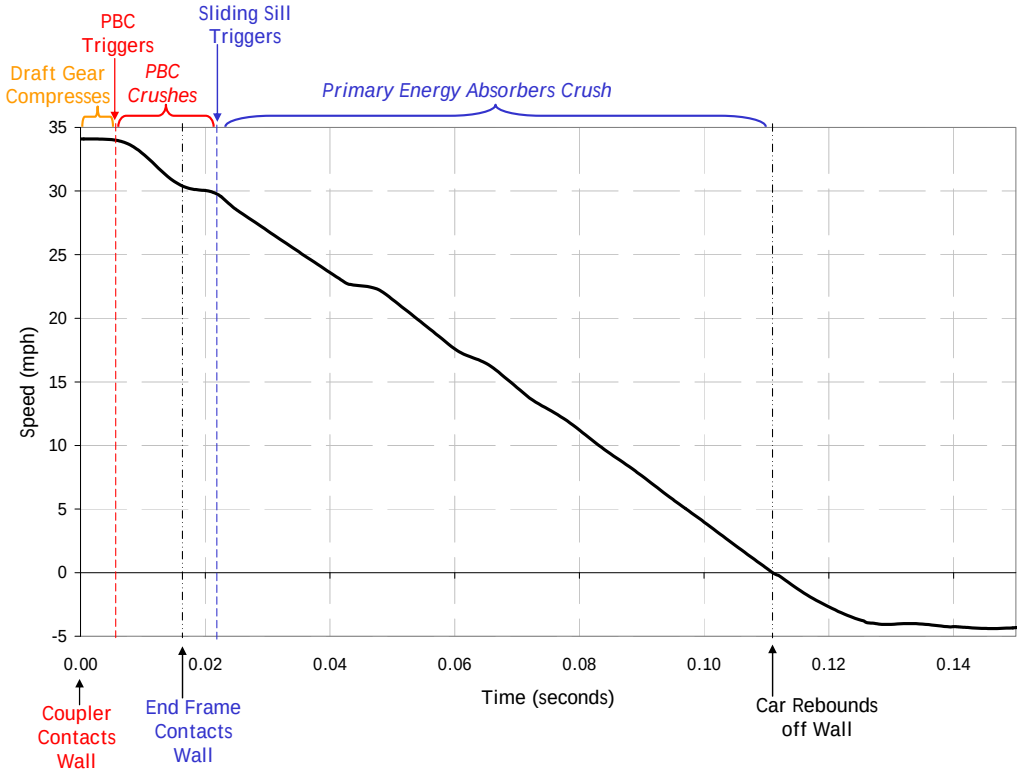

Figure 46. Collision dynamics velocity plot indicating the sequence of events

6.1.4 Non-longitudinal Motions

In the single-car test slight truck motions are observed in the high-speed film of the CEM equipment. The three-dimensional model simulates the pitching motion of the trucks relative to the car body. In this section the model is used to evaluate the progression of relative motions between the car body and the trucks.

During the CEM single-car impact test, the car body comes to rest in 0.11 seconds, which means the car body is experiencing a severe deceleration. As described above, the sequence of events begins such that a longitudinal impact force initially enters the car at the coupler pulling face, which is below the car body's center of gravity. This instigates a pitching motion in the car body. Additionally, if the coupler is at angle an the time of impact, lateral motions are introduced. In the single car test, the pushback coupler triggers at about 0.005 seconds after the impact and begins to slide back, which minimizes the introduction of lateral loads into the car body. The end frame then contacts the wall and is pinned against it as the crush zone crushes in-line with the car body's longitudinal centerline and the car body decelerates. There is no vertical motion of the end frame, as is observed in the high speed film and by the distinct imprint of the end frame on the impact wall. The crush zone triggers at about 0.02 seconds which causes the end frame to slide back in-line with the car body longitudinal centerline and minimizes the pitch of the car. By comparison, in the conventional single car impact test, the draft sill folds under causing a significant pitching motion of the rear of the car. Figure 25 shows a set of sequential stills from the high-speed cameras of both the conventional single car test and the CEM single car test. In the conventional test the car impacted the wall and both the car body and trucks significantly pitched forward. In the CEM single car

test, the pitching of the car body was reduced due to the controlled crush of the car end. The sliding sill and the progressively collapsing design of the crushable structure minimized the vertical motions of the car by keeping the collapse of the structure to be parallel to the severe longitudinal forces.

In the single car test of conventional equipment, the car crushed by approximately 6 feet and the wheels of the lead truck lifted off the rails by 9 inches as it crushed. In contrast, the CEM car crushed by 3 feet and all the wheels lifted off the track by less than an inch. Figure 47 shows a set of images from the single car test model. The series shows 1) the steady state positions of the car body on the trucks just prior to impacting the wall, 2) very little truck pitching at the time the pushback coupler triggers, 3) truck pitching forward at the time the PEAM triggers and 4) the time at which the car has completely decelerated and the crush completed. The pitching of the trucks is about 10 degrees in the model. Because the modeling of the truck connections is somewhat crude, the trucks' pitching motions appear closer in rotation to the conventional single car test, but the vertical lift of the truck's CG is less than an inch. From the high-speed video of the CEM test, the wheels spin as the car body is impacting the wall, which implies the trucks lifted off the tracks just enough to allow the wheels to rotate as the trucks decelerated with the car body. The exaggerated pitch of the trucks is satisfactory because the vertical lift is very small the truck motions do not necessarily affect the significant results of the model.

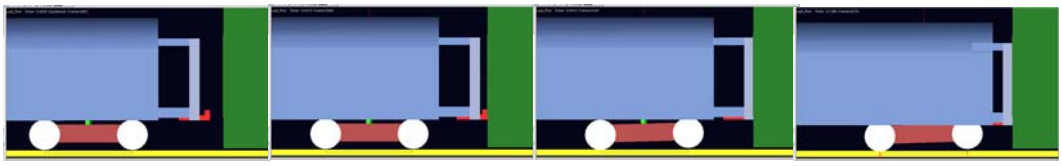

Figure 47. Sequential stills from the 3D multi-body model showing the pitching motions of the truck

6.1.5 Wheel-to-rail Interaction

The final feature of the single-car model is the multi-dimensional motion of the wheel-to-rail connection. (Appendix A provides more information about the definition and implementation of the derailment characteristic.) The results show that the wheel-to-rail characteristic is measuring a lateral force between the truck and the rail which follows the wheel-to-rail characteristic as defined. The trucks oscillate back and forth between the rails, with negligible displacement with respect to the rail. Accordingly, the lateral force between the truck and the rail is negligible. This demonstrates that the forces between the truck and the rail are not high enough to cause derailment. This observation was confirmed in the test. For a single-car impact condition the forces remain longitudinal. The crush zone is designed to promote longitudinal forces into the car body and performs sufficiently in the single-car impact.

6.2 TWO-CAR MODEL COMPARISON

The objective of the three-dimensional multi-mass two-car model is to develop a two-car lumped-mass model of CEM passenger rail equipment that includes all the features developed in the single-car model and a coupled connection with three-dimensional motion. The results of the two-car impact test of CEM passenger

railcars are used to validate the model results. Selected results are shown in this section for the model run with the test conditions of the corresponding two-car impact test. The key comparisons include the total crush values for each component, the longitudinal gross motions of the CG of the cars and the sequence of events and timing of each component in the crush zone. Additionally, the motion at the coupled connection is shown and evaluated for the three-dimensional model compared to the test.

In the two-car impact test, two-coupled cars impacted the test wall at a speed of 29.3 mph. The crush zone on the lead car was activated and nearly exhausted the crushable structure (approximately 3 feet of total crush). At the coupled connection, both pushback couplers were activated and pushed back, allowing the end frames to come into contact and both crush zones to activate. There was about three feet of crush at the coupled interface. The collision dynamics model results agree with the test data in terms of gross motions and crush.

6.2.1 Force-crush Behavior

A comparison of initial kinetic energy to energy absorbed through crush is in general agreement between the model and test data. The total energy absorbed by the crush zone represents the energy required to bring the test vehicle to rest from an initial speed of 29.3 mph. The kinetic energy in the test condition is about 4.3 million ft-lb and the energy absorbed by the crush zone is about 4.2 million ft-lb. In the two-car CEM test the crush zone on the front of the coach car crushed and both crush zones at the coupled interface crushed. Figure 48 shows the force-crush behavior of each component in the crush zones of the two-car test scenario model. The light blue trace shows the behavior of the draft gear and pushback coupler. As

in the single-car test, at the crush zone at the front car was exhausted. The pushback coupler reached its maximum stroke and the primary energy absorbers crushed by about 30 inches. The dark blue trace shows the crush of the primary energy absorbers. The PEAM at the rear end of the lead car and the front end of the trailing car crushed by approximately 10 inches and 1 inch, respectively. The force crush was modified from the initial design values of the components in response to post-test observations. The most noticeable observation was that the PEAM did not crush in a consistent folding pattern as expected. The individual cells of the primary energy absorbing elements were intended to collapse in a progressive mode of deformation with no material failure, but in the test it was observed that some cell deformation included material failure and experienced a "bursting" behavior. To represent the buildup of crushed material due to the erratic crushing behavior of the "bursting" cells in the model, input force-crush characteristics were modified. A slightly increasing crush force represents the uniform crush of the first half of the PEAM stroke and a steeper increasing crush force represents the bursting behavior of the second half of the PEAM stroke.

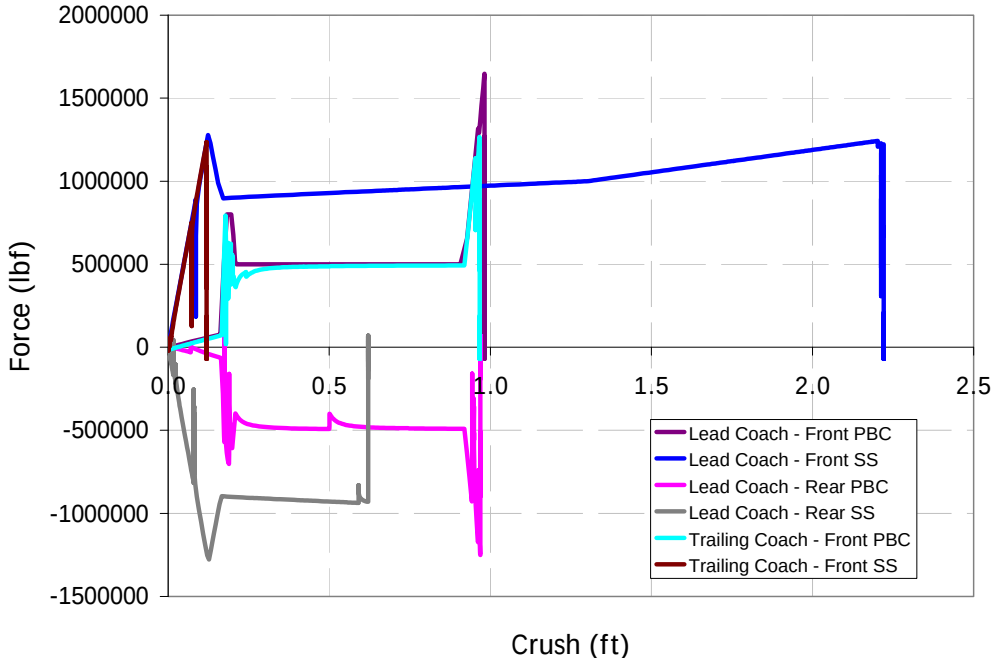

Figure 48. Two-car test scenario: Force-crush results from two-car model

6.2.2 Gross Motions

Figure 49 shows a comparison of the velocity-time histories for the car body motion test data and the two-car multi-mass three dimensional collision dynamics model. As with the pre-test model shown in Figure 31 there is close agreement between the model and test in terms of the longitudinal measurements of crush and average deceleration. In the comparison of the pre-test model to the test results (Figure 31) the trailing car loses speed at approximately the same rate, but the initial timing of the trailing car beginning to decelerate is slightly delayed. The collision takes less than 0.2 seconds. The lead car impacts the wall at time zero and begins to decelerate. There is a 0.03-second delay before the trailing car begins to decelerate. The thesis model provides a more accurate comparison in terms of timing of the trailing car. There were two modifications to the model to improve the timing. The force-crush characteristic of PEAM was modified as described and shown in Section

6.2.1, and the draft gear stroke was shortened. With these modifications, the deceleration of the coupled cars follows the test data very closely, including rebound off the wall. The first car rebounds off the wall at about 0.15 seconds and the trailing car bounces off the wall just shy of 0.2 seconds. The force of the trailing car on the first car causes it to get pinned back against the wall after its initial rebound and consequently a second rebound occurs at about 0.21 seconds. The difference in the final speeds of the test cars is attributable to an oversight in the prototype design. Once a crush zone was triggered, the car end's structure provided essentially no draft load. With the sliding sill shear bolts triggered, the coach car crush zone design did not include a post-triggering retention device. This became apparent during the test when the car rebounded off the wall and the trailing car's end frame pulled out of the sill. The test data show that the trailing car has a cruise speed away from the wall of about 6 mph and the lead car has a cruise speed of about 3 mph for the time period shown. The design requirements of the CEM system were modified to include a retention device for post-triggering draft loads, and this modification was included in the CEM cars built for the train-to-train test.

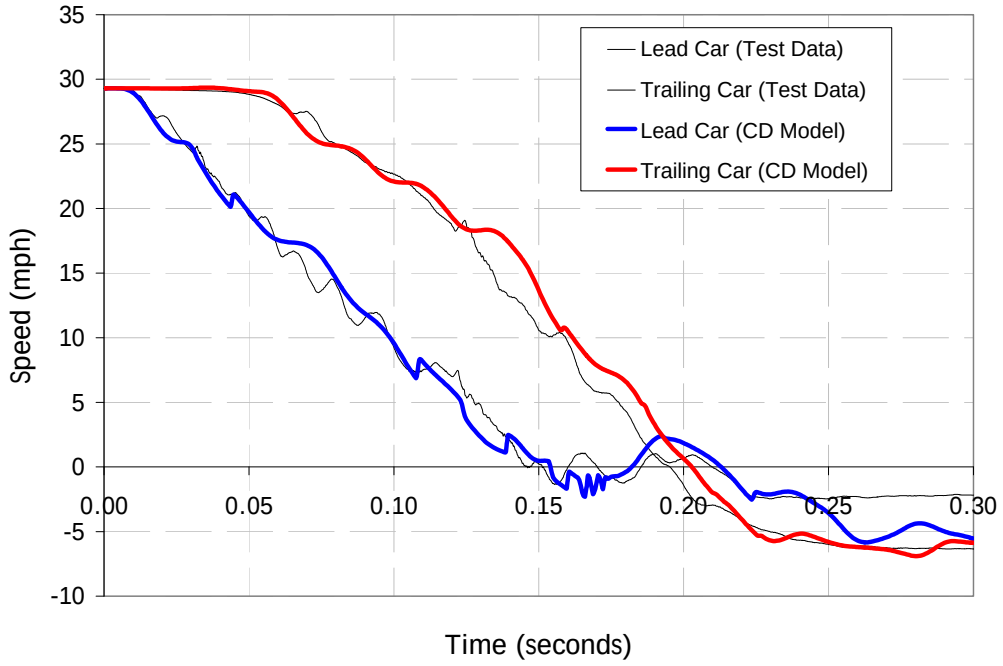

Figure 49. Two-car impact scenario: Comparison of car body motions in 3D multi-mass collision dynamics model and test data

The two-car scenario tests the performance of the crush zones at the coupled interface. The timing of events between the three crush zones in the test can be investigated by examining model results of each component's force crush behavior. Figure 50 shows the loads on each spring of each component. Figure 51 shows the contact forces of the PBC and the wall, the lead car end frame and the wall, and the end frames at the coupled interfaces. The lead crush zone performs similarly as in the single car test. The pushback coupler at the coupled interface triggers at about 0.057 seconds. As the collision force travels through the two-car consist, the coupler at the rear of the lead car is loaded and triggers just prior to the adjacent coupler. As the couplers push back, the end frames come together and make contact at 0.143 seconds, at which point the sliding sill is loaded. Referring back to the velocity trace, it should be noted that the first car comes to a complete rest at about

0.15 seconds and then begins to rebound off the wall. Because the first car rebounds at the same time as the sliding sills at the coupled crush zones are reaching peak levels, the PEAM at the rear of the first car is loaded from both sides – by the acceleration of the first car as it moves away from the wall and by the trailing car as it accelerates toward the wall. The timing is such that the sliding sill at the back of the first car is activated and begins to crush the PEAM. As the PEAM crushes, the load is temporarily relieved on the adjacent crush zone. The PEAM at the back of the lead car crushes by a total of 10 inches, whereas the PEAM at the front of the second car crushes by only an inch. This sort of crush zone activation illustrates how timing of the forces through the consist and the deceleration of the individual cars can affect the timing and activation of crush zones. It is important to consider such influences in the design of crush zones.

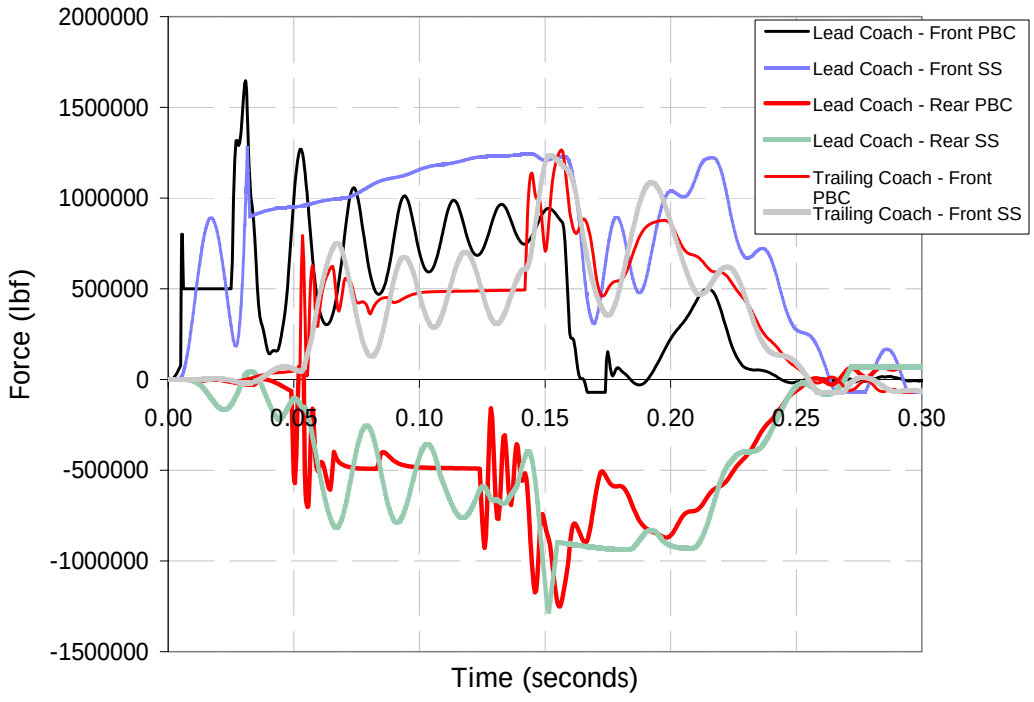

Figure 50. Model results of the force-time histories for each crush zone component in the two-car impact scenario

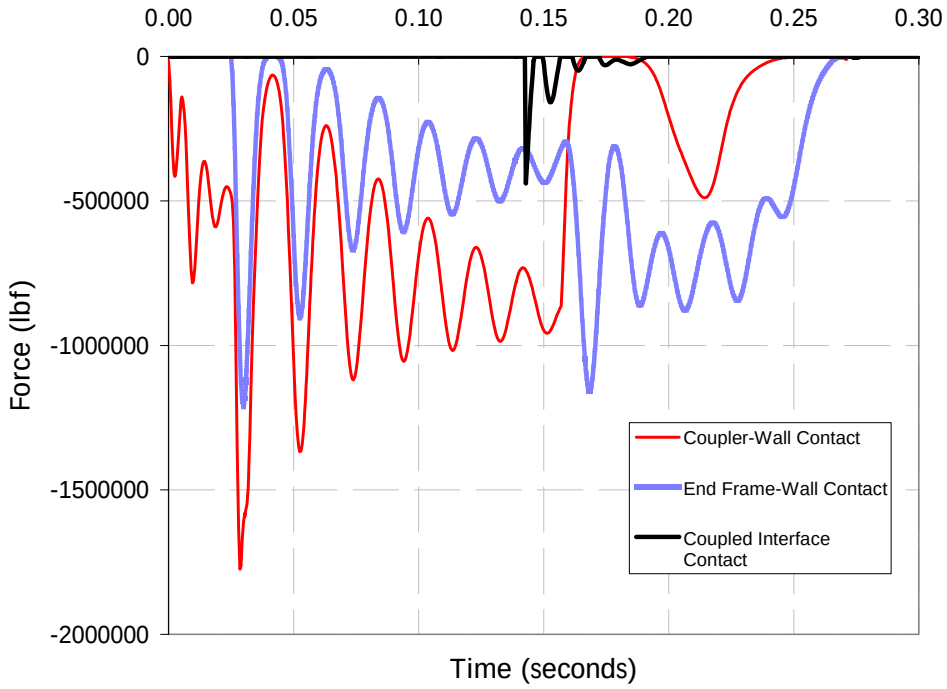

Figure 51. Model results of the contact forces in the two-car impact scenario

The plot in Figure 52 uses all of the results shown in the above plots from the collision dynamics model to identify the sequence of events on the velocity traces. Annotations along the bottom of the plot indicate the contact events: initial contact of the lead car's PBC with the wall, contact of the lead car's end frame with the wall, contact of the coupled cars' end frames, rebound of the lead car off of the wall (twice), and rebound of the rear car off of the wall. The key events of the crush zone on the front of the lead car are indicated beneath the lead car's trace (blue). The key events are indicated for the crush zones at the coupled interface above the trailing car's trace (red). The first shallow deceleration seen in the lead car indicates compression of the draft gear. In the trailing car, the draft gear compression occurs over a longer time period since the stroke of the draft gear is doubled with two draft gear sets between the coupled cars. The activation and crush of the PBC causes the

car to slow down at a higher rate. The sliding sill's activation is noted by the next change in slope. The PEAM of the lead car then crushes until the car rebounds off the wall.

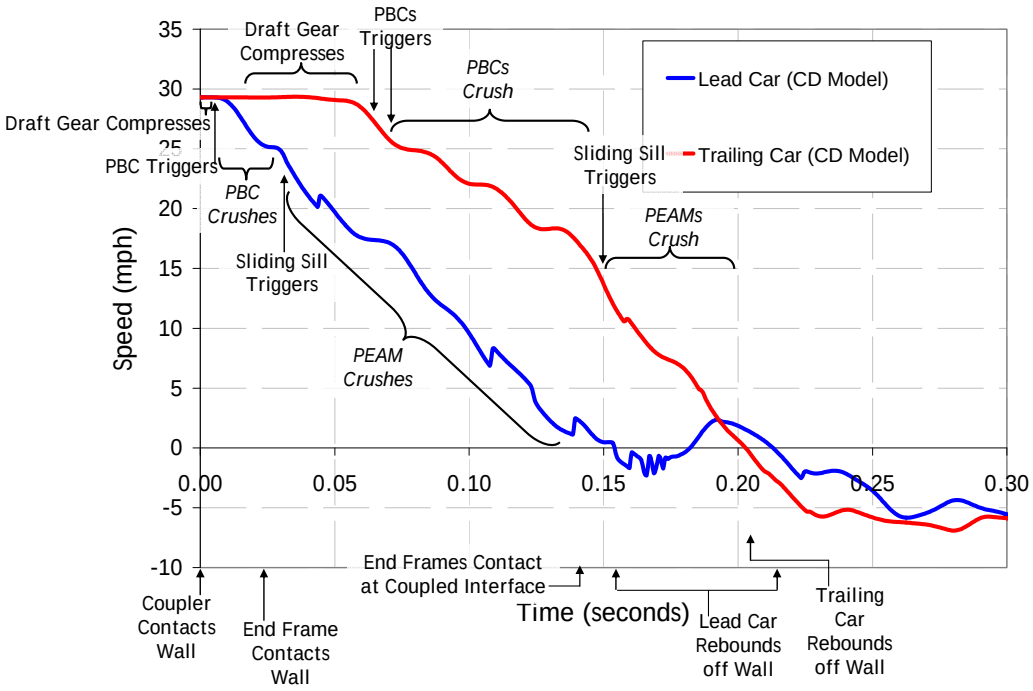

Figure 52. Velocity-time histories of two-car model annotated with sequence of events

Understanding the effects of the crush events on the gross motions of the cars makes the next task of investigating the train-to-train collision more manageable. It is apparent each car's deceleration is affected by the forces being applied from the front and the back. For instance, the first car rebounds off the wall at about 0.15 seconds, but is pushed back into it by the force applied from the coupled car behind it. These interactions will become more complicated as cars are added to the consist.

6.2.3 Three-dimensional Motions

High speed film from the full-scale tests shows that the non-longitudinal car body motions were minimized by the controlled collapse of the CEM crush zones.

Figure 30 shows a plan view of the coupled interface, comparing the conventional cars to the CEM cars in the two-car impact test. Coupled cars can reach an operational offset of about 2 inches. During the impact of the conventional cars, a lateral load was introduced into the consist that progressed high enough to derail the cars. During the CEM test, the crush at the front end of the lead car was designed to crush symmetrically along the centerline of the cars (in the direction of travel), so that the introduction of lateral loads was minimized. Additionally, the pushback feature of the couplers removes the moment arm between cars and brings the end frames together so that the transfer of lateral loads between cars is eliminated.

Passenger cars have vertical and lateral motions in typical operation due to the connections between the car body and trucks and at the couplers. The following results show that the model of two-coupled CEM cars simulates vertical and lateral motions within typical limits.

6.2.3.1 Pitching Motions

In the two-car test of conventional equipment, the lead car impacted the wall and climbed it as it crushed by approximately 6 feet. In contrast, the CEM car crushed by 3 feet and all the wheels lifted off the track by less than two inches. At the coupled interface, the conventional cars laterally buckled and the left track rolled due to high lateral loads. (Refer to Figure 30 for images of the lateral offsets during the collision and Figure 29 for images of the final positions of the cars.) Figure 53 shows a set of images from the two-car test model. The series shows the time of 1) initial contact between the PBC and the wall, 2) activation of the PEAM of the lead car's front crush zone, 3) activation of the second PBC at the coupled interface, 4) contact of the end frames at the coupled interface and 5) rebound of both cars off

the wall. The first image shows the steady state positions of the coupled cars at the instant of impact with the wall (velocity is 29.3 mph). Note both car bodies have a slight upward pitch. The second still shows that as the pushback coupler crushes, the trucks of the lead car have begun to pitch upward and the car body pitch has leveled off. The trucks pitch forward at their connection because the car body is dramatically decelerating. This is consistent with the results of all full-scale testing. The third still shows that as the PBCs at the coupled interface trigger, the trucks of the trailing car are pitching upward. At time 0.143 seconds, the image shows the lead car body pitching downward as the end frames contact. The final image shows the position of the cars at the time both have rebounded off the wall. During the total time of the collision event, the pitching of the trucks is less than 9 degrees in the model and the vertical lift of the truck's CG is less than an inch. Like the single-car test of CEM equipment, the high-speed video indicates that the trucks lift off the tracks just enough to allow the wheels to rotate. The car body motions are consistent with those observed in the full-scale tests.

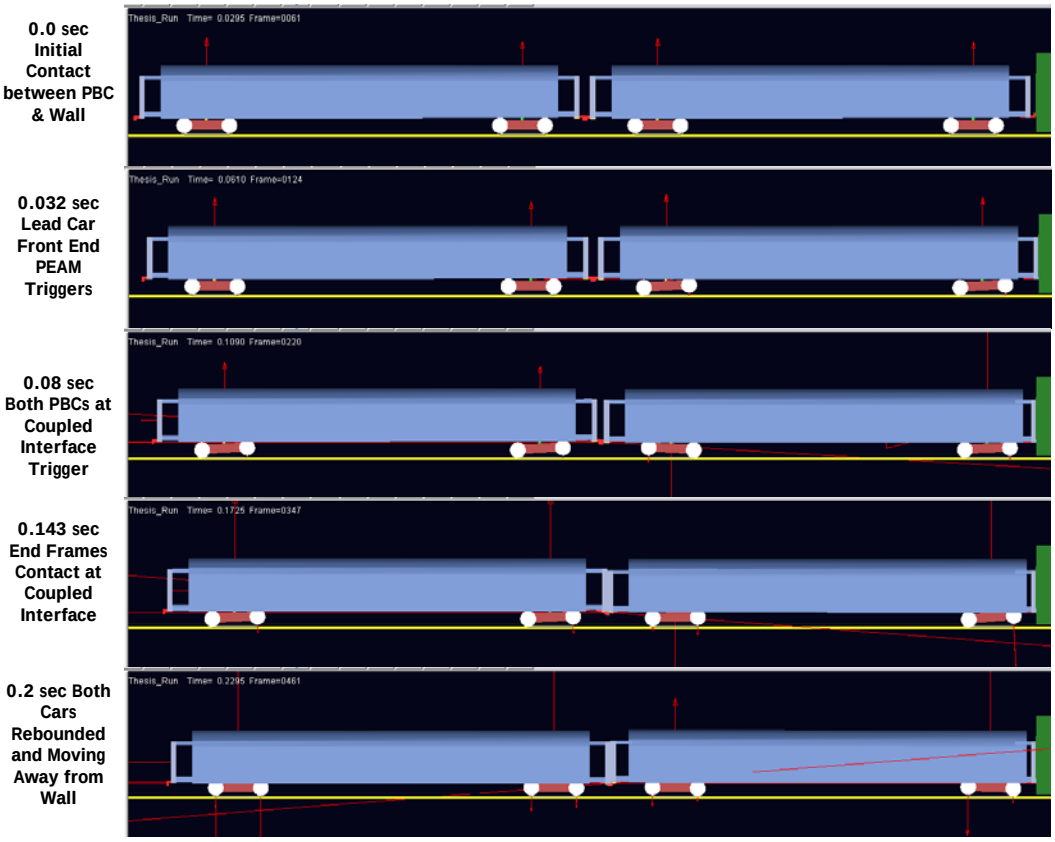

Figure 53. Sequential stills from the simulation of the two-car impact scenario showing truck and car body pitching motions

6.2.3.2 Coupled Connection

Figure 54 shows a set of images focusing on the coupled connection of the two-car model during a simulation of the two-car test. The images are described along with the results of relative car body motion and coupler swing provided in Figure 55. The series shows the time of 1) initial contact between the PBC and the wall, 2) activation of the first PBC (at the rear of the lead car) at the coupled interface, 3) activation of the second PBC (at the front of the trailing car) at the coupled interface, 4) contact of the end frames at the coupled interface and 5) rebound of both cars off the wall. The first image shows that the coupled ends of the cars are essentially

vertically and laterally aligned at the time of impact with the wall. The second image shows that by the time the first PBC at the coupled interface is triggered, there is about 2 inches of vertical misalignment between the cars. The third image shows that as the couplers pushback and the end frames move together, the length of the moment arm shortens and the vertical misalignment of the cars begins to reduce at about 0.15 seconds. The representation of the coupler allows for motion in both the vertical and lateral directions. At the time of the fourth image, a small lateral misalignment has developed between the cars of about 3 inches. This is within the range of usual misalignments between cars. The last image is at the time both cars are moving away from the wall. The end frames are beginning to pull apart and the vertical heights of the end frames have reversed from the previous image since the end frames are not contacting as they pull apart. This series of images demonstrates allowable motions due to modeling of the coupler connection and the resultant relative car body motions within an acceptable range of the known car body motions.

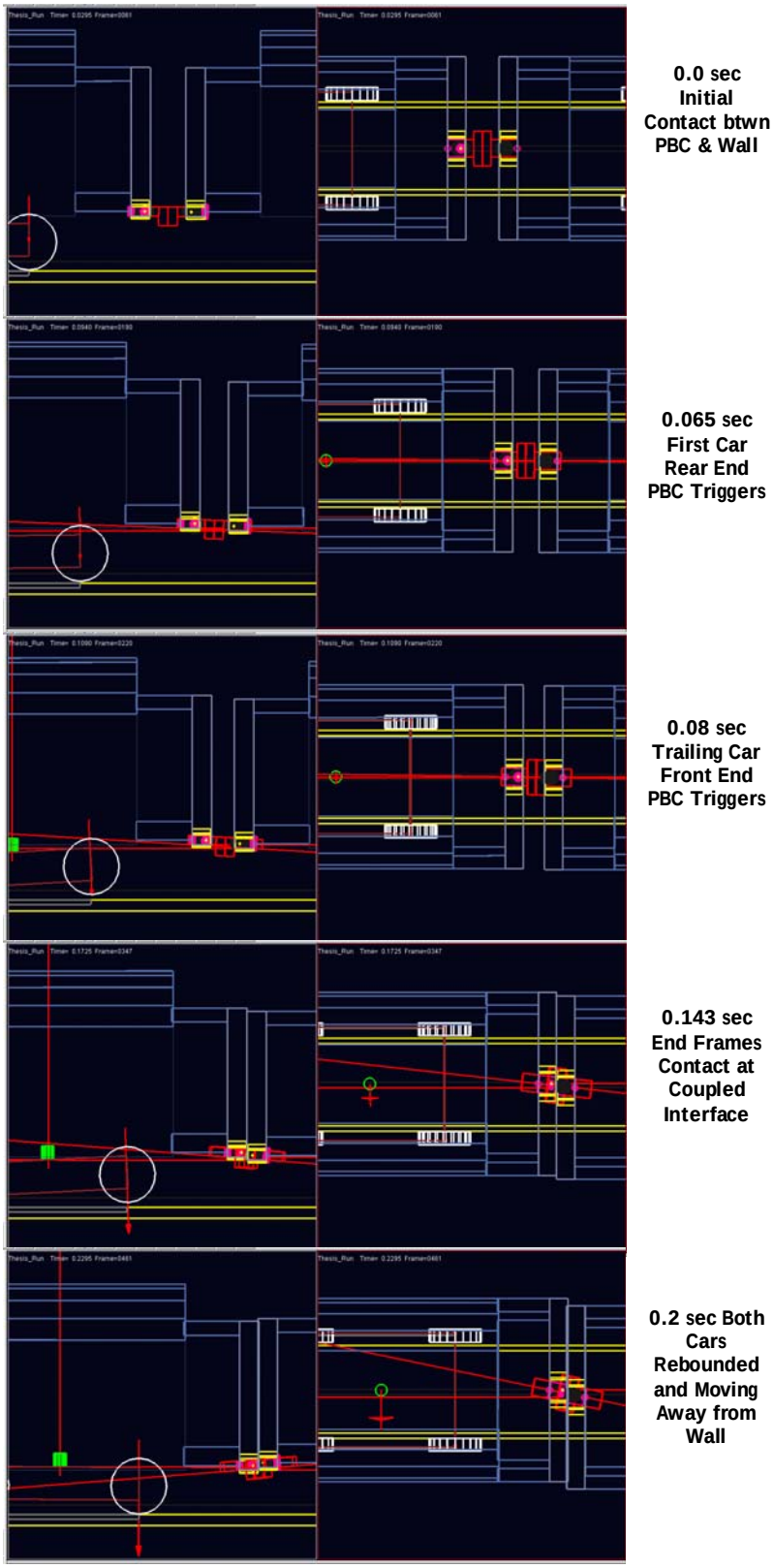

Figure 54. Sequential stills from the simulation of two-car scenario showing the car-to-car interaction

(A)

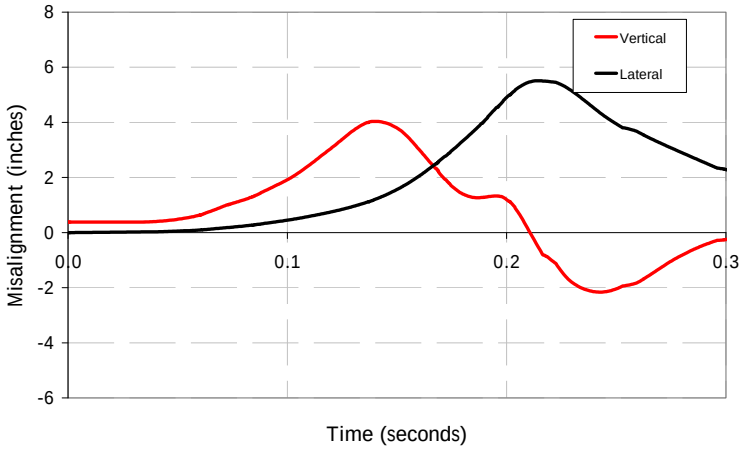

(B)

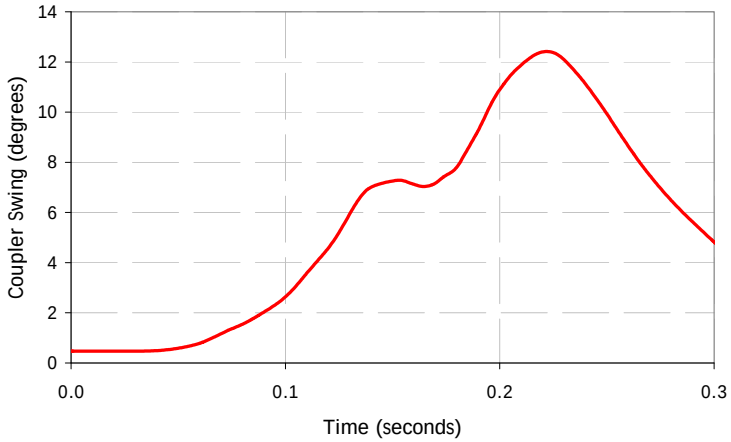

Figure 55. Model results of the relative car motions in the simulation of the two-car scenario: (A) vertical and lateral offset between end frames and (B) coupler rotation

6.3 TRAIN-TO-TRAIN

In the train-to-train impact test, a cab-car led train impacted a standing locomotive-led train at a speed of 30.8 mph. Both consists were of equal mass (individual vehicle weights are listed in Appendix A – Modeling Parameters). Upon impact, the lead cab car engaged the locomotive, thereby preventing override and crushed by approximately 3 feet in a controlled manner. Structural crush was passed

back to all of the trailing car crush zones, demonstrating that all of the space for crew and passengers can be preserved for this collision scenario.

This section presents the results of the three-dimensional model of a train-to-train impact test of CEM equipment. The key comparisons to validate the model include the total crush values for each component, the longitudinal gross motions of the cars and the sequence of events as crush is distributed through the train. Additionally, the model is used to investigate some details of the full-scale test that were unexpected and not considered with the pre-test one-dimensional model.

The results are shown for a baseline run of the model. Modifications are then incrementally applied to the model to improve the comparison with the test data. The improvements to the gross motions are presented and discussed. Comparisons between the models and test data of the crush distribution through the train are shown and discussed. Further variations to the force-crush characteristics are applied in order to further explain the selected events of the full-scale test.

6.3.1 Gross Motions

The gross motions of the train-to-train event are more challenging to predict than in the two previous tests. A one-dimensional model was used prior to the test to make predictions for planning of the test. (Refer to Figure 40 for the post-test comparison of the one-dimensional collision dynamics model to the test data.) The one-dimensional model was accurate in estimating the timing of the collision event, the distribution pattern of crush throughout the consist and the average deceleration of each car.

The force-crush characteristics used in the one-dimensional model are used to set a baseline run for the three-dimensional multi-mass model. Modifications to the

force-crush characteristics are applied in an effort to improve the agreement of the velocity traces and crush measurement with the test data based upon the variations in the crush zones and their performance in the test. Details of these variations are based upon post-test observations, autopsies performed on each crush zone and material tests conducted on selected components.

The model was exercised using the same parameters for force-crush characteristics as used in the one-dimensional model in order to set a baseline comparison between the models and test data. The baseline results for the car body gross motions of the three-dimensional model are compared against the test results and the one-dimensional model in Figure 56.

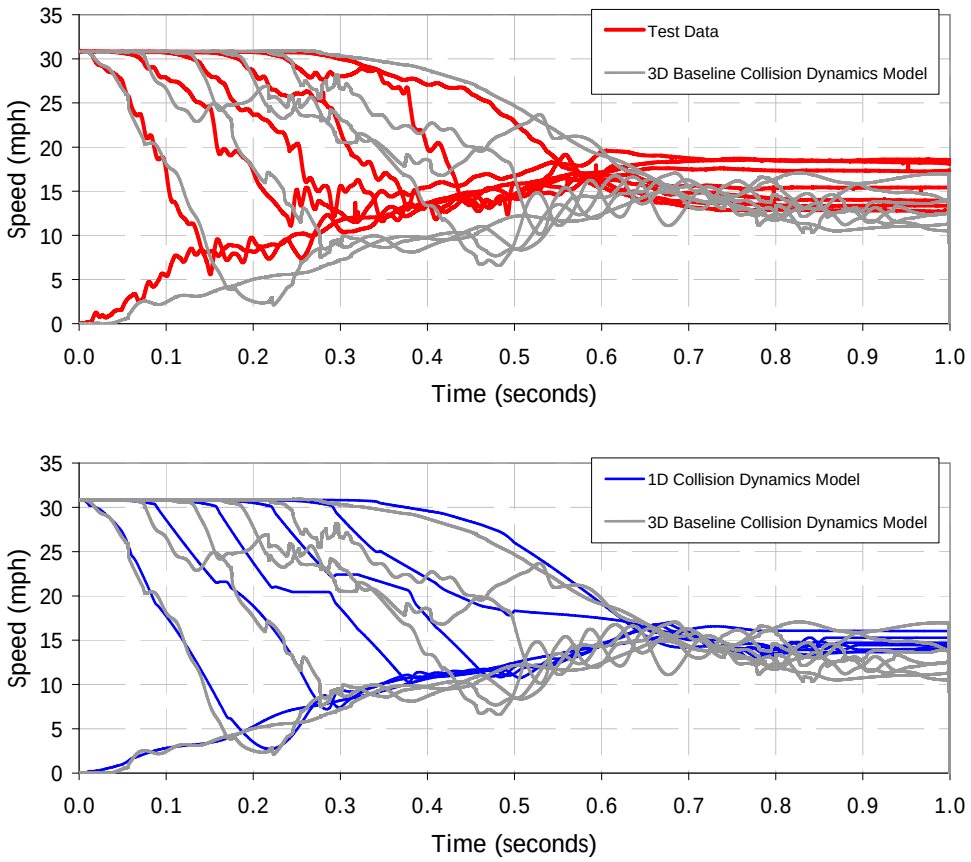

Figure 56. Velocity-time histories for the initially standing locomotive and each car in the moving consist: train-to-train test data (red), 1D collision dynamics model (blue) and the baseline 3D collision dynamics model (grey)

A series of modifications to the input parameters were implemented in order to incrementally improve agreement with the test data. In validating the two-car model with test data it was learned that agreement with the lead car must be captured, else a slight delay in timing of one car is amplified down the length of the consist. Table 4 lists the modifications selected for discussion in the following series of graphs.

Table 4. Modifications to three-dimensional collision dynamics model

Model Simulation	Modifications to Input Parameters
Baseline	*Parameters Used in 1D Post-test Model*
Mod A	Standing Consist ▪ Switched the weights of the ballasted hopper cars
Mod B	Cab Car PBCs ▪ Shortened stroke Coach PBCs ▪ Lowered trigger value ▪ Shortened trigger length
Mod C	Coach Car PBCs ▪ Shortened pushback stroke ▪ Strengthened draft gear
Mod D	Trailing Locomotive ▪ Softened crush force on spring (approx. 4" crush) Trailing Cab Car PEAM ▪ Added an intially high and sustained load by the LTM/SS/PEAM ▪ Increased average crush load by 20%

In comparing the test data to the baseline models, it is apparent that the standing consist is more severely accelerated by the initial impact with the moving consist than the models capture. This delay in the velocity trace affects the timing of each successive car. In the model each car decelerates for a longer period of time before reaching the consist's closing speed than in the test. Figure 57 shows the velocity traces of the impacting vehicles for the test data, the baseline case of the three-dimensional model and the first modification of the three-dimensional model. The first modification was made to the weights of the two ballasted hopper cars in the standing consist. In the test, one hopper was ballasted to nearly four times the weight of the adjacent hopper (refer to Appendix A for exact values). The configuration of two hopper cars was not known. In the baseline simulation the heavier hopper car was coupled to the lead locomotive and the lighter hopper car

was at the rear of the consist. In Mod A, the position of the hopper cars were reversed so that the lighter hopper car is coupled to the locomotive, followed by the heavier hopper car. With these modifications, the velocity traces match up more closely for the impacted locomotive. The circled region in Figure 57 shows that with the lighter hopper car directly behind, the initially standing locomotive is accelerated to about 8 mph in 0.15 seconds behind. Over that time interval, the agreement is improved because the lighter hopper provides less resistance than the heavier hopper.

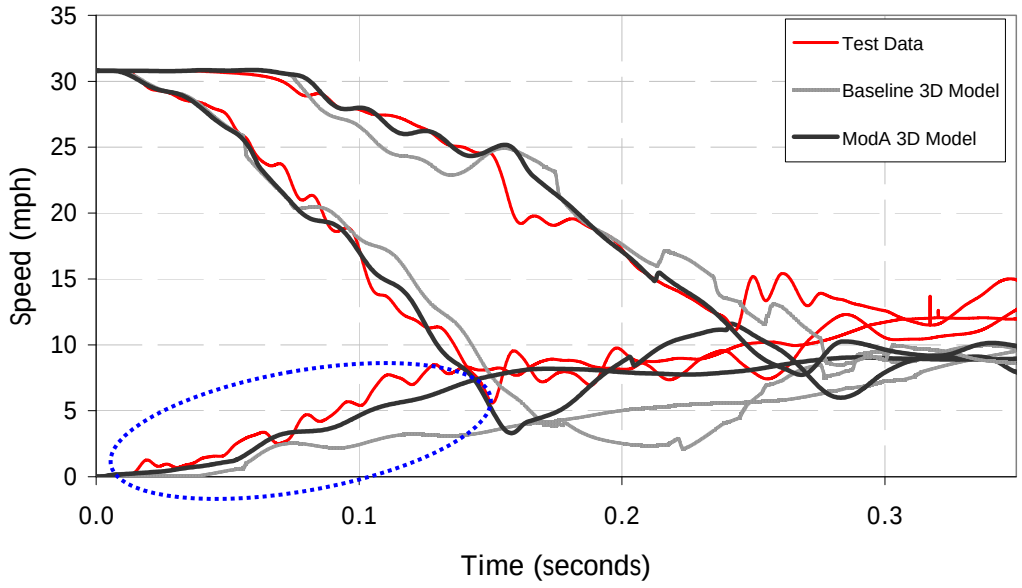

Figure 57. Comparison of velocity-time traces for the initially standing lead locomotive and the initially moving lead cab car and first trailer car: train-to-train test data (red), baseline 3D model (thin black), and Mod A of the 3D model (thick black)

Further modifications are made to improve the agreement of the deceleration of the cab car. At about 0.15 seconds the lead cab car in the model decelerates for longer than the test data, which delays the timing of the first coupled coach car and each successive car thereafter in the model. To address the timing issues of the initially moving consist the next modifications focus on the agreement of the first

coach coupled to the cab car in the moving consist. Figure 58 shows the velocity-time traces for all cars in the passenger consist and the impacted locomotive for the next set of modifications (Mod B). A review of the post-test crush zone autopsy provides evidence that the lead cab end PBC did not reach its full stroke [55]. The circled region in Figure 58 highlights the improvement discussed. Note that the deceleration of the lead cab car only reaches a speed of 5 mph at 0.15 seconds which is closer to the test data than with Mod A, for which the cab car slowed to 3 mph. With this modification applied to the model, the lead cab car's deceleration time decreases so that the initial deceleration of the first coach car following the cab car is shifted to the left slightly and more closely matches the test data (indicated by the arrow).

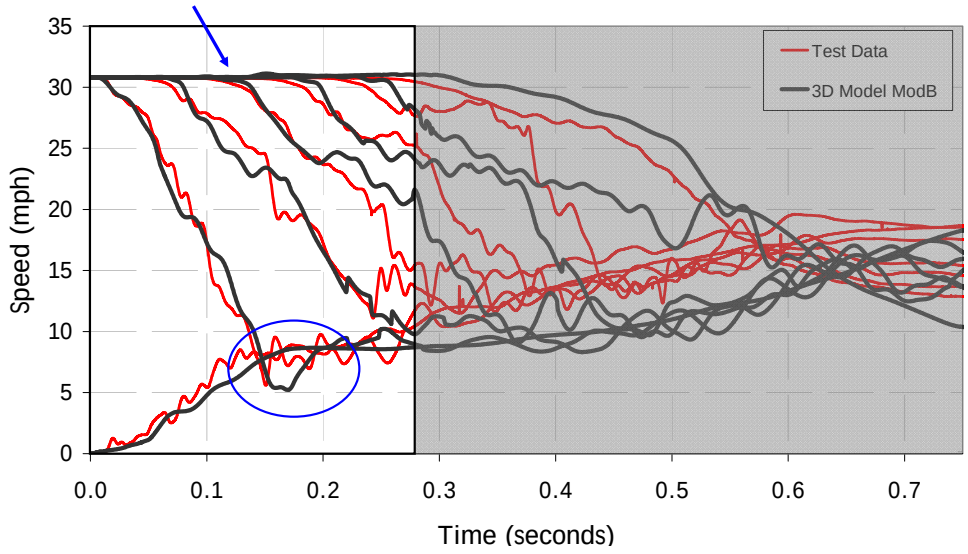

Figure 58. Velocity-time histories for the initially standing locomotive and each car in the moving consist: train-to-train test data (red) and Mod B of the 3D model (thick black)

Figure 59 shows the velocity traces for all cars in the passenger consist and the impacted locomotive for the next set of modifications (Mod C). In this simulation, the length of the pushback coupler stroke is shortened for all the cars and the draft

gear is stiffened to twice the strength. The initial deceleration of each car matches the test data more closely with this modification of the stiffened draft gear, as indicated by the arrows. The circled region identifies the region that is not captured well by the model. In this investigation into the details of the train-to-train test, it became apparent that the second car's premature sign change in deceleration at 0.24 seconds is not simulated in the model. One unexpected incident in the train-to-train collision involved the uncoupling of some of the cars during the collision. As the pushback coupler crushed, the coupler head interacted with the coupler carrier and at some ends activated the lift pin for release of the tight-lock coupler connection. As the collision progressed, the cab car and first coach uncoupled, the second coach car and third coach car uncoupled and the cab car and locomotive uncoupled. The discrepancy in the circled area is a result of the uncoupling of the cab car and first coach car. When both the cab car and first coach car are accelerating (in the circled area), a difference in the motions allows the cab car to pull away from the coach car and uncouple. This premature surge in the first coach accelerating is reflected in the successive deceleration traces of each car. Consequently, the velocity traces do not match up after 0.24 seconds because the model does not include an uncoupling feature.

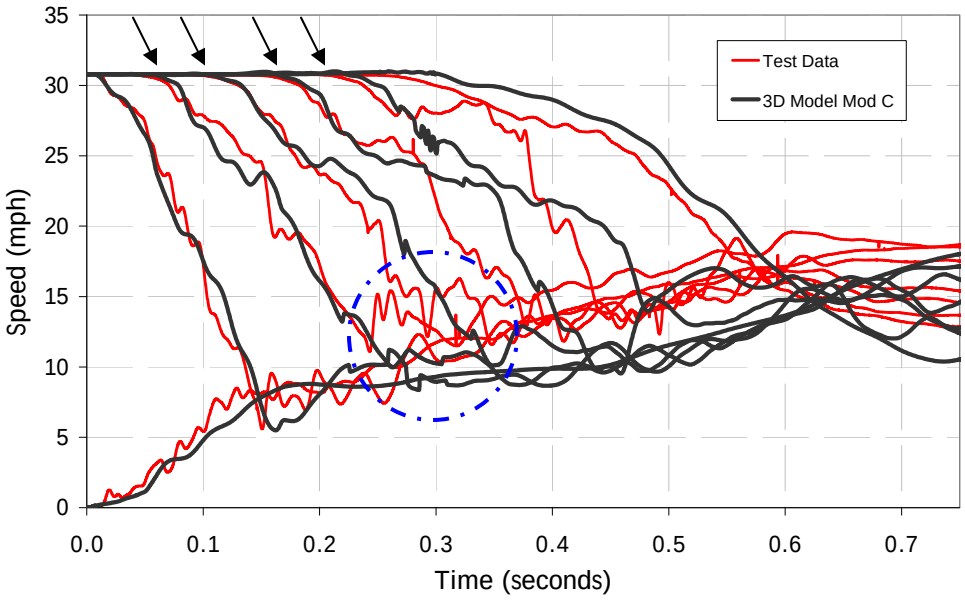

Figure 59. Velocity-time histories for the initially standing locomotive and each car in the moving consist: train-to-train test data (red) and Mod C of the 3D model (black)

Figure 60 illustrates the make-up of the trains pre-impact and post-impact. Schematic A shows the moving consist (5 passenger cars and a locomotive in the rear) moving at an initial speed toward a stationary consist (a locomotive followed by two hopper cars). Both consists are approximately the same weight. Schematic B shows the expected configuration of the two consists post-impact. When the lead cab car and locomotive engage during the impact and all cars remain coupled, the two consists continue together down the tracks when all crush is complete. Assuming this collision is perfectly plastic, the average cruise speed of the two consists post-crush is approximately half the initial speed. Schematic C shows the actual configuration of the cars post-impact. The uncoupling of cars took place between the lead cab car and the first coach car, between the second coach car and the third coach car and between the trailing cab car and the trailing locomotive, as shown in the schematic. The effects of the uncoupling event are observed as the

cars converge into an average post-impact cruise speed. In the first 0.22 seconds the speed of the locomotive in the model follows the test results very closely. After this time, the locomotive moves at a faster speed in the test measurements than in the model. If both Schematic B and Schematic C have the same initial conditions and configuration as shown in Schematic A, and the collision is assumed to be perfectly plastic between the cab car and locomotive, v_B will be slower than v_C because M_B is larger than M_C. This is observed in the gross motions plot shown in Figure 61, which shows the model versus test comparison over a longer period of time. The test data show the locomotive and cab car moving together at about 18 mph. The model results show that the cars of the CEM consist are converging at an average speed of about 14 mph. It should be noted that the model does not replicate the idealized Schematic B shown in Figure 60. The impacted locomotive and lead cab car do not stay engaged after the crush has completed and so the locomotive continues at a higher speed than the CEM consist after 0.65 seconds.

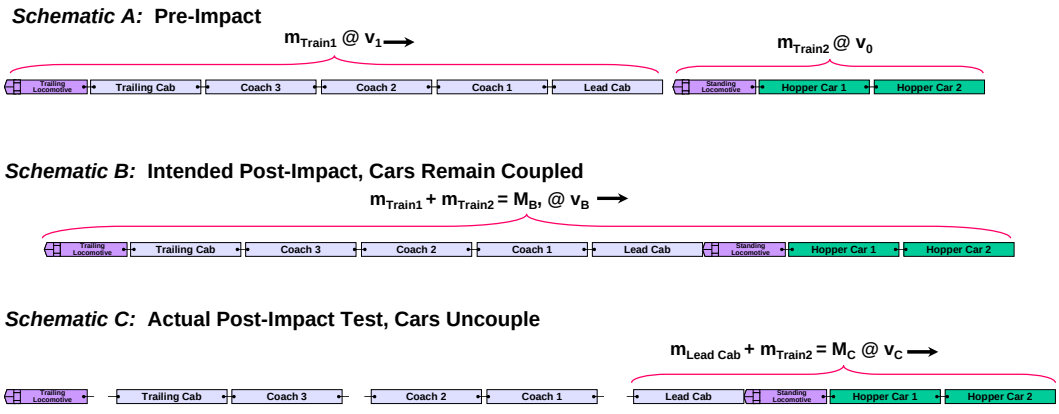

Figure 60. Illustration of the pre-impact and post-impact train configurations

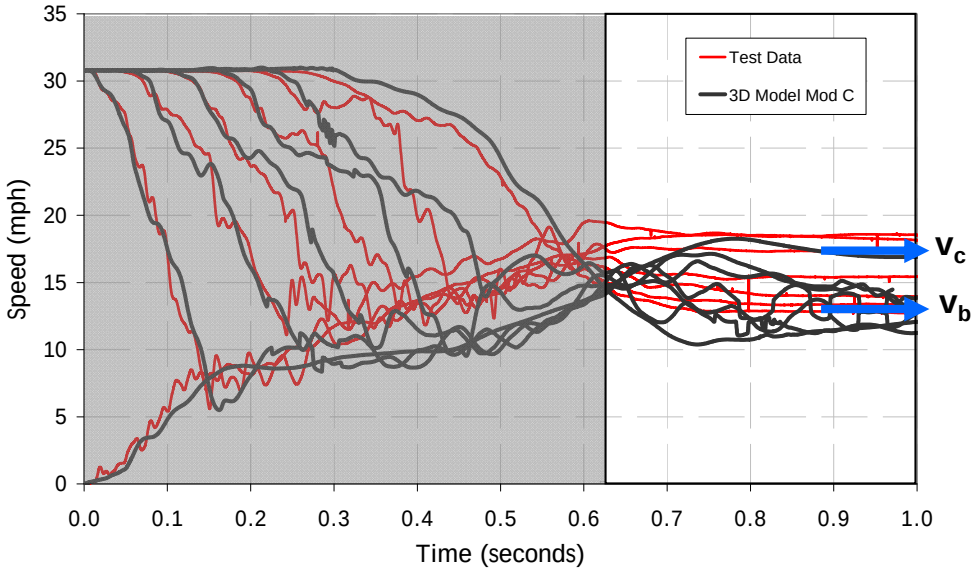

Figure 61. Velocity-time histories for the initially standing locomotive and each car in the moving consist: train-to-train test data (red) and Mod D of the 3D model (black)

Figure 62 shows the velocity traces for the cars in the front and back of the CEM consist and the impacted locomotive for the next set of modifications (Mod D). This simulation is an investigation into the damage observed at the coupled interface between the trailing cab car and trailing locomotive. The cab car sustained damage in the end frame and bellmouth, and crushed asymmetrically due to the lateral load of the offset locomotive. Modifications were made to the force-crush characteristic of the cab car in order to investigate the effect of higher loads applied to the cab end. The gross motions are plotted in the next figure. The boxed region shows the time at which the trailing cab car is beginning to crush. The arrows indicate similar behavior in the model and test data which suggests that the car end sustained high loads around 0.5 seconds. This incident is discussed further in the next section.

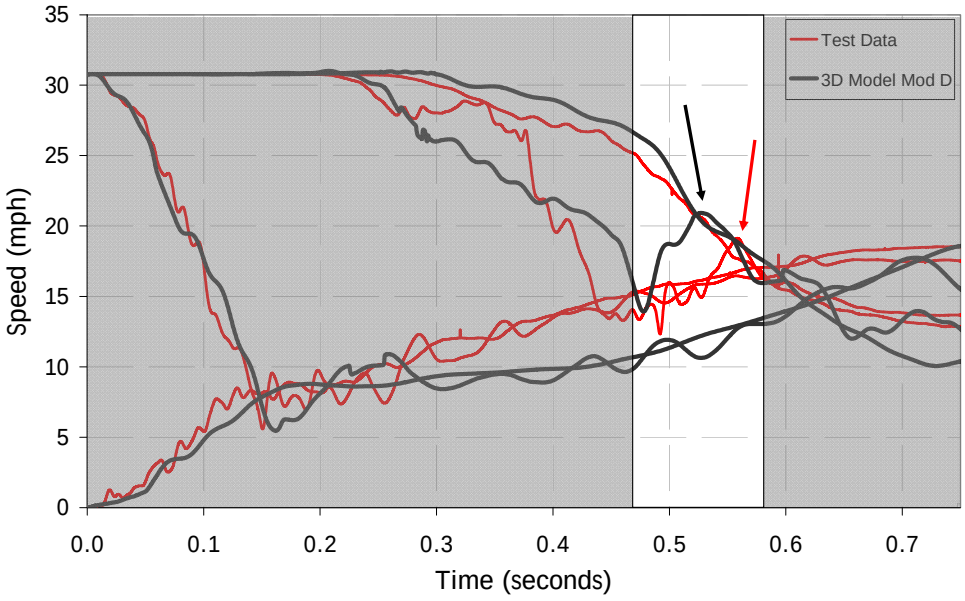

Figure 62. Velocity-time histories for the initially standing locomotive and the initially moving lead cab car, trailing cab car and trailing locomotive: train-to-train test data (red) and Mod D of the 3D model (black)

6.3.2 Crush

The overall crush distributed throughout the train totals about 14 feet. The one-dimensional model estimates the crush per crush zone as a single composite characteristic (each event of the crush zone occurs in series). The multi-mass model developed for this thesis includes a separate characteristic for each component of the crush zone. Load enters the crush zone through the couplers and through contact of the end frames, which provides a more accurate representation of the load path and activation of individual components.

The plots in Figure 63 compare crush results for the test measurements, the one-dimensional collision dynamics model and the three-dimensional multi-mass model for both the baseline and the modified simulation (Mod D). Figure 63A shows the crush sustained by each CEM passenger car and Figure 63B shows the

crush summed at coupled interfaces. The data are plotted to highlight the crush distribution through the length of the train. The test data are shown in black with the square markers. Overall, the model results over-predict the amount of crush in the train. The post-test autopsy of the crush zones uncovered evidence of variations in the expected performance of specific components [55]. The modifications listed in Table 4 were made in the model to address some of these events. As described in the previous section, agreement with the measured gross motions was improved. Likewise, the modifications made to the thesis model improve crush distribution agreement with the test data as shown by the red trace with circular markers in Figure 63. The red trace represents the results of Mod D, which includes the cumulative set of modifications listed in Table 4.

(A)

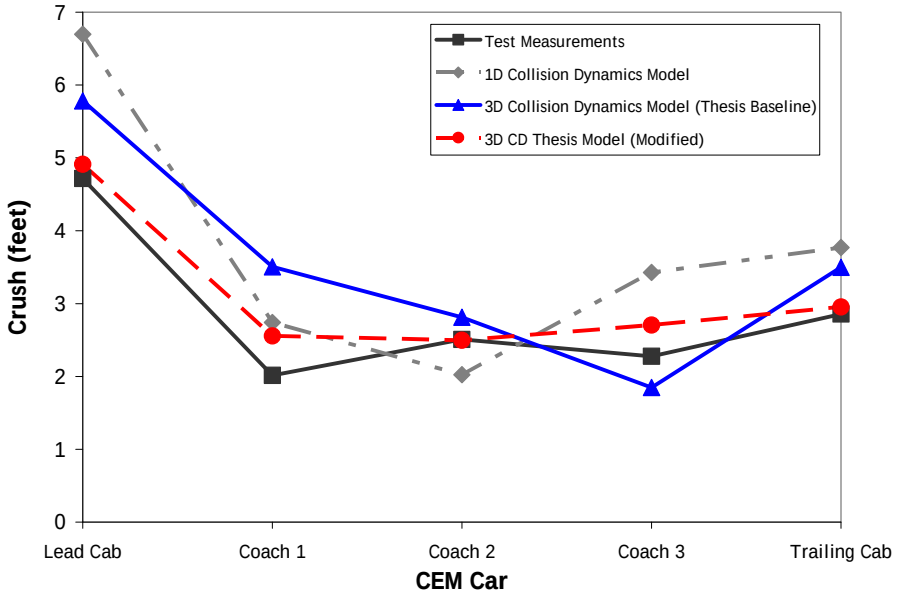

(B)

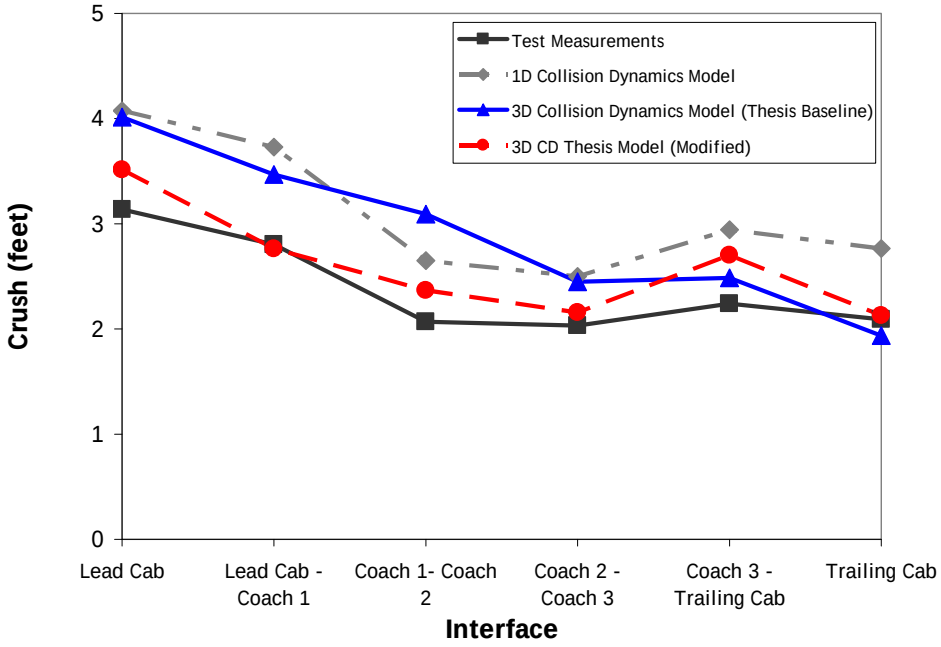

Figure 63. Crush distribution in the CEM train: comparison of the for the test results and the collision dynamics models for A) each CEM car and B) each CEM end or coupled interface

The red trace shows improved crush agreement at the lead cab car's crush zone. Modifications were made to the cab car crush zone (see Mod B in Table 4) which improved the agreement of the crush of the lead cab car crush zone. In the test, as

the lead cab car's coupler pushed back, the coupler pin which connects the draft gear box to the coupler yoke, interfered with an adjacent plate of the surrounding coupler carrier. Such interference suggests that the average crush loads may have been higher in the test than prescribed. With modifications to the cab car crush zone characteristics the model more accurately estimates the crush at this interface, as shown in the first red circle marker in Figure 63B.

Improved crush agreement is also observed at the rear of the CEM consist. The modification made to the trailing cab car and trailing locomotive (see Mod D in Table 4) improved the crush agreement at this coupled interface. In the test the coupled locomotive contacted the cab car's end frame with a lateral offset, causing the cab car crush zone to crush asymmetrically and sustain damage in structure that was not intended to deform. Evidence such as scraping marks in the cab car sliding sill/fixed sill mechanism and the final offset position of the cab car end frame indicate that the loads endured by the structure were higher than prescribed in an ideal in-line impact. Such events likely caused the cab car to experience less crush in the PEAM than predicted because collision energy was transferred into deforming other parts of the end frame structure. In order to investigate the effect of higher loads applied to the cab end, modifications were made in the model to the force-crush characteristic of the cab car (refer to Figure 68 in Appendix A for details). The force-crush characteristic of the coupled cab car was modified to require a larger load in order to crush the first three inches of the car end. The stiffness of the coupled locomotive end structure was modified to crush about four inches, as was observed in the test. With these modifications to the coupled end structures, the crush at the trailing cab more closely agrees with the test results, as shown by the last circle

marker in both graphs of Figure 63. Furthermore, the crush distribution pattern through the train is improved over the baseline results.

6.3.3 Non-longitudinal Motion

Figure 64 shows a comparison of the relative vertical and lateral motions at each coupled interface in the CEM consist. The maximum value of vertical offset between cars is about three inches. These are indications of the individual pitching of each car due to the severe decelerations. The vertical motions are very similar for all cars. The maximum value of lateral offset between cars is almost six inches. Although there are no lateral perturbations introduced to either consist, once the first coupled connection develops a lateral offset, it progresses down the length of the train. This behavior agrees with that observed in the test. While the push back of the couplers minimized the transfer of lateral forces between cars, the cars still experience minor offsets. In the test, the coupled cab car and locomotive experienced misalignment during the collision event. Pictures from onboard high speed cameras indicate the lateral misalignment may have been as high as 6"-8" during the collision. The buildup of lateral forces occurs successively in each car and is an indication of how a small lateral perturbation at the front of the train is transferred down the length of the train.

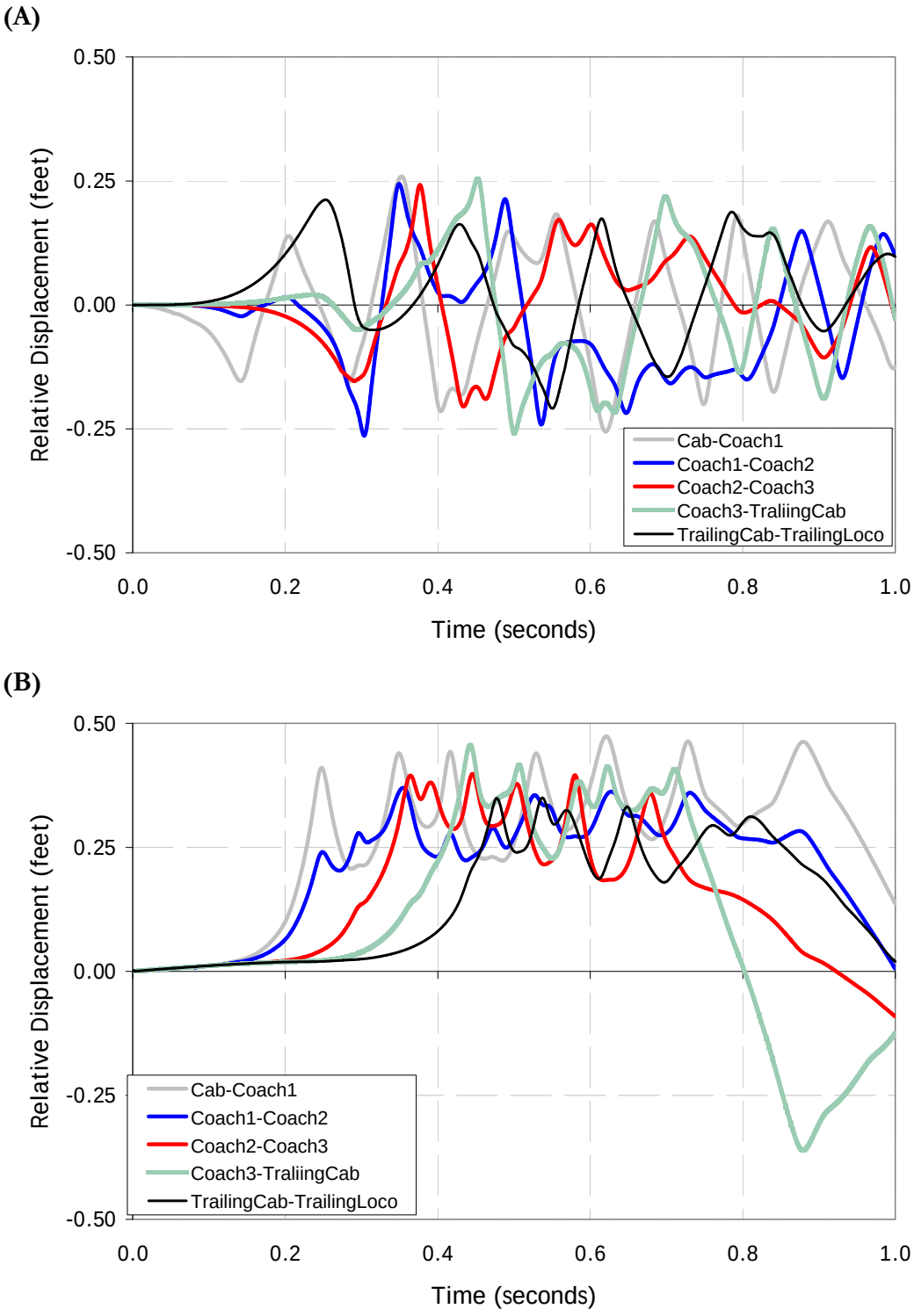

Figure 64. Model results for relative displacements between end frames at each coupled interface; (A) vertical displacement and (B) lateral displacement

7 CONCLUSIONS AND RECOMMENDATIONS

The three-dimensional collision dynamics model developed for this thesis serves two roles: to explain the events of the train-to-train test and to develop a tool for evaluating other collision conditions and equipment variations. The first role is accomplished and demonstrated through comparison of results with the full-scale test. The second role is accomplished through the documentation and demonstration of the features needed to assess other conditions and demands on CEM.

7.1 SPECIFIC CONTRIBUTIONS

The development and validation of a three-dimensional multi-body model for CEM passenger rail equipment is accomplished in this thesis. The work drew upon lumped-mass modeling techniques used in practice over the last thirty years to develop more advanced capabilities for evaluating CEM passenger rail equipment. The model features were developed and validated in three stages by comparison with full-scale test results. First, a multi-body lumped-mass representation of a single railcar with crush zones demonstrated that the three-dimensional motions of the car body and trucks correspond with those observed in the CEM single-car test. A two-car model demonstrated that the representation of the coupler produces the three-dimensional inter-car motions and pushback of the coupler. A train-to-train model demonstrated the performance of the three-dimensional features of a full train of CEM railcars in a train-to-train impact.

The three-dimensional thesis model adapted some modeling techniques previously used in dynamic modeling practice and developed new features required

for capturing the three-dimensional motion and car-to-car interactions unique to CEM railcars. A user-defined FORTRAN subroutine, developed in past research, was employed to compute the non-linear force-crush behavior as structural crush. Contact forces were chosen based upon the findings of previous parametric studies conducted by Severson [9] during the development of the single and two-car full-scale tests of conventional equipment.

Multi-body representations of the crush zones were developed similar to those developed by Jacobsen, Tyrell and Perlman [10, 11] in preparation for the single and two-car CEM full-scale tests. In this thesis, the multi-body crush zone configuration was improved upon, so that the load path can be traced through each component of the crush zone and timing of events can be evaluated. The end frame is constrained to crush in-line with the car body, which assumes the sliding sill/fixed sill mechanism functions. A more accurate representation of the coupler was developed which captures the motions of a conventional coupler during typical operation and also pushback features of the coupler during prescribed collision loads. The bellmouth structure and coupler mechanism are modeled with a series of contact forces and joints. This representation allows for the coupler to achieve pitch, yaw and one translational motion. With the appropriate connections and range of coupler swing represented, three-dimensional loads are transferred between cars. In a collision, when a prescribed longitudinal load is reached, the pushback triggers, allowing the coupler arm to shorten and the car ends to move together. Fingered anti-climbers required on passenger cars are simulated so that vertical motion is limited once the cars come together.

New truck representations were developed for suspension characteristics and the wheel-to-rail interaction. A series of parts were connected in which the inertial properties are lumped into a single mass and "dummy" masses were used to constrain motion along the rails but still allow rotational and pitching motions relative to the car body. Lateral interaction between the truck and rail is simulated and a force-displacement characteristic is defined to estimate a derailment event.

Typically, in collision dynamics modeling, a lumped-mass representation is developed at the impacting interface and simplified railcar representations are used for the cars further away from the impact point. For this thesis, by constructing a full train of the multi-body CEM railcars, the three dimensional performance of CEM equipment could be simulated through the entire train length. With the uniting of three-dimensional motion and component level representation, the train-to-train model can be used to investigate the performance of CEM at three equally important levels: as a full train system, for car-to-car interactions and at a component level within each crush zone. With this capability established, the model can be used to evaluate how variations at one level affect the performance at all three. More complicated performance issues are quickly being raised about CEM in the U.S. as development of regulations and incremental introduction into service are in sight.

7.2 OBSERVATIONS AND DISCUSSION

The full-scale tests point out the need to design a reliable and robust CEM system. Each crush zone did not perform identically, nor is it realistic to expect the ideal performance of each crush component. Determining the specific timing and activation of each crush zone throughout a consist is complicated and depends upon

the loading conditions and interaction of adjacent CEM cars. The force applied to a particular crush zone depends on the timing of the collision force traveling through the consist and the motions of the cars in front and behind. For example, the force on a crush zone at a given instant is larger if the lead car is decelerating and the rear car is accelerating than if the lead car is accelerating and the trailing car is decelerating. Because the performance of a crush zone is force dependent, and the performance of a system of crush zones is force and time dependent, it is challenging to engineer a CEM train that will vary in length and configuration during regular operation to have an exact sequence of events. Instead, good practice for designing CEM railcars for U.S. commuter rail service should focus on developing reliable and robust CEM systems that can accommodate a range of collision conditions for a variety of consist configurations.

As CEM designs evolve and become more common in North American passenger rail operation one-dimensional and three-dimensional collision dynamics models are both useful design and evaluation tools. The use of the three-dimensional model has been demonstrated by achieving close agreement with crush and three-dimensional motions measured in full-scale tests. Because the models run in minutes instead of hours or days, as do detailed finite element models, collision dynamics models are useful in evaluating design choices such as how changes in components affect crush distribution or the severity of the collision. Although not discussed in depth herein, the model also estimates the secondary impact velocity which is used to predict the likelihood of serious injury to the passengers. There is a tradeoff between designing stiff railcar structures to absorb collision energy and increasing the severity of SIVs.

7.3 CONCLUSIONS

The train-to-train full-scale test of CEM equipment conducted on March 23, 2006, was a success in demonstrating the feasibility of CEM. The prototype designs of CEM cab and coach ends were retrofitted onto existing passenger railcars and absorbed the collision energy involved in a 31 mph impact with a like train, so that all the occupied space was preserved. Haphazard collision modes observed in the conventional full-scale test such as override, lateral buckling and bulk crushing of the lead passenger car were prevented. The tests unequivocally showed that CEM provides a higher level of occupant protection over conventional passenger rail equipment.

The full-scale tests also pointed out that the CEM system can be further improved. Some details did not occur as expected. Several improvements can be addressed through design modifications and some events should be flagged for further consideration.

The uncoupling of cars during push back of the couplers can be easily corrected with a design modification, such as a protective cover for the lift pin on the coupler head or redesign of the coupler carrier where the interference occurs. Additionally, mention of such a feature to protect the lift pin should be included in specifications of CEM equipment.

The primary energy absorbers were observed to have uneven crush. While the crush did not affect the overall energy absorption capability of the components, the bursting behavior of the cells due to material failure cause the cells to interfere with surrounding structure. It is likely that the erratic bursting of PEAM cells affected the crush force and likely produced higher oscillations in the crushing force. This

behavior makes the collapse of each crush zone a less controlled event. Other forms of crushable structures, such as deformation tubes which crush in a more predictable and uniform manner, are a better option for designing a controlled system. A number of companies in Europe currently provide this technology off-the-shelf.

Trigger elements also provided some difficulty through the development process to ensure a tolerable range of activation. Conventional bolts were used as the shear bolts in the pushback coupler and sliding sill for the prototype designs. Purchasing specifically designed shear bolts can ensure a tighter range of the trigger loads if shear bolts are chosen as the trigger mechanism.

The build up of lateral forces in each CEM car is a noteworthy reminder that a small lateral perturbation at the front of the train is easily transferred down the length of the train. As such, the proper functioning of crush zone components that minimize non-longitudinal motion is extremely important in ensuring a less chaotic collision environment. The deformable anti-climber, the pushback coupler and the sliding sill arrangement, each serve important roles in minimizing non-longitudinal motions. The cab car crush zone was designed to withstand an offset impact with a locomotive of 6" in the vertical and lateral directions. The sliding sill-in-fixed sill design configuration, which allows pushback of the crush zone, essentially prevents significant relative motion between the main car body and the end frame for a vertical and lateral load applied longitudinally with a 6" offset. During the full-scale tests, the lead cab car resolved the non-longitudinal forces introduced by the locomotive through the pushback of the coupler, the conforming of the deformable anti-climber to the shape of the locomotive skirt and maintaining longitudinal crush of the end structure. By comparison, at the interface of the coupled cab car and the

trailing locomotive, the cab car crush zone experienced some unexpected damage due to the non-longitudinal loads that developed.

In the test, the locomotive's lateral offset relative to the centerline of the coupled cab car, followed by the initiation of the crush zone caused the bellmouth and coupler housing to be loaded obliquely. Permanent deformation resulted, as evidenced by failed welds in the end frame assembly and formation of a 5-inch crack in the bellmouth structure. Inspection of the crack revealed that it radiated out from a curved transition in the bellmouth/end structure assembly. Due to this deformation the end frame crushed the PEAM in an asymmetric manner. Investigation of the coupled cab car/locomotive interface was evaluated with the collision dynamics model. The investigation attempted to reproduce the crush and gross motions measured at that interface. By simulating crush of the locomotive end structure and stiffening the cab car crush zone to simulate the high loads caused to damage the support structure, the gross motions at that interface were more closely recreated.

In the test, introduction of lateral and vertical loads through a coupled connection provided a severe set of loads on the CEM support structure. The performance of the coupled cab and locomotive highlight the need for the support structure to be designed against an appropriate range of dynamic crush loads, particularly non-ideal loading conditions. Specific structural details of the prototype CEM design are currently being re-evaluated in a related FRA project to improve cab car end frame structures. Additionally, research is needed to incorporate CEM features into locomotives. In the full-scale test, had the coupled locomotive included

CEM features such as a deformable anti-climber and a pushback coupler, the non-longitudinal loads at the coupled connection would have been minimized.

7.4 RECOMMENDATIONS FOR FURTHER WORK

While the benefits of CEM have clearly been recognized by the U.S. rail industry, acceptance of CEM as a standard practice still hinges on a few issues: consideration and development of standards and regulations, performance in non-ideal collision conditions and service experience. The model developed for this thesis is designed to be a tool for evaluating future concerns about CEM performance. Following are some of the anticipated efforts:

1) Future Designs
2) Further CEM Development
    a. Higher Speeds
    b. Oblique Collisions
3) Inclusion of CEM Features on Locomotives

With the safety benefits and design feasibility demonstrated by FRA research, the inclusion of CEM designs in future passenger rail equipment is already happening. Metrolink awarded a contract to Rotem in March 2006 for an order of multi-level cab cars and coach cars that include CEM requirements. Other major cities such as Austin, Texas are proceeding with development of existing and new commuter rail service and will place orders for new passenger rail equipment. With such expansion of commuter rail service around the country and the continued use of shared track, a number of new railcar designs which might include CEM principles, will enter into the U.S. market over the next decade. For each new

design, railcar manufacturers must demonstrate through testing and analyses the crashworthiness performance to the buyer. The three-dimensional multi-body collision dynamics model will be a valuable tool in terms of design assessment and evaluation of train-level performance, car-level performance and crush zone component performance. Evaluating the activation of each crush zone is particularly important in the design of a reliable and robust CEM system.

The U.S. demands CEM systems with reliability and robustness to meet a range of impact conditions, variation in equipment types and irregularity of consist configurations, associated with the typical rail operating environments. Further research into CEM performance in other conditions is still needed. CEM performance in a grade crossing collision will be analyzed in the near future with the possibility of tests to evaluate the design issues. The model can also be used to investigate the performance of the train in non-ideal conditions (i.e. oblique collision or curved track). The three-dimensional multi-mass representation of the model allows for relative motions between the coupler, crush zone, car body and trucks. Such features of the model can estimate loads transferred between individual components. This feature is important as collision conditions are further explored and accidents provide more information. The design and performance of CEM at higher speeds will also need to be addressed in the future. The prototype design succeeded in meeting the design requirements at 30 mph. This is not the top speed for which collisions occur. CEM will continue to evolve and analyses will continue to aide in evaluation.

Further inclusion of CEM features on locomotives, both passenger and freight locomotives, is highly recommended. The benefits of CEM can be applied outside

of passenger rail equipment. CEM can help to control chaotic collision events by implementing deformable anti-climbers and pushback couplers, at a minimum, on locomotives. The model is set up to evaluate the inclusion of CEM features on the locomotives in the model. Such features will help minimize chaotic collision events such at lateral buckling and override.

REFERENCES

[1] Lewis, J.H. "Validation of Measures to Improve Vehicle Safety in Railway Collisions," 1995 ASME International Mechanical Engineering Congress and Exposition, AMD-Vol. 210, BED-Vol. 30, pp. 17-34.

[2] Cleon, L.M., J. Legait, M. Villemin. "SNCF Structural Crashworthiness Design Strategy: Design Examples of Duplex TGV and XTER Diesel Multiple Unit." Ed. D.C. Tyrell and A.H. Rubin. Symposium on Rail Vehicle Crashworthiness, June 1996, U.S. Department of Transportation, DOT/FRA/ORD-97/08, 1998.

[3] "Train Crashworthiness for Europe," SAFETRAIN Final Report, for the European Community under the Industrial and Materials Technologies Programme, Issued 27/07/2000.

[4] U.S. Department of Transportation, Federal Railroad Administration, "49 CFR Part 216 et al., Passenger Equipment Safety Standards; Final Rule," Federal Register, May 12, 1999.

[5] Dias, J., M. Pereira. Chapter 2, "Multicriteria Optimization of Train Structures for Crashworthiness," *Advances in Computational Multibody Systems*, Vol. 2, pp. 295-316.

[6] Mayville, R.A., R.J. Rancatore, L. Tegler, L. "Investigation and Simulation of Lateral Buckling in Trains," Proceedings of the 1999 IEEE/ASME Joint Railroad Conference, Institute of Electrical and Electronics Engineers, Catalog Number 99CH36340, 1999.

[7] Jacobsen, K., D. Tyrell, A.B. Perlman. "Rail-Car Impact Tests with Steel Coil: Collision Dynamics," American Society of Mechanical Engineers, Paper No. JRC2003-1655, April 2003.

[8] Priante, M. "A Collision Dynamics Model of a Bi-level Train," Tufts University Master's Thesis, May 2006.

[9] Tong, P. "Mechanics of Train Collision," 1976, Final Report, FRA-OR&D-76-246, Cambridge, Massachusetts.

[10] Jacobsen, K., D. Tyrell, A.B. Perlman. "Impact Test of a Crash-Energy Management Passenger Rail Car," American Society of Mechanical Engineers, Paper No. RTD2004-66045, April 2004.

[11] Jacobsen, K., D. Tyrell, A.B. Perlman. "Impact Tests of Crash Energy Management Passenger Rail Cars: Analysis and Structural Measurements," American Society of Mechanical Engineers, Paper No. IMECE2004-61252, November 2004.

[12] French, P. "U.S. Railroad Safety Statistics and Trends," AVP – Safety and Performance Analysis, presented for Association of American Railroads, July 3, 2007.

[13] Tyrell, D. "Rail Passenger Equipment Accidents and the Evaluation of Crashworthiness Strategies," presented at 'What Can We Realistically Expect from Crashworthiness? Improving Train Design to Withstand Future Accidents' Rail Equipment Crashworthiness Symposium, Institute of Mechanical Engineers, May 2, 2001, London, England.

[14]"Report to the House and Senate Appropriations Committees: The Safety of Push-Pull and Multiple-Unit Locomotive Passenger Rail Operations," Federal Railroad Administration, Office of Safety, Office of Railroad Development, June 2006.
[15]National Transportation Safety Board, "Head On Collision of Boston & Maine Corp Extra 1731 East & MBTA Train No. 570 on Former Boston & Maine Corp. Tracks, Beverly, Massachusetts, August 11, 1981", RAR-82-01, March 1982.
[16]National Transportation Safety Board, "Head On Collision of National Railroad Passenger Corporation (Amtrak) Passenger Trains Nos. 151 and 168, Astoria Queens, New York, NY, July 23, 1984", RAR-85-09, May 1985.
[17]National Transportation Safety Board, "Collision of National Railroad Passenger Corporation (Amtrak) Trains 59 with a Loaded Truck-semitrailer Combination at a Highway/Rail Grade Crossing in Bourbonnais, Illinois, March 15, 1999", NTSB/RAR-02/01, February 2002.
[18]Mayville, R.A., K.N. Johnson, R.G. Stringfellow, D.C. Tyrell. "The Development of a Rail Passenger Coach Car Crush Zone," ASME/IEEE Paper No. ASME RTD 2003-1653, April 2003.
[19]Martinez, E., D. Tyrell, R. Rancatore, R. Stringfellow, G. Amar. "A Crush Zone Design for An Existing Passenger Rail Cab Car," American Society of Mechanical Engineers, Paper No. IMECE2005-82769, November 2005.
[20]Tyrell, D.C., A.B. Perlman. "Evaluation of Rail Passenger Equipment Crashworthiness Strategies," Transportation Research Record No. 1825, pp. 8-14, National Academy Press, 2003.
[21]Severson, K., D. Tyrell, A.B. Perlman. "Analysis of Collision Safety Associated with Conventional and Crash Energy Management Cars Mixed Within a Consist," American Society of Mechanical Engineers, Paper No. IMECE2003-44122, November 2003.
[22]Jacobsen, K., K. Severson, A.B. Perlman. "Effectiveness of Alternative Rail Passenger Equipment Crashworthiness Strategies," American Society of Mechanical Engineers, Paper No. JRC2006-94043, April 2006.
[23]Priante, M., D. Tyrell, A.B. Perlman. "The Influence of Train Type, Car Weight, and Train Length on Passenger Train Crashworthiness," American Society of Mechanical Engineers, Paper No. RTD2005-70042, March 2005.
[24]Tyrell, D., E. Martinez, K. Jacobsen, D. Parent, K. Severson, M. Priante, A.B. Perlman. "Overview of a Crash Energy Management Specification for Passenger Rail Equipment," American Society of Mechanical Engineers, Paper No. JRC2006-94044, April 2006.
[25] Contract No. EP142-06 Metrolink Commuter Rail Cars – Technical Specification, Issued 03/14/06.
[26]Chatterjee, S. and J.F. Carney, III. "Crash Energy Dissipation Management and Interior Crashworthiness in Passenger Trains," Report to Advanced Railroad Research Centre, Sheffield, U.K., Vanderbilt Engineering Center for Transportation Operations and Research, Nashville, TN, December 1994.
[27]Cadete, R., J. Dias, M. Pereira. "Optimization in Vehicle Crashworthiness Design Using Surrogate Models," 6th World Congresses of Structural and Multidisciplinary Optimization, Rio de Janeiro, Brazil, June 2005.

[28]Tyrell, D., K. Severson, B. Marquis. "Crashworthiness of Passenger Trains: Safety of High–Speed Ground Transportation Systems," DOT/FRA/ORD – 97/10, U.S. Department of Transportation, Washington, D.C., February 1998.

[29]Severson, K., "Development of Collision Dynamics Models to Estimate the Results of Full-scale Rail Vehicle Impact Tests," Tufts University Master's Thesis, November 2000.

[30]"Railway Tests Crash-worthy Coaches," *The Tribune*, The Tribune News Service, Chandigarh, India, February 22, 2006.

[31]National Transportation Safety Board, "Collision and Derailment of Maryland Rail Commuter MARC Train 286 and National Railroad Passenger Corporation AMTRAK Train 29 Near Silver Spring, MD February 16, 1996", RAR-97-02, 06/17/1997.

[32]Tyrell, D., K. Severson, A.B. Perlman. "Single Passenger Rail Car Impact Test Volume I: Overview and Selected Results," U.S. Department of Transportation, DOT/FRA/ORD-00/02.1, March 2000.

[33]Tyrell, D., K. Severson, A.B. Perlman. "Passenger Rail Two-Car Impact Test Volume I: Overview and Selected Results," U.S. Department of Transportation, DOT/FRA/ORD-01/22.I, January 2002.

[34]Tyrell, D., K. Severson, A.B. Perlman, R. Rancatore. "Train-to-Train Impact Test: Analysis of Structural Measurements," American Society of Mechanical Engineers, Paper No. IMECE2002-33247, November 2002.

[35]Tyrell, D., K. Jacobsen, E. Martinez, A.B. Perlman. "A Train-to-Train Impact Test of Crash-Energy Management Passenger Rail Equipment: Structural Results," American Society of Mechanical Engineers, Paper No. IMECE2006-13597, November 2006.

[36]White, J.H., Jr. "The American Passenger Car," The John Hopkins University Press, 1978.

[37]Smith, Roderick. "Crush Zone Development" from Tyrell, D.C., A Rubin, editors, "Proceedings of the Symposium on Rail Vehicle Crashworthiness, June 1996", U.S. Department of Transportation, DOT/FRA/ORD-97/08, 1998.

[38]Pike, Jeffrey A. *Automotive Safety: Anatomy, Injury, Testing and Regulation*, Warrendale: Society of Automotive Engineers, 1990.

[39]Smith, R.A. "Crashworthiness of Trains: Principles and Progress," ASME, AMD-Vol. 210/BED-Vol. 30, pp 79-88.

[40] "High Speed Technical Specification of Interoperability – Rolling Stock," *Official Journal of the European Union*, 2002/735/EC, L245/402-506, Published 9/12/2002.

[41]National Transportation Safety Board, "Rear-End Collision of Amtrak Passenger Train 94, The Colonial and Consolidated Rail Corporation Freight Train ENS-121, on the Northeast Corridor, Chase, Maryland January 4, 1987," January 1988, RAR-88-01.

[42]Tyrell, D. "U.S. Rail Equipment Crashworthiness Standards," Journal of Rail and Rapid Transit, Proceedings Part F, Institute of Mechanical Engineers, August 2002.

[43] American Public Transportation Association, Member Services Department, Manual of Standards and Recommended Practices for Passenger Rail Equipment, Issue of July 1, 1999.
[44] International Union of Railroads *Annual Report 2006*, UIC Communications Department, Paris, France, December 2006.
[45] "Caltrain.com – Caltrain 2025" Caltrain, 2007. www.caltrain.com/caltrain2025.html
[46] "MBTA, About the MBTA, Transit Projects." Massachusetts Bay Transportation Authority, 2007.
[47] "TriMet: Washington Country Commuter Rail." TriMet, 2007. http://www.trimet.org/commuterrail/index.htm http://www.mbta.com/about_the_mbta/t_projects/?id=990
[48] "Commuter Rail in Minnesotta – MN/DOT." Minnesotta Department of Transportation, 2007. http://www.dot.state.mn.us/passengerrail/commuter.html
[49] Mayville, R.A., R.G. Stringfellow, R.J. Rancatore, T.P. Hosmer. "Locomotive Crashworthiness Research, Volumes 5: Cab Car Crashworthiness Report," DOT/FRA/ORD-95/08.5, 1996.
[50] Tyrell, D.C., K.J. Severson, R.A. Mayville, R.G. Stringfellow, S. Berry, A.B. Perlman. "Evaluation of Cab Car Crashworthiness Design Modifications," Proceedings of the 1997 IEEE/ ASME Joint Railroad Conference, Institute of Electrical and Electronics Engineers, Catalog Number 97CH36047, 1997.
[51] Mayville, R., K. Johnson, D. Tyrell, R. Stringfellow. "Rail Vehicle Car Cab Collision and Corner Post Designs According to APTA S-034 Requirements," American Society of Mechanical Engineers, Paper No. MECE2003-44114, November 2003.
[52] Kirkpatrick, S., R. MacNeil. "Development of a Computer Model for Prediction of Collision Response of a Railroad Passenger Car," Proceedings of the 2002 IEEE/ASME Joint Railroad Conference, Institute of Electrical and Electronics Engineers, Catalog Number CH37356-TBR, 2002.
[53] Iwnicki, Simon. *Handbook of Railway Vehicle Dynamics*. Boca Raton: Taylor and Francis Group, 2006.
[54] *Adams*™. Vers. 2005 R2. Santa Ana: MSC Software Corporation, 2005.
[55] Priante, M. and E. Martinez. "Crash Energy Management Crush Zone Designs: Features, Functions, and Forms," Proceedings of the 2007 ASME/IEEE Joint Rail Conference and Internal Combustion Engine Spring Technical Conference, JRCICE2007-40051, March 2007.
[56] SAE J211/1, "Surface Vehicle Recommended Practice – Instrumentation for Impact Tests," March 1995.
[57] Tyrell, D., K. Jacobsen, D. Parent, A.B. Perlman. "Preparations for a Train-to-Train Impact Test of Crash-Energy Management Passenger Rail Equipment," American Society of Mechanical Engineers, Paper No. IMECE2005-70045, March 2005.

APPENDIX A – MODELING PARAMETERS

Mass Properties

Table 5 shows the weights of each test vehicle in the set of three full-scale impact tests of CEM equipment. Each car is retrofitted with two crush zones. The coach cars have a coach end crush zone on each end. The cab cars have a cab end crush zone on one end and a coach end crush zone on the other end. In Chapter 4, Table 2 showed the distribution of mass properties for each lumped mass in a single car. Each car is made up of a car body, two trucks, and two crush zones, as shown in Figure 17. In the collision dynamics models, the mass representing the main car body is the total car weight minus the weight of two crush zones and two trucks.

Table 5. Inertial properties of each lumped mass in the collision dynamics models

Fullscale Impact Test	Test Vehicle	Mass (lb)
Single Car	Coach Car, Budd Pioneer, #244	71,650
Two-Car	1st Coach Car, Budd Pioneer, #248	74,875
	2nd Coach Car, Budd Pioneer, #244	75,250
Train-to-train	Cab Car, M1, #9358	81,150
	1st Coach Car, M1, #9358	82,225
	2nd Coach Car, Pioneer, #244	72,450
	3rd Coach Car, Pioneer, #248	72,100
	Trailing Cab Car, M1, #9614	81,300
	Trailing Locomotive, EMD F40, #202	258,775
	Standing Locomotive, EMD F40, #234	245,000
	1st Ballasted Hopper Car	78,459
	2nd Ballasted Hopper Car	312,598

Spring characteristics

Force-crush Characteristics

The characteristics used in the runs presented for the single-car results of the thesis model are shown in Figure 65.

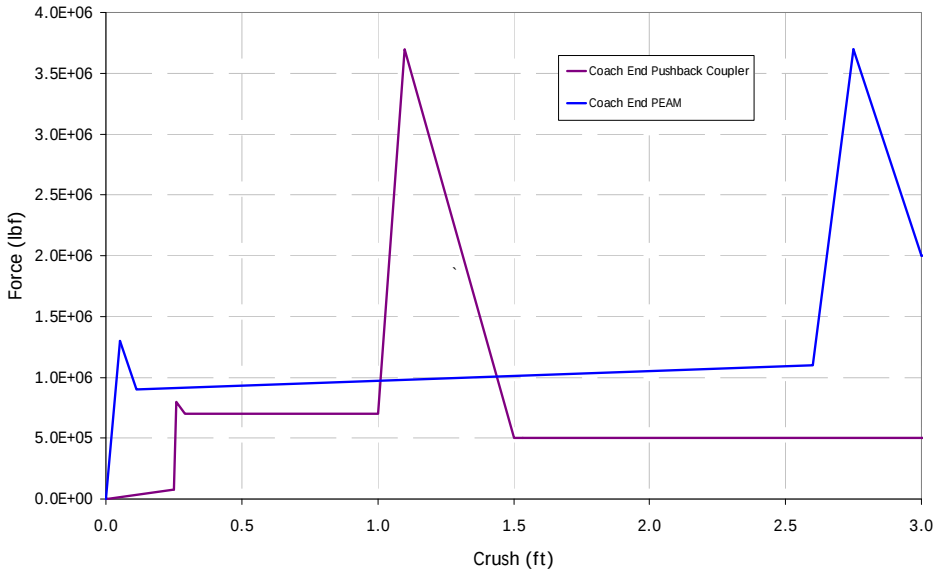

Figure 65. Force-crush characteristics used in the 3D multi-body single-car thesis model

The characteristics used in the runs presented for the two-car results of the thesis model are shown in Figure 66. There were three crush zones in this test and were modeled as identical.

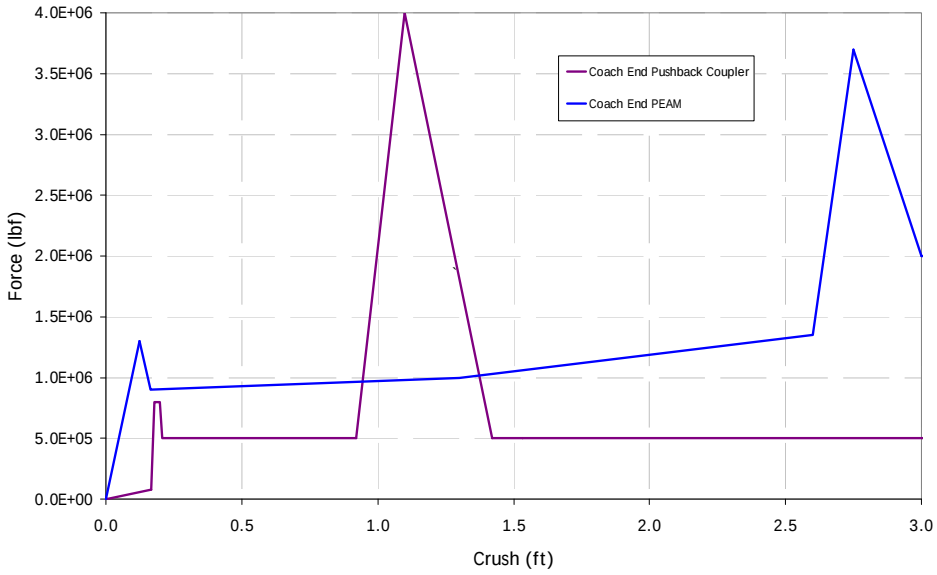

Figure 66. Force-crush characteristics used in the 3D multi-body two-car thesis model

The characteristics used in the runs presented for the baseline train-to-train results of the thesis model are shown in Figure 67. There were ten crush zones on the five passenger cars.

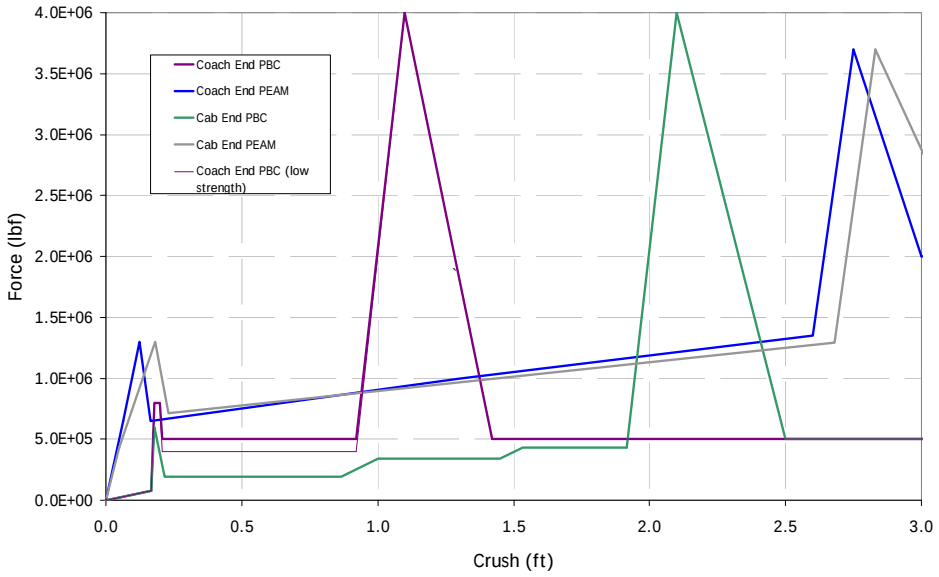

Figure 67. Baseline force-crush characteristics used in the 3D multi-body train-to-train model

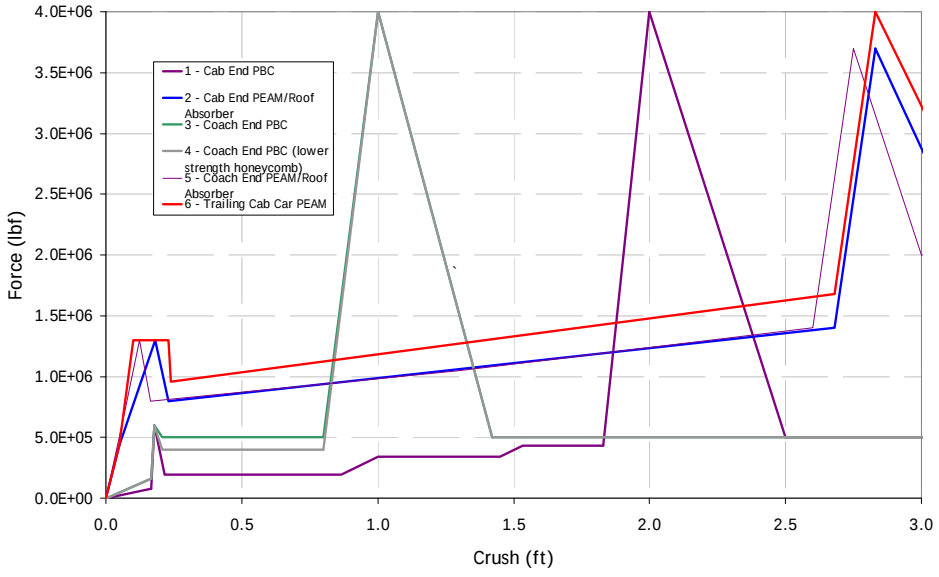

Figure 68. Mod D force-crush characteristics used in the 3D multi-mass train-to-train model

Primary Suspension

The primary suspension characteristic is built into the force vector connecting the truck mass to the dummy truck part. The spring constant for the vertical component of the force vector is 1E8 lb/ft to represent a very hard stiffness. For these trucks the primary suspension is a set of rubber bushings in the wheel set attachment.

Secondary Suspension

The information for a single component force, representing the suspension forces acting between an example truck and the car body is shown below.

```
Object Name      :  .T2TModel.SecSusp_TRc
Object Type      :  Single_Component_Force
Parent Type      :  Model
Adams ID         :  21
Active           :  NO_OPINION
I Marker         : .T2TModel.Truck_R.MARKER_164
J Marker         : .T2TModel.CoachBody.MARKER_165
Length           : None
Mode             : Translational
Actiononly       : FALSE
Function         :
   1.662e4*(VARVAL(.T2TModel.SSspring_Rc)**2)*step(VARVAL(.T2TM
   odel.SSspring_Rc),0,1,.01,0) -
   1.662e4*VARVAL(.T2TModel.SSspring_Rc)*step(VARVAL(.T2TModel.
   SSspring_Rc),0,0,.01,1)*step(VARVAL(.T2TModel.SSspring_Rc),.
   91,1,.92,0) -
   (1.662E4*.92+1e6*(VARVAL(.T2TModel.SSspring_Rc)-
   .92)**2)*step(VARVAL(.T2TModel.SSspring_Rc),.91,0,.92,1)
```

The plot in Figure 69 shows the function programmed into the Adams™ single component force. There are four springs per truck.

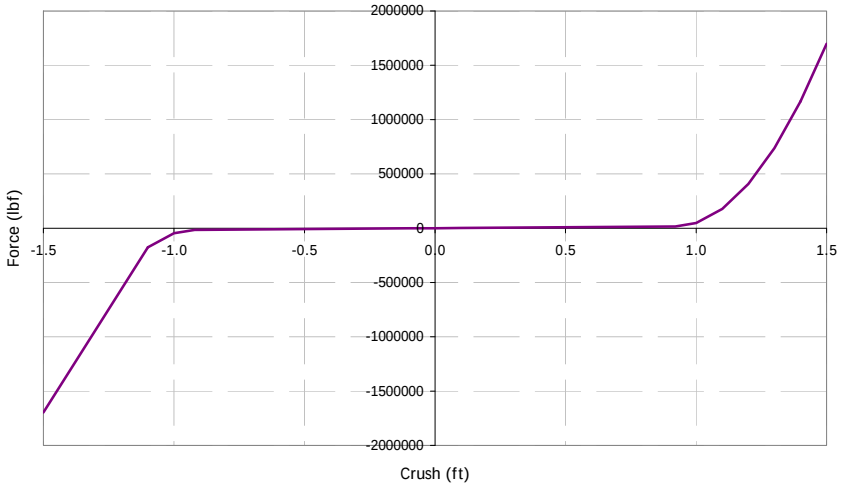

Figure 69. Vertical spring characteristic for secondary suspension

The plots below show the bounce of the lead car in a train-to-train collision scenario. The secondary suspension has a frequency of about *7 Hz*.

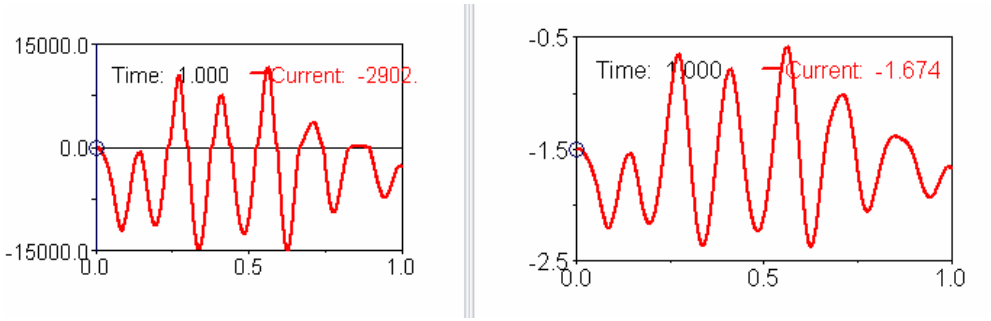

Figure 70. Results for a full train model simulation showing force vs. time (left) and displacement vs. time (right)

Wheel-to-rail Characteristics

The definition for a force vector that transmits forces transmitted between an example truck and the rail (via a dummy mass) is shown below.

```
Object Name:  .T2TModel.TruckRailInteract_TR
Object Type:  Force_Vector
Parent Type:  Model
Adams ID:  2
Active:  NO_OPINION
I Marker: .T2TModel.Truck_R.MARKER_95
J Marker: .T2TModel.TruckDummy_R.FMARKER_97
Reference Marker: .T2TModel.TruckDummy_R.MARKER_96
X Force Function: -1E6 *
   DX(.T2TModel.Truck_R.MARKER_95,.T2TModel.TruckDummy_R.MARKER
   _96,.T2TModel.TruckDummy_R.MARKER_96) - 1000.0 *
   VX(.T2TModel.Truck_R.MARKER_95,.T2TModel.TruckDummy_R.MARKER
   _96,.T2TModel.TruckDummy_R.MARKER_96,.T2TModel.TruckDummy_R.
   MARKER_96)
Y Force Function: -1E8 *
   DY(.T2TModel.Truck_R.MARKER_95,.T2TModel.TruckDummy_R.MARKER
   _96,.T2TModel.TruckDummy_R.MARKER_96) -1000.0 *
   VY(.T2TModel.Truck_R.MARKER_95,.T2TModel.TruckDummy_R.MARKER
   _96,.T2TModel.TruckDummy_R.MARKER_96,.T2TModel.TruckDummy_R.
   MARKER_96)
Z Force Function : -1*
   0.2*(.T2TModel.CoachBody_weight+2*(.T2TModel.Coupler_weight+
   .T2TModel.CZ_weight+.T2TModel.Truck_weight))/2*step(DZ(.T2TM
   odel.Truck_R.MARKER_95,.T2TModel.TruckDummy_R.MARKER_96,.T2T
   Model.TruckDummy_R.MARKER_96),-0.2,-1,-0.19,0)
   +.T2TModel.lateral_derail*(DZ(.T2TModel.Truck_R.MARKER_95,.T
   2TModel.TruckDummy_R.MARKER_96,.T2TModel.TruckDummy_R.MARKER
   _96))*step(DZ(.T2TModel.Truck_R.MARKER_95,.T2TModel.TruckDum
   my_R.MARKER_96,.T2TModel.TruckDummy_R.MARKER_96),-0.2,0,-
   0.19,1)*step(DZ(.T2TModel.Truck_R.MARKER_95,.T2TModel.TruckD
   ummy_R.MARKER_96,.T2TModel.TruckDummy_R.MARKER_96),0.19,1,0.
   2,0)
   +0.2*(.T2TModel.CoachBody_weight+2*(.T2TModel.Coupler_weight
   +.T2TModel.CZ_weight+.T2TModel.Truck_weight))/2*step(DZ(.T2T
   Model.Truck_R.MARKER_95,.T2TModel.TruckDummy_R.MARKER_96,.T2
   TModel.TruckDummy_R.MARKER_96),0.19,0,0.2,1))
```

The plot below shows the force versus displacement characteristic used to estimate the occurrence of derailment. In the Adams™ model the above code characterizes the three-dimensional spring characteristic between the truck and dummy mass, which allows the loads to be exerted on the rail. The plot below shows the lateral nonlinear characteristic. A linear relationship exists up to about 2 inches. Beyond two inches (at a load about half the total car weight), derailment is assumed to occur and a constant load is applied represented the trucks continuing along the ties or ballast with a steady coefficient of friction.

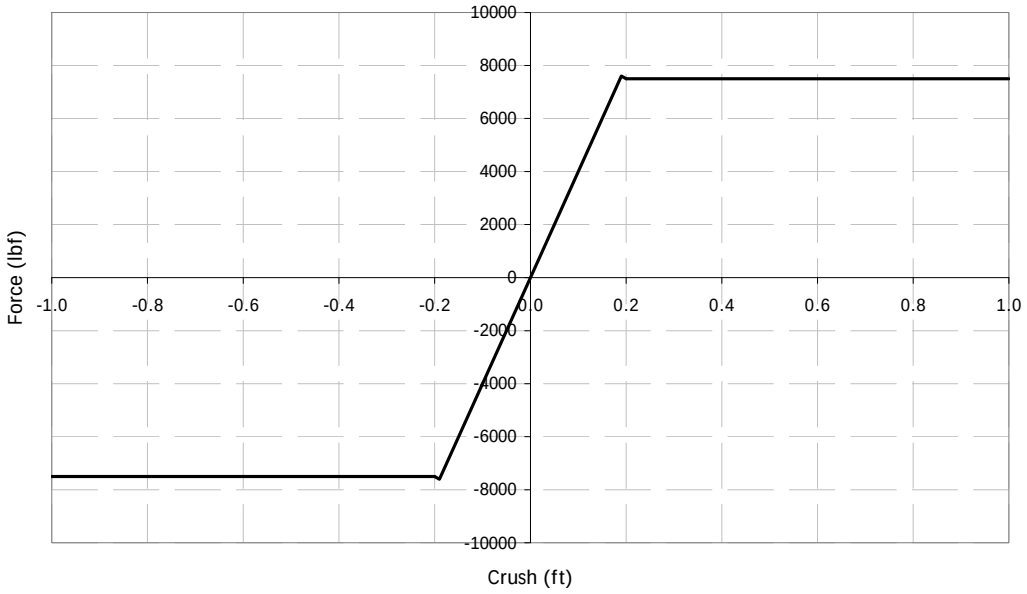

Figure 71. Lateral spring characteristic for wheel-to-rail representation

The plot below shows the results of force versus displacement of the trucks in the Adams™ model in the single-car impact scenario.

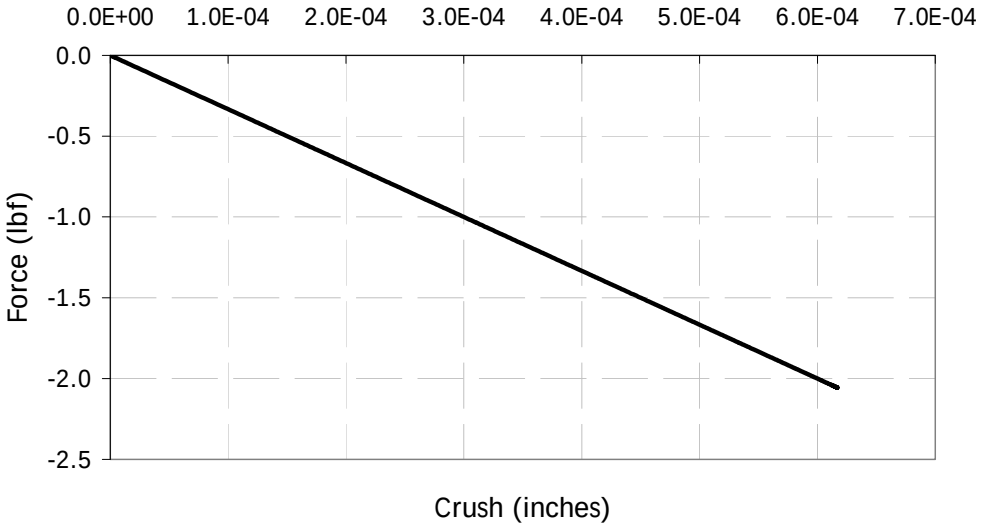

Figure 72. Force-displacement plot of truck-to-wheel interaction in the single-car test impact simulation

The plot below shows the results of force versus displacement of the trucks in the Adams™ model when a lateral perturbation is applied to the car body to induce derailment.

Figure 73. Single-car model exercised with lateral perturbation: results of the derailment characteristic, force vs. displacement between the truck and dummy mass

APPENDIX B – ADDITIONAL SIMULATION RESULTS

Two-Car Model

The plot below shows the results of modifications to the two-car model.

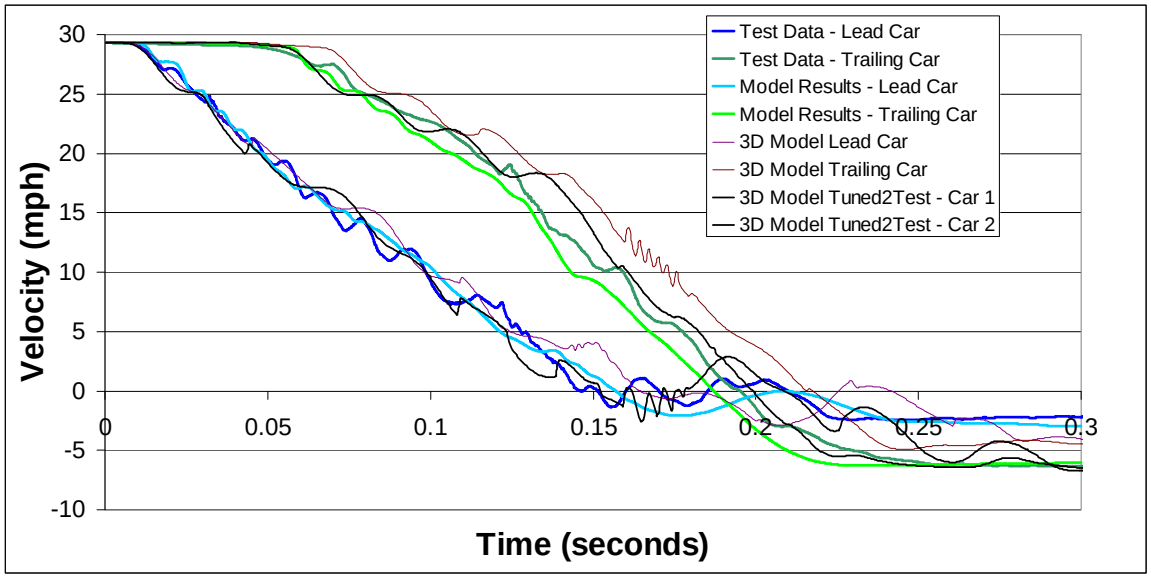

Figure 74. Velocity-time history comparison of test data, 1D model and 3D model for the two-car impact

The secondary suspension motions are shown below for the simulation of the two-car impact scenario.

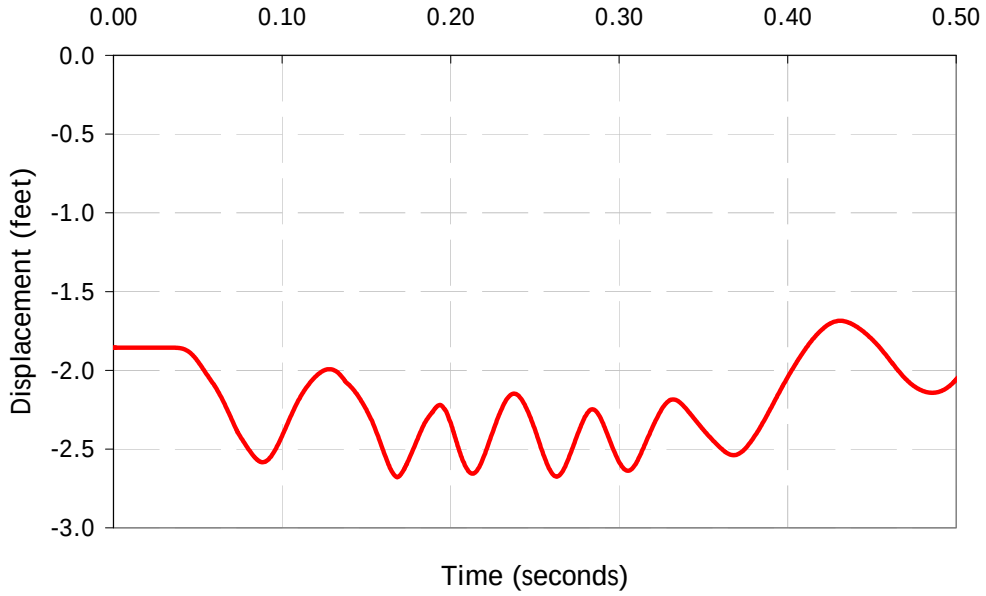

Figure 75. Displacement of secondary spring in two-car simulation

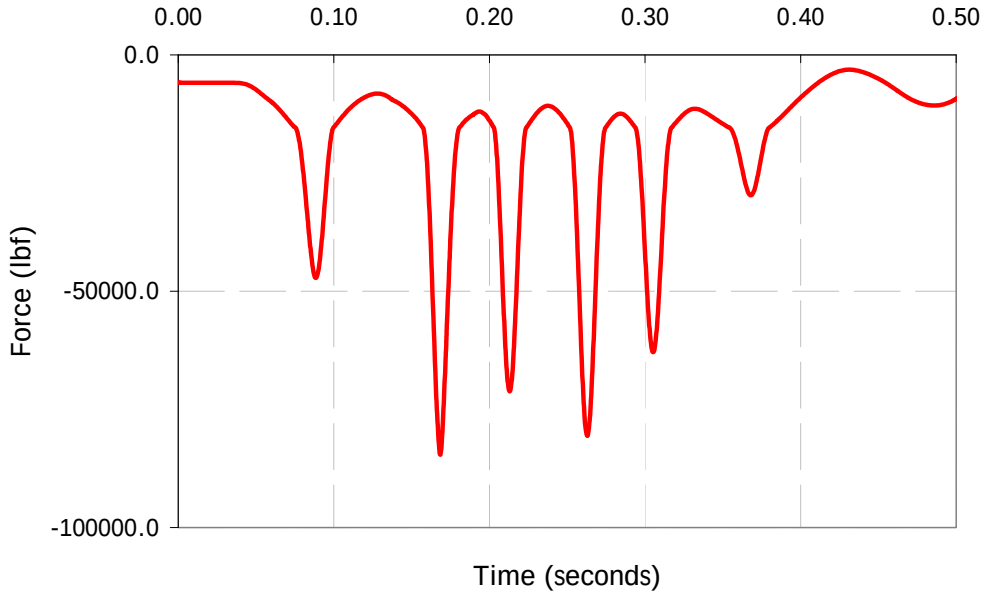

Figure 76. Force of secondary suspension spring in two-car simulation

Train-to-Train Model

The plot below shows the results of Mod A to the train-to-train model.

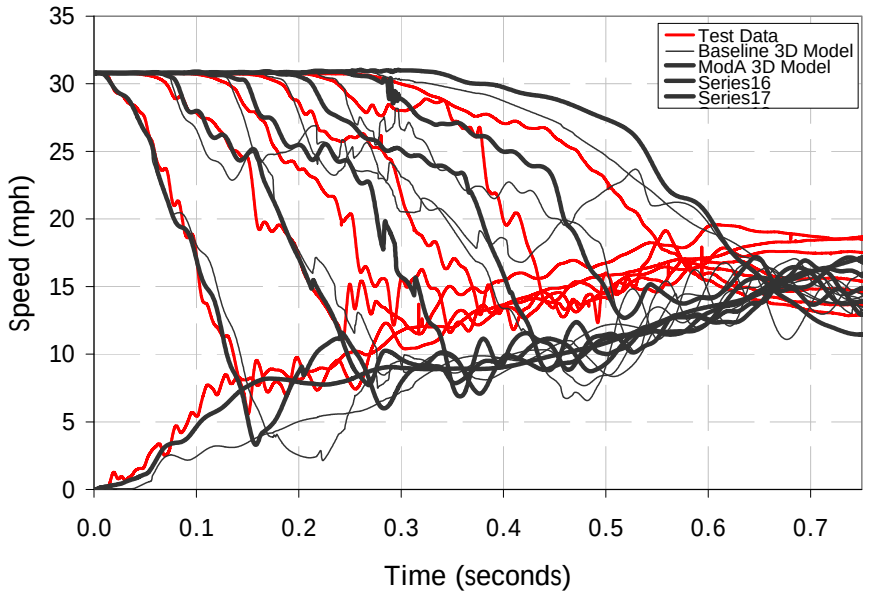

Figure 77. Comparison of train-to-train velocity-time histories: test data (red), baseline 3D model (thin black) and Mod A of 3D model (thick black)

The plot below shows the results of Mod D to the train-to-train model.

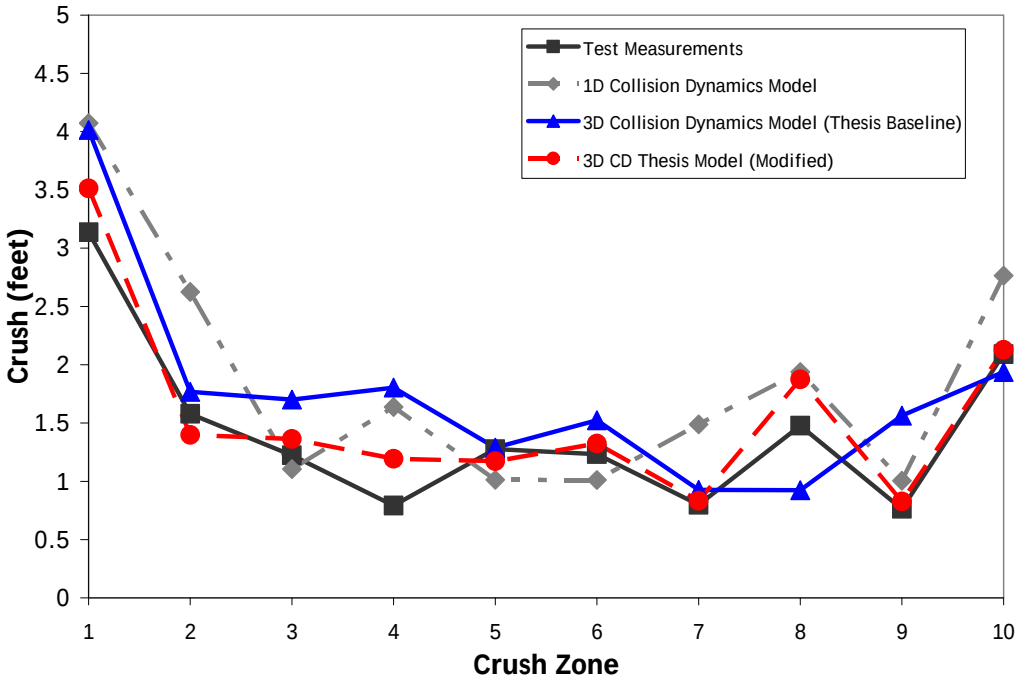

Figure 78. Graph comparing the crush distribution of the test results and the collision dynamics models for each crush zone